NASA Contractor Report 158919

Evaluation of Aero Commander Propeller Acoustic Data: Static Operations

A. G. Piersol
E. G. Wilby
J. F. Wilby

BOLT BERANEK AND NEWMAN INC.
Canoga Park, Ca. 91303

CONTRACT NO. NAS1-14611-15
MAY 1978

NATIONAL AERONAUTICS AND SPACE ADMINISTRATION
LANGLEY RESEARCH CENTER
HAMPTON, VIRGINIA 23665

ABSTRACT

Acoustic data have been analyzed from a series of ground tests performed on an Aero Commander propeller-driven aircraft with an array of microphones flush-mounted on one side of the fuselage. The analyses were concerned with the propeller blade passage noise during static operation at several different engine speeds and included calculations of the magnitude and phase of the blade passage tones, the amplitude stability of the tones, and the spatial phase and coherence of the tones. The results indicate that the pressure field impinging on the fuselage represents primarily aerodynamic (near field) effects in the plane of the propeller at all frequencies. Forward and aft of the propeller plane aerodynamic effects still dominate the pressure field at frequencies below 200 Hz; but at higher frequencies, the pressure field is due to acoustic propagation from an equivalent center located about 0.15 to 0.30 blade diameters inboard from the propeller hub.

TABLE OF CONTENTS

LIST OF TABLES

LIST OF FIGURES

LIST OF FIGURES (Cont'd)

1. INTRODUCTION AND OBJECTIVES

A series of ground runup experiments have been performed by personnel of the NASA Langley Research Center involving a reciprocating engine-propeller driven Aero Commander airplane with an array of exterior microphones flush-mounted on the starboard side of the fuselage. Some analyses of the resulting acoustic data have already been performed [1]. However, additional analyses are now desired to obtain detailed information concerning the magnitude and character of the noise impinging on the fuselage originating from the propellers only. The specific analyses required fall into four categories, as follows:

a) The magnitude of all significant propeller blade passage tones at various locations on the fuselage.

b) The magnitude stability of the propeller blade passage tones at selected locations on the fuselage.

c) The relative phase among the propeller blade passage tones at each of several selected locations on the fuselage.

d) The spatial correlation and velocity of the propeller blade passage tones over the fuselage.

This report summarizes the procedures and results of various types of data analysis designed to obtain the above desired information. The analyses were performed by Bolt Beranek and Newman (BBN) for the NASA Langley Research Center (LRC) under Task Assignment No. 15 of Contract NAS1-14611.

2. DATA AND INSTRUMENTATION

The data were provided for analysis by LRC in the form of magnetic tape recordings of sound pressure signals on a 14-channel tape. The data were Frequency Modulated with a carrier frequency of 104 kHz on intermediate range providing a recorded data frequency range of 0 to 10 kHz at 30 ips.

2.1 Summary of Data

The recorded data included eleven channels of sound pressure signals representing eleven different measurement locations for nine specific test runs, as summarized in Table 1. The ten exterior microphone locations are detailed in Figure 1. Microphone 11 was located in

TABLE 1

Summary of Aero Commander Test Runs

Run Number		Operating Engines	Nominal Engine Speed (rpm)	Blade Passage Frequency (Hz)	
LRC No.	BBN No.			Nominal	Measured*
1	1	both	2100	66.7	67.6
2	2	both	2400	76.2	75.8
3	3	both	2600	82.7	82.1
4	-	port only	2100	66.7	68.4
3b	4	both	2600	82.7	82.0
5	5	stbd only	2100	66.7	66.9
6	6	stbd only	2100	66.7	66.8
7	7	stbd only	1700	54.0	54.5
8	8	stbd only	1700	54.0	52.8

*Determined from narrow band analysis of the data.

Location	1	2	3	4	5	6	7	8	9	10	11*
x (Meters)	-.622	-.368	0	0	0	0	.368	.622	1.841	2.785	0
y (Meters)	0	0	.584	.279	0	-.305	0	0	.152	.152	.279

Propeller Diameter = 2.36m

Distance From Microphone to Propeller Tip (Along Radius)	3	4	5	6
	.140	.121	.178	.330

* Location 11 is inside the fuselage 0.25 meters directly left of Location 4

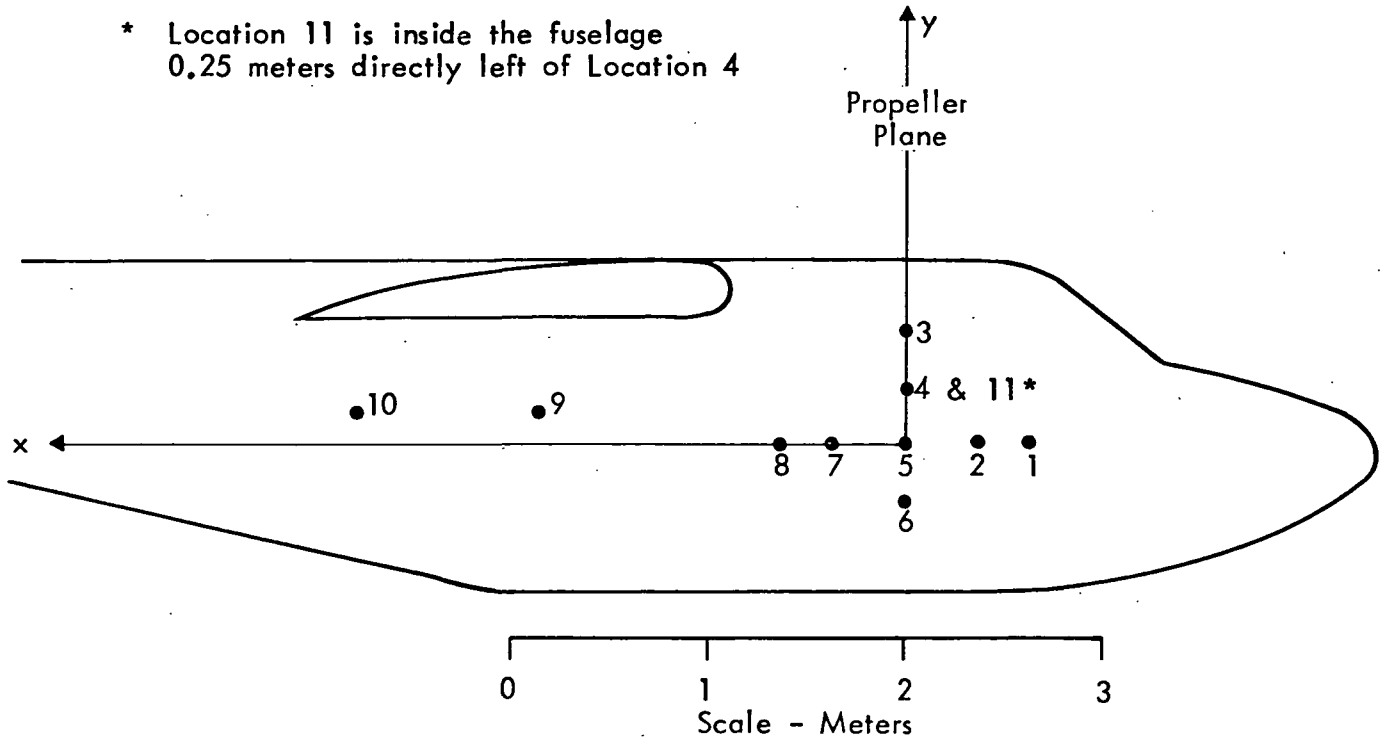

FIGURE 1. LOCATION OF MICROPHONES FOR AERO COMMANDER TEST RUNS

the interior of the aircraft. Each channel of recording was preceded by a 124 dB acoustic calibration signal at 250 Hz. The individual data samples were from 30 seconds to one minute in duration.

Referring to Table 1, note that one of the test runs, designated by LRC as Run No. 4, involved operation of the port engine only. Since all the measurements were made on the starboard side of the fuselage, the data from this run proved to be acoustically uninteresting. Hence, the data from this run were dropped early in the analysis and the Number 4 was assigned to the repeat of Run No. 3, originally designated by LRC as Run No. 3b. Nevertheless, for completeness in the data reporting, the acoustic spectra calculated at all locations during operation of the port engine (LRC Run No. 4) are presented in Table A-12 of Appendix A.

2.2 Summary of Analysis Instrumentation

The data records were reproduced for analysis using a Hewlett Packard 3924B magnetic tape recorder with appropriate FM reproduce electronics. All analyses were performed using the appropriate function on a Spectral Dynamics Model SD360 Digital Signal Processor. The stability studies of the propeller blade passage tones required a narrowband analog filtering operation prior to the SD360 Processor. This was provided by a General Radio Model 1564A Sound and Vibration Analyzer. Exact frequencies were generated using a General Radio Model 204D oscillator and calculated with a General Radio Model 1192-B counter. A schematic diagram of the data analysis setup is shown in Figure 2.

Some post analysis evaluations were performed by key punching raw data for input to a general purpose digital computer. Such evaluations were carried out on the CDC 6600 remote terminal in the BBN Canoga Park office.

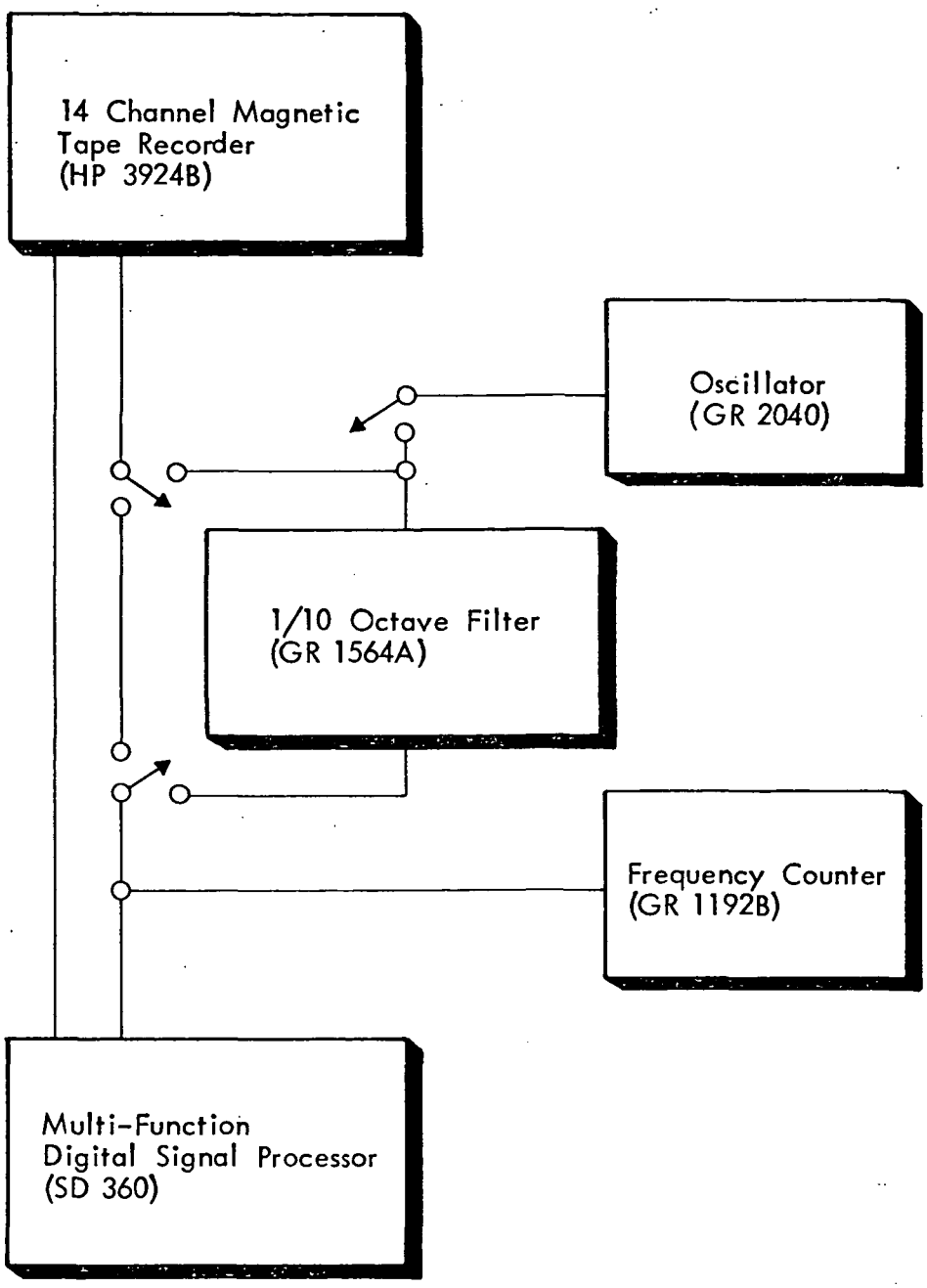

FIGURE 2. SCHEMATIC DIAGRAM OF DATA ANALYSIS INSTRUMENTATION

3. DATA ANALYSIS PROCEDURES

The required data analyses broadly divide into four categories, as previously summarized in Section 1. For each type of analysis, certain preliminary steps were required to select appropriate analysis parameters and establish necessary calibrations.

3.1 Magnitude of Propeller Blade Passage Tones

This analysis was performed directly on the SD360 using Function 2 (1024 point forward transform) or Function 3 (2048 point forward transform) with a Kaiser-Bessel time window. The first step was to establish an appropriate resolution bandwidth for the analysis. On the one hand, it is desirable to use as narrow an analysis bandwidth as feasible so as to suppress the random background noise and engine exhaust tones entering the resolution window. On the other hand, since the propeller blade passage tones are not perfect sine waves, but in fact have finite bandwidths, it is desirable to use a resolution bandwidth which is at least as wide as the tones being analyzed. Nothing is gained by using a smaller resolution, and it further would complicate the calibration problem. The desired compromise on resolution was achieved by repeatedly analyzing selected records with various resolution bandwidths to identify that bandwidth which provided the maximum tone level to background noise ratio without significantly reducing the absolute value of the tone magnitude. By trial-and-error procedures, a resolution bandwidth of B_e = 2 to 4 Hz appeared to provide a good compromise.

The next step was to select a frequency range for the analysis. The minimum resolution requirement of B_e = 2 Hz allows a maximum frequency range of 0 to 2 kHz. Using the frequency translation box on the analyzer, any multiple of this upper cutoff frequency could

also be achieved. However, preliminary analyses of selected data samples indicated that the propeller blade passage tones usually became insignificant in magnitude before the frequency reached 2 kHz. Hence, all data analysis was performed in the frequency range from 0 to 2 kHz.

The third step was to calibrate the processor. This was accomplished by analyzing the 124 dB calibration signals on the tape using exactly the same parameter settings as would be used later for the actual data analysis. The peak spectral value of the calibration signal on each channel was then fixed at 0 dB and all spectral values for the actual data were read off relative to this reference. It should be mentioned that because the digital processor calculates spectral values at discrete frequencies 4 Hz apart, the indicated magnitudes of the calibration signals, as well as the data signals, are influenced by the exact ratio between the signal frequency and the A/D conversion rate of the processor. An effort was made to correct for this during calibration, but the resulting data should not be considered accurate to more than ± 1 dB relative to the calibration signal at the calibration frequency. Based upon the calibration of individual components in the data acquisition system by LRC personnel, the frequency response function of the acquisition system was assumed to be acceptably flat.

Having selected analysis parameters and calibrated the processor, the magnitudes of all significant spectral components at all eleven locations in Figure 1 were calculated for all test runs in Table 1. These data were then key punched along with the associated attenuator settings used for the recordings, and input to the CDC 6600 computer for attenuator corrections and post processing.

3.2 Stability of Propeller Blade Passage Tones

Perhaps the best way to evaluate the stability (closeness to a true sine wave) of blade passage tones would be to use signal enhancement procedures where the pressure time histories measured at a given location during each revolution of the propeller are ensemble-averaged. Any variations of each tone from a true sinusoid will appear as noise and, hence, ultimately cancel out in the ensemble-averaging operation. However, for signal enhancement procedures to be effective, particularly at the frequencies of higher order tones, it is necessary to have a very accurate reference mark defining when the propeller is in a specific position. Unfortunately, no such propeller position marker was superimposed on the data records.

Another way to evaluate the stability of blade passage tones is to first isolate them one by one using a narrow bandpass filter and then compute the probability density function of each tone. Discrepancies from a true sine wave will appear as narrowband noise superimposed on a sine wave yielding a probability density function of the form [2]

$$p(x) = (\pi\sigma_n)^{-1} \int_0^{\pi} \psi\left[\frac{x - A\cos\theta}{\sigma_n}\right] d\theta \qquad (1)$$

where $\psi[u] = \frac{1}{\sqrt{2\pi}} e^{-u^2/2}$

A = amplitude of sine wave component

σ_n = standard deviation of narrowband noise component.

Plots of the function in Eq. (1) for various sine wave to noise power ratios are shown in Figure 3.

This type of analysis procedure has been used in the past to evaluate the stability of tones from large fans [3]. It has the advantage of not being sensitive to time base variations and, hence, does not require an accurate reference mark defining the exact position of the propeller. The primary disadvantage of the procedure is that it will not identify sine wave to noise ratios of less than unity.

To implement the procedure on the data at hand, the output of the tape recorder was passed through a narrow bandpass filter which could be tuned to isolate individual propeller blade passage tones. The output of the bandpass filter was then analyzed on the SD360 using Function 14 (probability density histogram), as previously illustrated in Figure 2. The bandpass operation was achieved using a 1/10 octave (7 percent) filter which provided a bandwidth of at least 4 Hz at the frequency of the fundamental blade passage tone. This is consistent with the optimum analysis bandwidth determined in Section 3.1. On the other hand, since the filter bandwidth increases with frequency, the filter would not provide a sufficiently narrow bandwidth to isolate propeller tones above about 500 Hz, depending upon the measurement location and test run. However, the stability of the propeller blade passage tones generally collapsed rapidly with harmonic order. Hence, except for the aft locations (9 and 10) where isolation from exhaust tones was most difficult, the 7 percent filter proved adequate for the purposes of this analysis.

The primary parameter of concern in this type of analysis is the record length T relative to the isolating filter bandwidth B. It must be remembered that the output of the narrow bandpass filter to a random noise input will appear as a sine wave with slowly varying amplitude and phase. Hence, if a probability density is

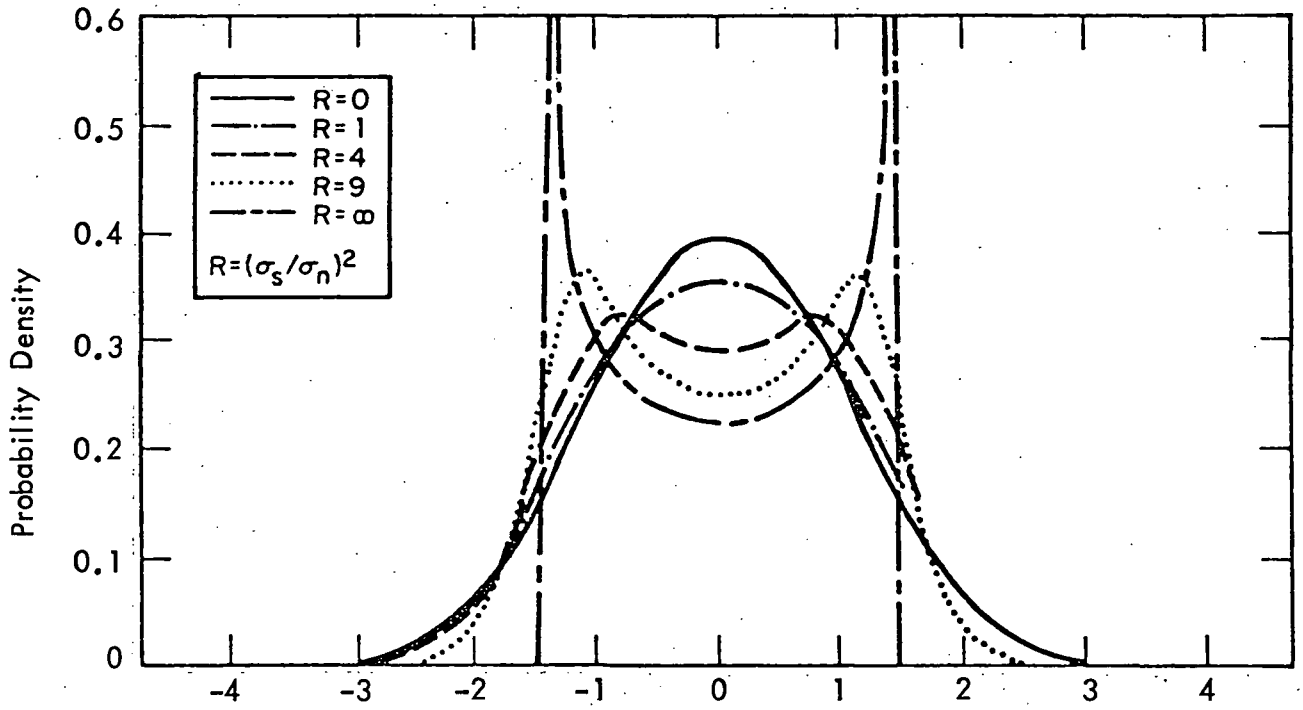

FIGURE 3. PROBABILITY DENSITY FUNCTIONS OF SINE WAVE IN GAUSSIAN NOISE

computed from too short a record, the result will tend to look like a sine wave, even though the tone probability density of the noise is probably Gaussian in form. As a rule of thumb, the analysis time T should be such that BT > 50 to assure that the narrowband noise will display a Gaussian probability density function. For the case at hand, this requirement is easily met with an analysis time of T = 30 seconds, which was used for these evaluations.

The instrumentation was calibrated for the tone stability studies by applying a sine wave from the oscillator in Figure 2 with the frequency fixed at the exact center frequency of the propeller blade passage tones summarized in Table 1. The narrow bandpass filter was tuned to have the sine wave at the center of its bandwidth. The probability density of this true sine wave was then computed using the same analysis parameters which were employed for the later analysis of the propeller blade passage tones.

Having selected the analysis parameters, the narrow bandpass filter was centered over various propeller blade passage tones of interest in the data, and the probability density functions of the tones were computed using the same input level that was employed for the sine wave calibration analysis. The resulting probability density plots were then reduced to a ratio of the average magnitude of the side peaks to the magnitude of the minimum density at x = 0, called the probability density ratio (PDR). This ratio can be converted to a sine wave to noise power ratio as shown in Figure 4. Such analyses were performed on the following tones.

a) The fundamental tone at all locations for Tests No. 2, 4, 5, and 7.

b) All tones at all locations for Test No. 4.

c) All tones at Location No. 6 for Tests No. 2, 4, 5, and 7.

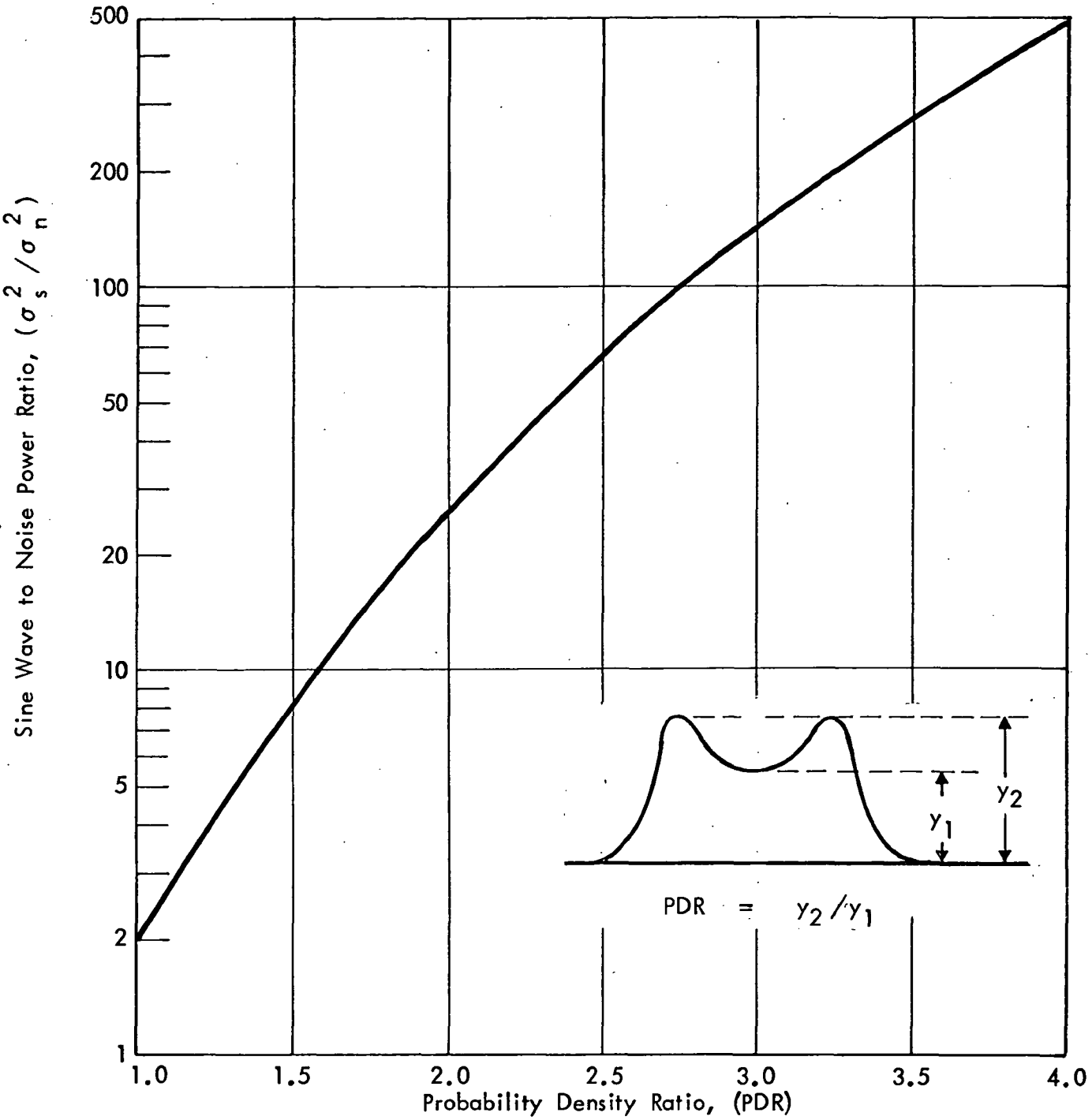

FIGURE 4. SINE WAVE TO NOISE RATIO VERSUS PROBABILITY DENSITY RATIO

Tests 1, 3, 6, and 8 were omitted from the analysis because they essentially represent repeats of the four test runs analyzed.

3.3 Relative Phase of Propeller Blade Passage Tones

The correct way to determine the relative phase among the various harmonics of the propeller noise signal measured at a given location would be to first eliminate the noise by ensemble averaging the signals for each revolution of the propeller, and then calculate the Fourier coefficients and phase of the residual deterministic signal. However, as discussed in Section 3.2, this was not feasible for the data at hand because no propeller position marker was provided with the data. Hence, it was necessary to calculate the phase angles of the individual tones using the raw sound pressure level signals from the data recording.

Using the same analysis parameters established for the tone magnitude measurements in Section 3.1, the phase of short segments (0.25 seconds long) of the pressure time histories at each measurement location of interest was computed on the SD360 using Function 2 (1024 point forward transform). To assess the stability of the phase calculations, the analysis was repeated five times on different segments of the pressure signals measured at Locations No. 1, 6, and 8 for Test Runs No. 2, 4, 5, and 7. The three locations were chosen for analysis because they represented interesting and relatively clean signals forward, mid, and aft of the propeller plane. As for the tone stability studies in Section 2.2, Test Runs No. 1, 3, 6, and 8 were omitted because they were essentially repeats of the test runs analyzed.

No special calibrations were required for this analysis since the SD360 calculates the phase of all components in a Fourier spectrum directly. However, since the calculations were started in each

case at arbitrary times, the phase angles had to be reduced in terms of a difference from the phase of the fundamental blade passage tone.

3.4 Spatial Correlation of Propeller Blade Passage Tones

The spatial correlation characteristics of the propeller blade passage tones over the fuselage surface were determined by computing the coherence and phase between pairs of sound pressure signals on the SD360 using Function 6 (transfer function B/A). Since coherence is dimensionless and phase is relative, no special calibrations were required. The coherence and phase measurements were made for Test Runs No. 2, 4, 5, and 7 at the location pairs summarized in Table 2.

The phase data measured at the exact frequencies of propeller blade passage tones were interpreted in terms of trace velocities using the relationship

$$U_c(f) = (360\ fd)/\phi(f) \qquad (2)$$

where f = frequency of tone

d = distance between locations

$\phi(f)$ = phase angle in degrees between locations at frequency f.

The coherence data at the exact frequencies of tones were analyzed with a view to fitting exponential functions of the form

$$\gamma^2(f) = \exp\left[\frac{-2\pi f|d|}{aU_c(f)}\right] \qquad (3)$$

TABLE 2

Location Pairs for Coherence and Phase Analysis

Direction	Position Relative to Propeller Hub	Location Numbers
Longitudinal	Forward	5 versus 2
		5 versus 1
		2 versus 1
	Aft	5 versus 7
		5 versus 8
		5 versus 9
		5 versus 10
		5 versus 11*
		7 versus 8
		7 versus 9
		7 versus 10
		8 versus 9
		8 versus 10
		9 versus 10
Circumferential	Above	4 versus 3
		5 versus 3
	Below	4 versus 5
		4 versus 6
		5 versus 6

*Test Run No. 4 only

where f = frequency of tone

$|d|$ = magnitude of distance between locations

$U_c(f)$ = trace velocity

a = decay constant.

Various evaluations of these data were performed using programable desk calculators.

In closing, it should be mentioned that the validity of the conclusions to be drawn later from the phase data are heavily dependent upon the assumption that there were no relative phase shifts introduced in the data acquisition and recording system. The available calibration data are insufficient to verify this assumption, but the analyzed data provided no reason to question its validity.

4. RESULTS AND DISCUSSIONS

The results of the various studies are now summarized with brief discussions of the interpretations of the results.

4.1 Magnitudes of Propeller Blade Passage Tones

The magnitude of all significant propeller blade passage tones measured with a resolution of $B_e \doteq 4$ Hz at all locations in Figure 1 and for all Test Runs in Table 1 are detailed in Appendix A. The overall values of the significant propeller blade passage tones are summarized in Table 3. Also presented in this table are the engine speed in rpm, the engine operation (both or starboard only), and the actual propeller blade passage frequency (bpf) in Hz.

TABLE 3

Overall Values of Propeller Blade Passage Tones (4 Hz Resolution)

Location (Fig. 1)	Overall Level in dB by Test Run (Table 1)							
	1	2	3	4	5	6	7	8
1	128.9	131.9	132.7	133.1	129.3	128.4	124.0	123.8
2	133.1	135.8	136.9	137.3	133.2	132.5	128.2	127.8
3	133.1	135.6	137.3	137.4	132.3	132.0	127.2	127.0
4	133.8	136.5	138.4	138.1	132.9	132.5	128.1	128.2
5	129.6	132.6	134.1	134.0	129.1	129.1	123.6	123.4
6	125.8	128.9	130.5	130.4	125.2	125.2	129.7	129.2
7	130.3	133.0	134.0	134.2	130.8	129.6	124.9	125.0
8	126.7	129.6	131.7	131.9	126.7	125.7	121.0	121.7
9*	127.0	129.6	131.7	132.1	125.4	124.8	117.9	118.9
10*	125.8	**	130.5	130.8	124.6	124.2	118.2	119.5
11	105.1	107.9	109.7	109.8	101.4	101.0	96.6	97.8
rpm	2100	2400	2600	2600	2100	2100	1700	1700
engine	both	both	both	both	stbd	stbd	stbd	stbd
bpf	67.6	75.8	82.1	82.0	66.9	66.8	54.5	52.8

*Levels too high due to engine noise contamination and reflections off the wing (see Appendix Tables A-9 and A-10).

**Data suspect due to auto-ranging of data acquisition equipment.

Three pairs of test runs represented essentially identical test conditions, namely, Runs 3 and 4 (2600 rpm), Runs 5 and 6 (2100 rpm), and Runs 7 and 8 (1700 rpm). A review of the results in Table 3 reveals no major differences between the overall levels of the two sets of data in each pair; at most locations, the levels agree within ±1 dB. Statistical tests performed by the computer on the harmonic magnitudes detailed in Appendix A confirmed the lack of a statistically significant difference at almost all locations. Based upon these results, the data for Test Runs 3, 6, and 8 were excluded from further analysis.

Also of interest are Test Runs 5 and 6 versus Run 1, which represented identical conditions (2100 rpm) except Runs 5 and 6 were performed with only the starboard engine operating while Run 1 was performed with both engines operating. The results in Table 3 reveal that the Test Run 1 levels are slightly higher than the average levels of Runs 5 and 6 at the far aft microphone locations (No. 9 and 10), and substantially higher (by about 3 dB) at Location No. 11 inside the aircraft, as would be expected. At all forward locations, however, there is no significant difference between the one and two engine runs. Hence, the data for Test Run 1 were excluded from further analysis.

Typical narrowband pressure spectra measured at Microphone Locations 1, 6, and 10 are shown in Figures 5, 6, and 7, respectively. Microphone 1 is located forward of the plane of rotation of the propeller, and the spectrum in Figure 5 is therefore fairly free from contamination by engine exhaust noise. Microphone 6 is located in the plane of rotation of the propeller, and the associated spectrum in Figure 6 is beginning to show more influence of the exhaust. Finally, Microphone 10 is well aft of the propeller plane, and the spectrum in Figure 7 is dominated

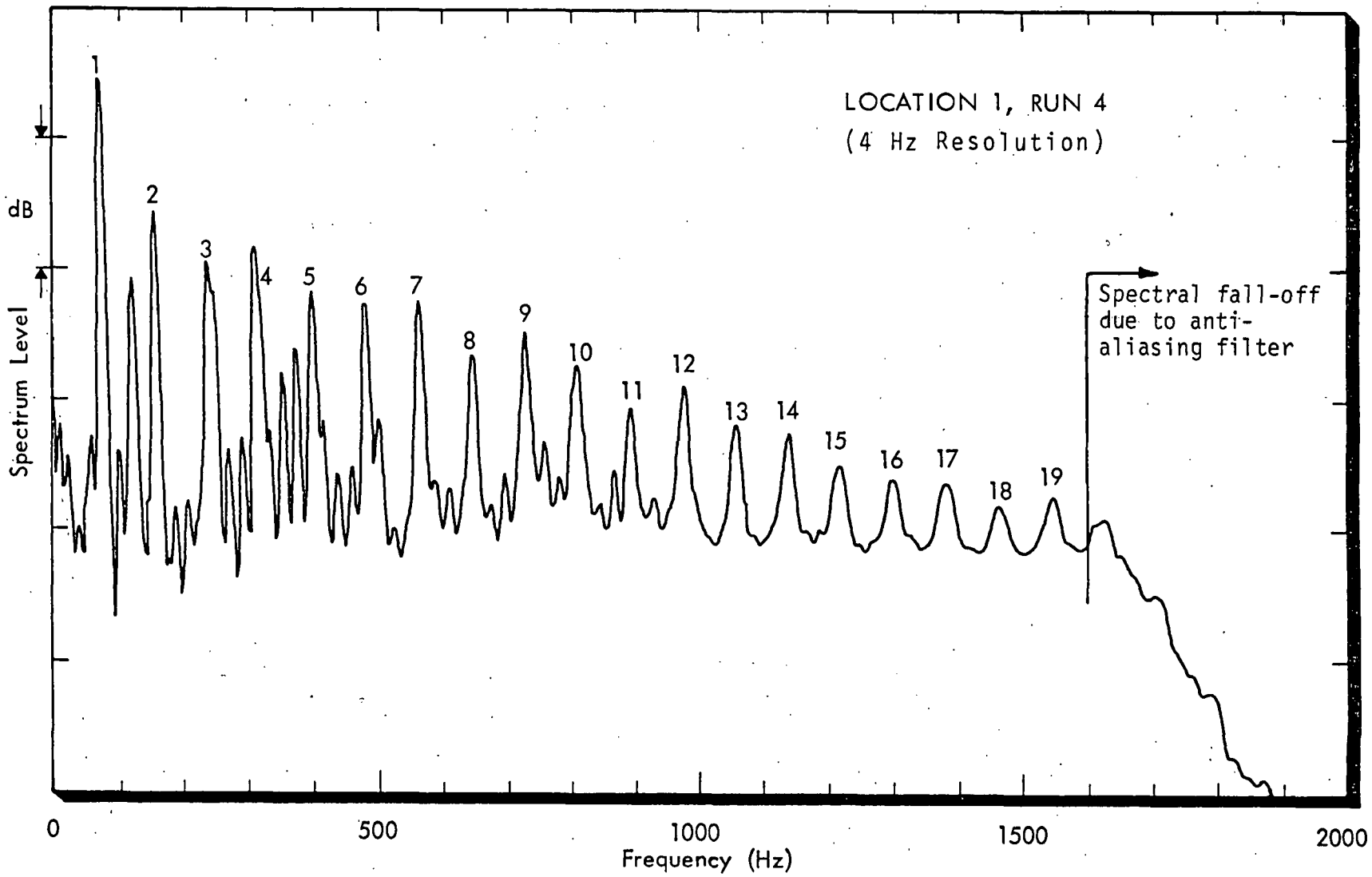

FIGURE 5. NARROWBAND PRESSURE SPECTRUM AT LOCATION 1, TEST RUN 4

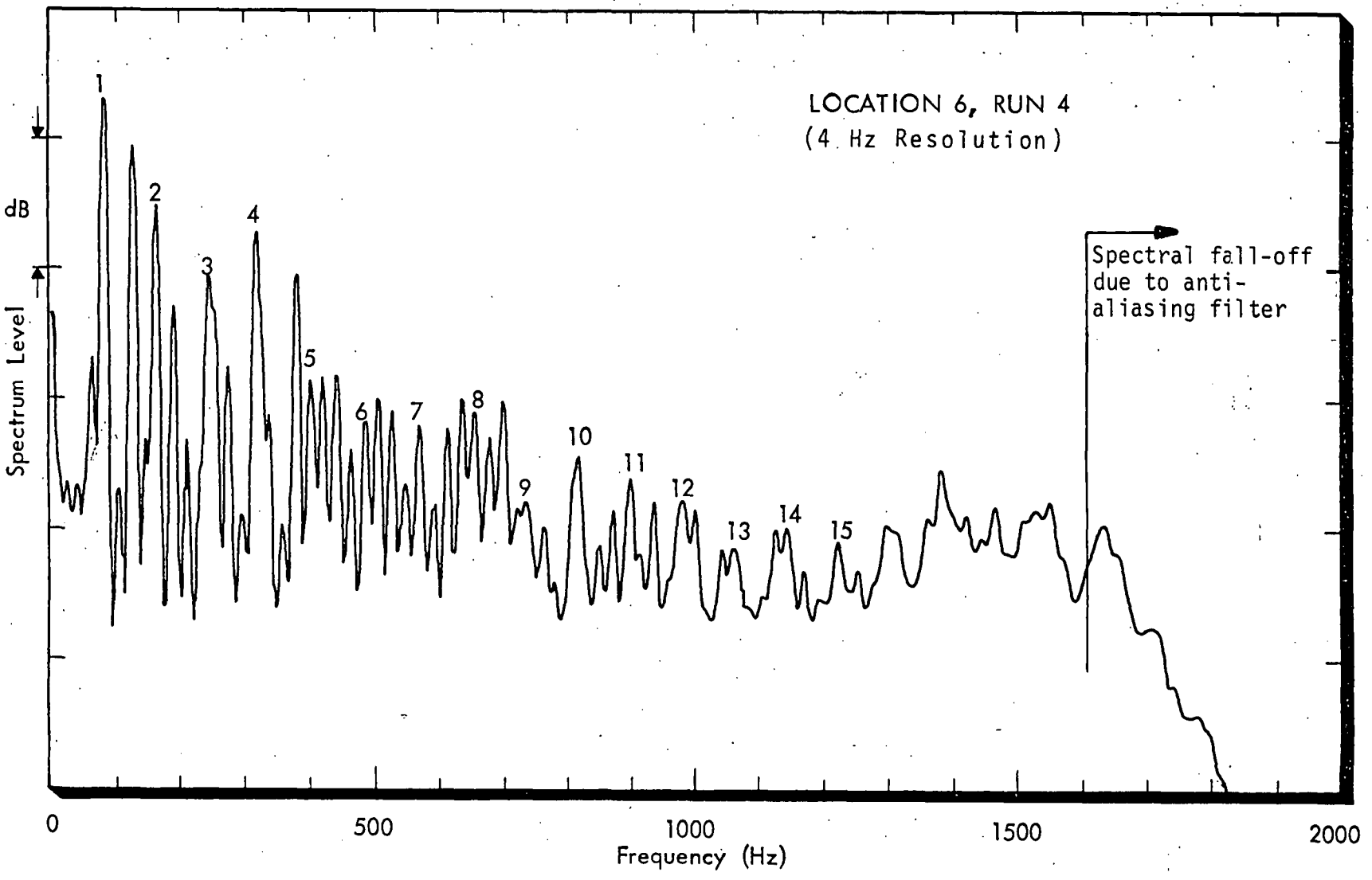

FIGURE 6. NARROWBAND PRESSURE SPECTRUM AT LOCATION 6, TEST RUN 4

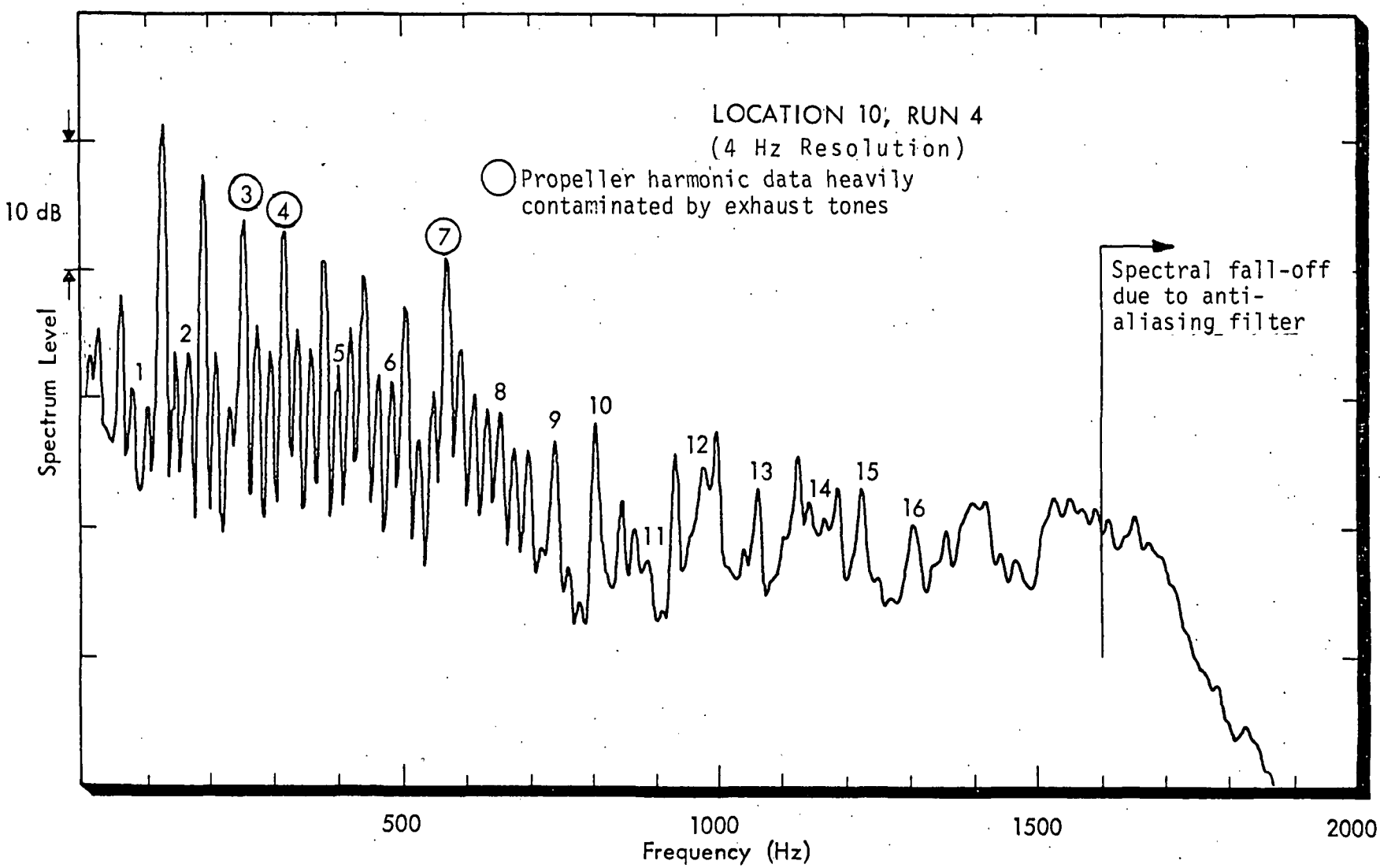

FIGURE 7. NARROWBAND PRESSURE SPECTRUM AT LOCATION 10, TEST RUN 4

by exhaust noise harmonics. These exhaust tones sometimes fall very close to the frequencies of propeller blade passage harmonics and, hence, contaminate the propeller noise level measurements. This is particularly true at Locations 9 and 10 where most of the harmonics are probably contaminated somewhat and the 3rd, 4th, and 7th harmonics appear to be contaminated heavily, as seen in Figure 7.

In an effort to suppress this problem, the data for the runs of interest (2,4,5, and 7) were reanalyzed using a resolution of B_e = 2 Hz, as opposed to 4 Hz. The results are presented in Appendix A (Table A-13 through A-16). The overall values of the significant blade passage harmonics determined with the 2 Hz resolution are summarized in comparison to the 4 Hz resolved data in Table 4. Note that the overall levels for the two analyses are similar at all locations except 9 and 10 where the 2 Hz resolved levels are

TABLE 4

Overall Values of Propeller Blade Passage Tones (2 Hz Resolution)

Location (Fig. 1)	Test Run 7 (1700 rpm)		Test Run 5 (2100 rpm)		Test Run 2 (2400 rpm)		Test Run 4 (2600 rpm)	
	4 Hz	2 Hz	4 Hz	2 Hz	4 Hz	2 Hz	4 Hz	2 Hz
1	124.0	123.3	129.3	128.4	131.9	130.9	133.1	132.9
2	128.2	127.0	133.2	132.2	135.8	134.8	137.3	137.1
3	127.2	126.3	132.3	131.2	135.6	134.0	137.4	136.3
4	128.1	127.1	132.9	131.7	136.5	135.2	138.1	137.2
5	123.6	123.2	129.1	128.5	132.6	131.8	134.0	133.9
6	129.7	128.6	125.2	123.9	128.9	127.2	130.4	129.9
7	124.9	124.2	130.8	129.6	133.0	131.5	134.2	133.2
8	121.0	119.8	126.7	124.8	129.6	127.5	131.9	129.9
9*	117.9	113.7	125.4	116.8	129.6	119.5	132.1	123.4
10*	118.2	112.2	124.6	115.1	**	**	130.8	123.5

*Levels may be too high due to reflections off the wing.
**Data suspect due to auto-ranging of the data acquisition equipment.

substantially lower. Referring to the appropriate data in Appendix A, this evolves from a dramatic reduction in the levels of the 3rd, 4th, and 7th harmonics in the 2 Hz analysis due to a better separation of the propeller and exhaust tones at these frequencies. However, even with the 2 Hz resolution, it should be remembered that the data for Locations 9 and 10 are still probably too high due to reflections off the wing which are not present in the data at the other locations.

Comparison of the measured noise levels with available prediction methods does not come within the scope of this investigation. However, it is interesting, and relatively simple, to consider the harmonic noise levels relative to the overall propeller noise levels since such an analysis requires no information regarding the propeller performance except for tip rotational Mach number. Measured data presented in this form are shown in Figures 8 and 9 for Microphones 1 and 5 and for the two extremes of the test rpm range. The test data are compared with values of the relative harmonic level obtained by means of the two prediction methods in [4] and [5]. The prediction methods call for the propeller tip helical Mach number, but as the test airplane had zero forward speed, the helical and rotational Mach numbers are the same. For an engine rpm of 2600, the tip rotational Mach number is 0.594 (Figure 8); and for 1700 rpm, the Mach number is 0.395 (Figure 9).

Figures 8 and 9 show that at the lower Mach number the predicted harmonic levels decrease more rapidly than do the measured values, as harmonic order increases from 1 to 5. At the higher Mach number, the measured and predicted harmonic levels decrease at about the same rate. For harmonic orders greater than 5, the prediction procedures diverge, one predicting harmonic levels which decrease more rapidly than do the test data, and the other less rapidly.

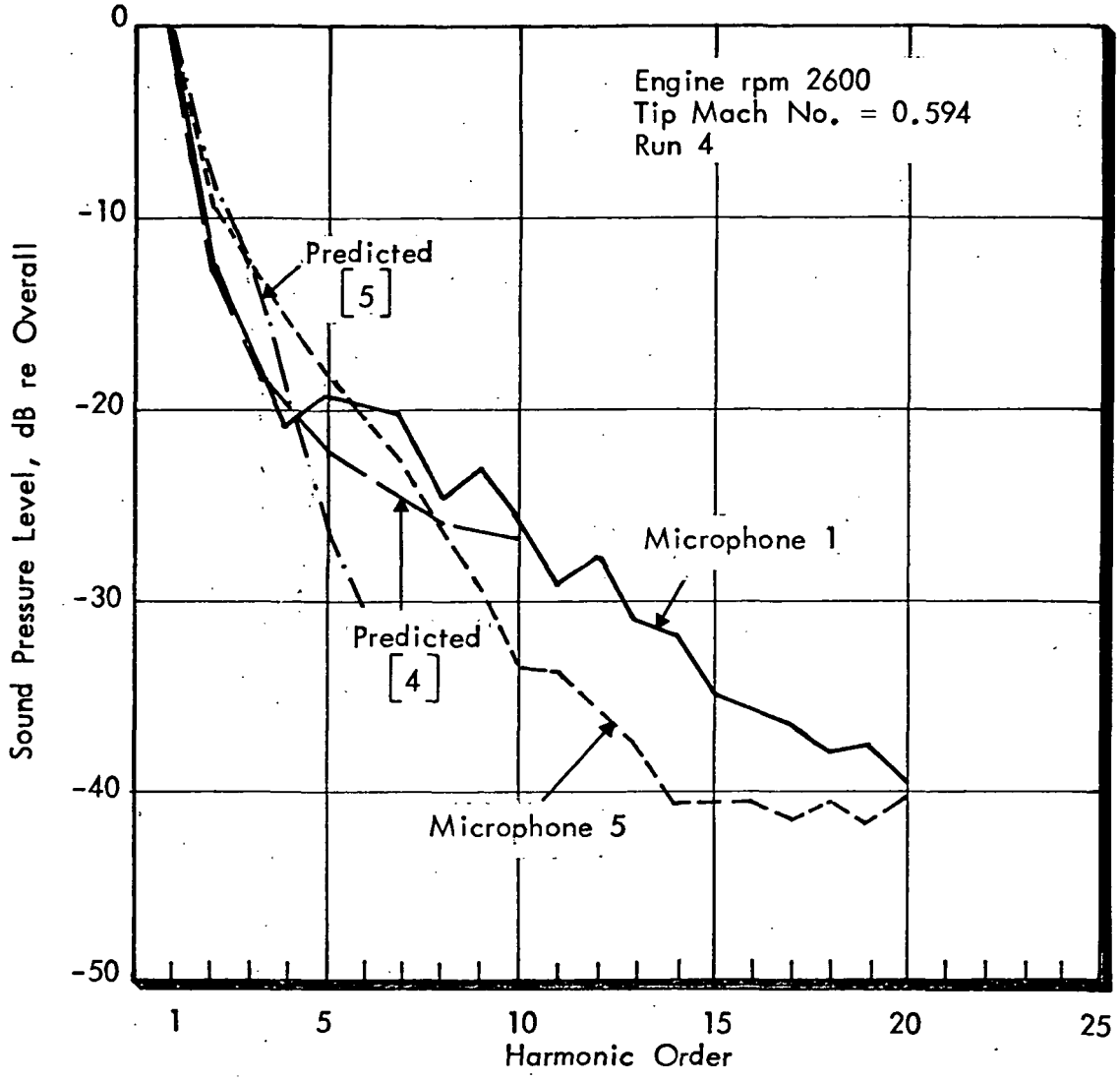

FIGURE 8. COMPARISON OF MEASURED AND PREDICTED PROPELLER HARMONIC LEVELS, TEST RUN 4

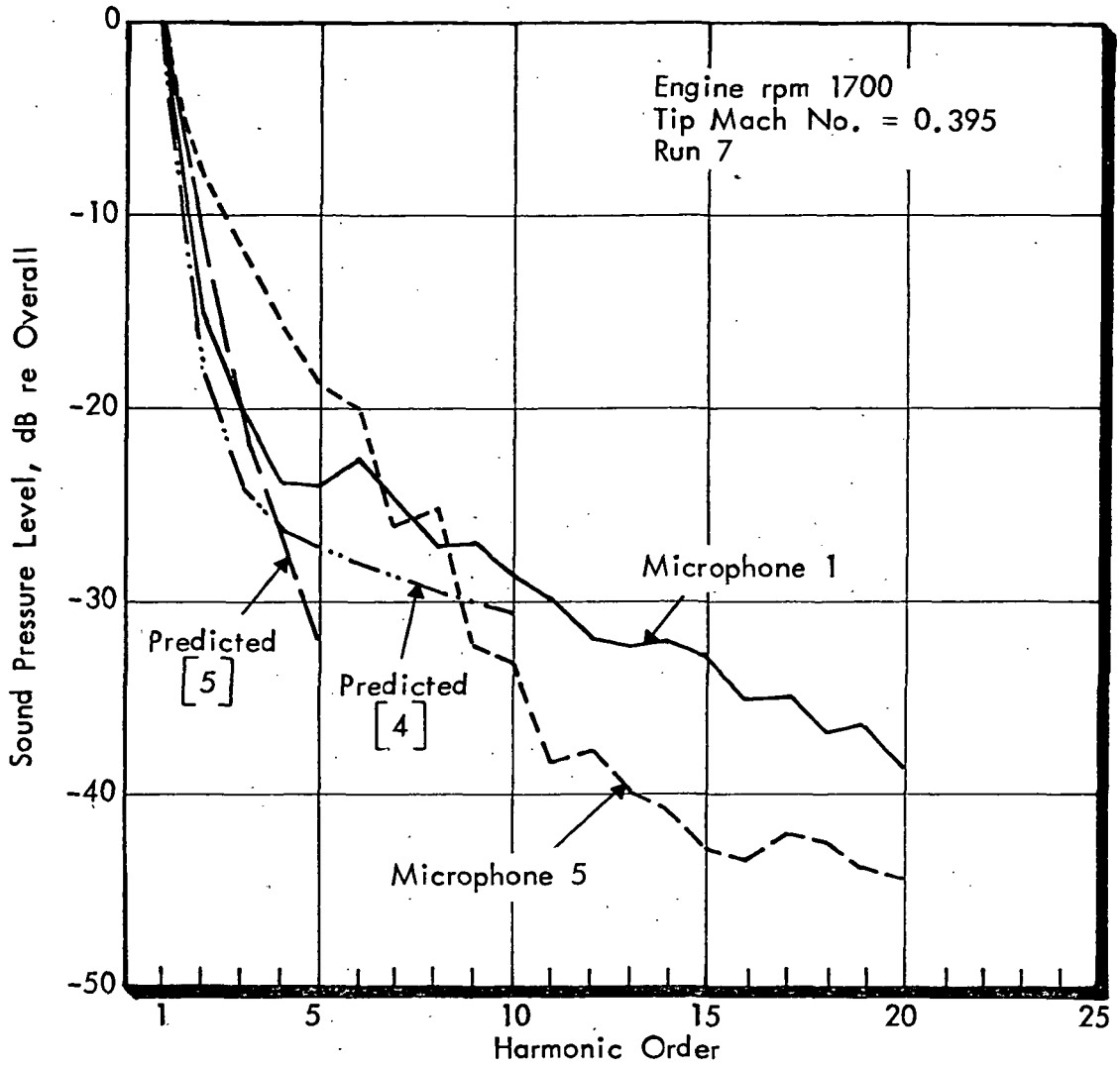

FIGURE 9. COMPARISON OF MEASURED AND PREDICTED PROPELLER HARMONIC LEVELS, TEST RUN 7

4.2 Stability of Propeller Blade Passage Tones

The results of the probability density analyses of the individual propeller blade passage tones were converted to sine wave to noise power ratios (σ_s^2/σ_n^2) using Figure 4. These ratios are summarized in Table 5. Typical probability density data for Test Run 4, Location No. 6, are presented in Appendix B.

Referring to the results in Table 5, the following general trends are observed from the data.

a) The fundamental propeller blade passage tones are relatively good sine waves at all locations and for all tests except at the two aft measurement locations (Nos. 9 and 10) and inside the fuselage (No. 11).

b) The sinusoidal character of the tones diminishes rapidly with harmonic order, producing a sine wave to noise ratio at all locations of less than unity at or prior to the fifth harmonic.

c) The most stable harmonics at higher frequencies appear to occur at Location No. 6 (See Appendix B).

These results are broadly typical of similar data for the tones generated by large jet engine fans [3]. They demonstrate clearly that the propeller blade passage pressures are not fully deterministic, but in fact have a stochastic character due to turbulence in the inflow to the propellers.

4.3 Relative Phase of Propeller Blade Passage Tones

The results of the tone stability studies in Section 4.2 suggest that the phase of the higher order propeller blade passage harmonics

TABLE 5. SINE WAVE TO NOISE RATIOS OF PROPELLER BLADE PASSAGE TONES

Test Run (Table 1)	Harmonic Number	Sine Wave to Noise Power Level by Location No. (Figure 1)										
		1	2	3	4	5	6	7	8	9	10	11
2	1	150	>500	60	60	150	170	90	40	<1	8	*
4	1	300	500	80	90	290	260	140	50	4	3	*
	2	30	120	110	140	100	60	30	12	***	***	*
	3	2	12	16	13	17	3	3	2	***	***	*
	4	<1	<1	<1	2	2	4	<1	<1	***	***	*
5	1	260	350	180	400	450	160	90	100	2	<1	90
	2	**	**	**	**	**	20	**	**	**	**	**
	3	**	**	**	**	**	7	**	**	**	**	**
7	1	240	450	200	140	240	130	130	40	3	2	10
	2	**	**	**	**	**	30	**	**	**	**	**
	3	**	**	**	**	**	3	**	**	**	**	**
	4	**	**	**	**	**	2	**	**	**	**	**

*Probability density functions revealed features typical of "beat" phenomenon (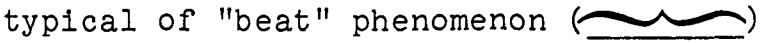)

**Not measured

***Data above the first harmonic distorted by the presence of intense engine exhaust tones

relative to the fundamental cannot be very stable. The relative phase studies confirm this expectation, as is seen from the phase data summarized in Table 6. Shown in this table are the relative phases computed from four separate segments of each record of interest plus the mean and standard deviation of the four calculations. It is clear from the standard deviation results that the most stable phase data were provided by Test Run 4 (2600 rpm). However, even for this case, the scatter in the phase data is relatively large.

These results come as no surprise when a sample time history of the propeller blade passage pressure at a given location is examined. A typical time history is shown in Figure 10. Note that the details of the time history change dramatically from one cycle to the next. Some of this variation, of course, is reflected in the random fluctuations of the Fourier component magnitudes, as evaluated in Section 4.2; but much of it also represents random variations in the phasing of the Fourier components.

4.4 Spatial Correlation

As indicated in Section 3.4, the spatial correlation of the propeller pressure field was reduced in terms of coherence and phase angle spectra for selected pairs of microphones. This format was used as it presents the data in a manner which is readily usable for describing pressure forcing fields in the calculation of structural response and noise transmission.

Sample coherence and phase angle spectra obtained for the pressure field on the Aero Commander are presented in Appendix C. The appendix also contains tabulated coherence and phase angle data for the noise components at the propeller blade passage frequency and higher order harmonics.

TABLE 6. PHASE OF PROPELLER BLADE PASSAGE TONES RELATIVE TO FUNDAMENTAL

Test Run (Table 1)	Harmonic Number	Phase Relative to Fundamental in Degrees by Location No. (Figure 1)																	
		Location No. 1						Location No. 6						Location No. 8					
		1	2	3	4	Ave.	S.D.	1	2	3	4	Ave.	S.D.	1	2	3	4	Ave.	S.D.
2	2	-44	94	95	124	67	75	-18	109	-28	122	46	80	326	278	280	306	298	23
	3	139	89	287	280	199	100	-13	49	-32	78	20	52	174	264	204	80	180	77
	4	368	347	161	173	262	110	353	339	128	224	261	106	331	331	402	341	351	34
	5	279	240	370	418	327	82	- 9	91	115	-	66	66	316	388	401	234	335	77
4	2	200	247	260	277	246	33	130	92	119	144	121	22	90	86	28	58	66	29
	3	103	157	175	170	151	33	296	228	276	305	276	34	212	177	53	158	150	68
	4	255	161	145	176	184	49	81	-28	49	96	50	55	234	219	297	369	280	68
	5	93	207	167	231	174	60	240	78	202	262	196	82	116	381	190	220	227	112
	6	249	227	70	247	198	86	31			57	44	-						
5	2	35	146	35	16	58	59	155	-15	42	82	66	71	67	1	- 9	16	19	34
	3	269	148	243	257	229	55	293	160	282	366	275	85	282	348	217	169	254	78
	4	208	353	309	95	241	115	95	-36	-16	105	37	73	275	201	356	223	264	69
	5	31	147	197	139	128	70	453	313	227	-	331	114	52	75	-	-	64	-
7	2	129	280	254	297	240	76	60	68	28	-69	22	63	239	253	82	64	159	100
	3	62	- 3	24	3	22	29	309	314	239	382	311	58	-38	- 5	25	135	29	75
	4	430	323	338	317	352	53	167	212	89	314	196	94	436	347	246	338	342	77
	5	188	180	321	172	215	71	-22	21	190	54	61	92	352	300	251	192	274	68
	6	- 6	188	37	173	98	97	-	-	-	-	-	-	-	-	-	-	-	-

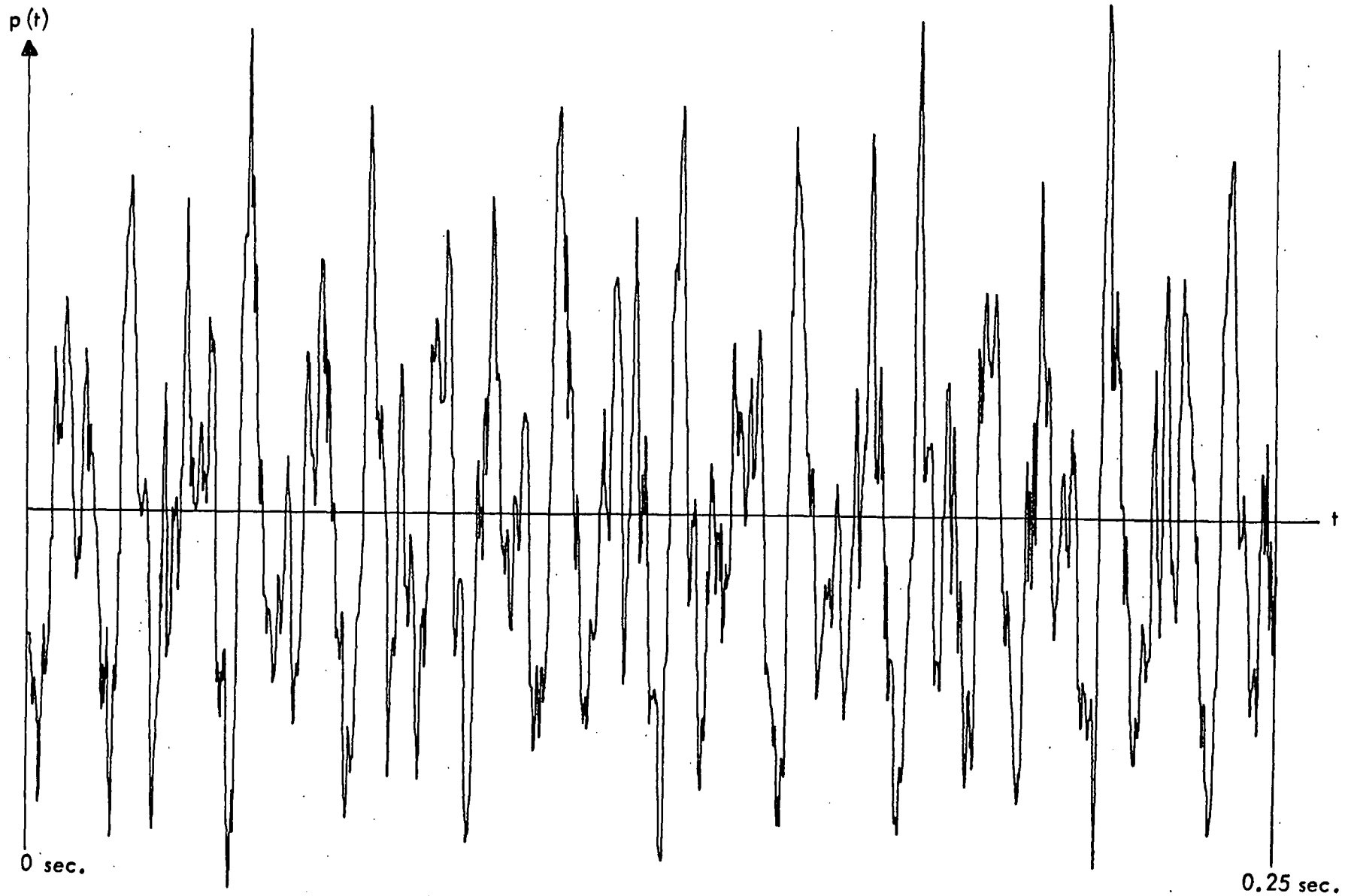

FIGURE 10. SAMPLE TIME HISTORY OF PROPELLER BLADE PASSAGE PRESSURE - TEST RUN 4, LOCATION NO. 6

The purpose of this section is to present a preliminary analysis of the coherence and phase information. The coherence data are considered in terms of the spatial decay over the fuselage, and the phase angle is interpreted in terms of the pressure field trace velocity. The analysis is preliminary because within the scope of the present investigation it was not possible to study the phenomena in great detail. Instead, an elementary analysis is presented on the assumption that further studies will provide a more comprehensive understanding of the phenomena involved. For example, factors such as reflections from the ground and wing surfaces, local airflow velocities induced by the propeller, the relative contributions from acoustic near and far fields, and the influence of the propeller potential field are either omitted from the present discussion or are introduced in a simplified manner.

4.4.1 Phase Analysis

The phase angle can be interpreted in terms of a trace or phase velocity, as indicated in Equation (2) of Section 3.4, when the pressure field is convected. This interpretation has been used in describing aerodynamic pressure fields associated with turbulent boundary layers and acoustic pressure fields generated by jet exhausts. Thus it is appropriate to apply the same approach to the measured propeller near field, which is probably a combination of aerodynamic and acoustic components.

The first step in the analysis is to express the phase angle $\phi(f)$ in terms of a continuously increasing or decreasing angle rather than an angle which varies only within the range $\pm\pi$. This conversion requires some judgment regarding the addition or subtraction of multiples of 2π to the measured phase angles given in Appendix C. An example of this computational procedure is given

in Table 7 for Microphones 9 and 10 and Test Run 2. The example shows several harmonic orders where 2π or 4π is subtracted from the measured phase angle. The example also shows two instances where there is some doubt as to the correct multiple of 2π to be subtracted from the data. The uncertainty arises because the phase angle values deviate from the general trend. In general, these deviations occur for harmonic orders with low values of coherence. Furthermore, on simple ray analysis there is also evidence that at the frequencies of concern there is destructive interference of sound waves due to reflections from the wing lower surface or the ground.

TABLE 7

Sample Phase Angle Analysis

Microphones 9 and 10 - Run 2

Harmonic Order	Frequency Hz	Coherence	Phase (degrees)	Phase (rad/π)	Multiples of 2π	Phase (radians/π)
1	76	.31	- 14	-.08	0	- .08
2	152	.11	-105	-.58	0	- .58
3	227	.41	168	.93	-2π	-1.07
4	303	.98	128	.71	-2π	-1.29
5	379	.34	-176	-.98	-0 or 2π	- .98 or -2.98
6	455	.43	116	.65	-2π or 4π	-1.35 or -3.35
7	531	.70	-119	-.66	-2π	-2.66
8	606	.48	121	.67	-4π	-3.33
9	682	.24	12	.07	-4π	-3.93
10	758	.33	- 21	-.12	-4π	-4.12

In order to minimize the influence of deviations in the phase angle data, no phase data have been included for harmonic orders where the coherence is less than 0.05; and phase data associated with coherence values less than 0.15 have been treated as having reduced statistical confidence. Estimates of pressure field trace velocity have been made mainly on the basis of data points where the coherence was greater than 0.15.

Consider first convection in the circumferential direction, as recorded by Microphones 3 to 6. Figure 11 shows, as an example, phase angle-frequency data for Microphone pairs 4-5 and two propeller rotational speeds. It is seen that the data points closely follow straight-line relationships. The empirical curves shown in the figures were fitted to the data using regression analysis, with each curve being constructed to pass through the origin of the axes. These and other similar curves were used to estimate trace velocities for the pressure fields, using Equation (2). A straight-line relationship indicates that the velocity is independent of frequency.

Circumferential trace velocities estimated for five microphone pairs are listed in the upper portion of Table 8, where it is seen that there is a general trend of increasing trace velocity with propeller rotational speed. It should be emphasized, however, that there has been no attempt made to establish an empirical relationship between trace velocity and propeller rpm, nor has the trend been checked for statistical significance.

As the microphone locations associated with the circumferential direction measurements are located in the plane of rotation of the propeller and are close to the blade tip, a crude engineering model is proposed whereby the pressure field on Microphones 3 to 6

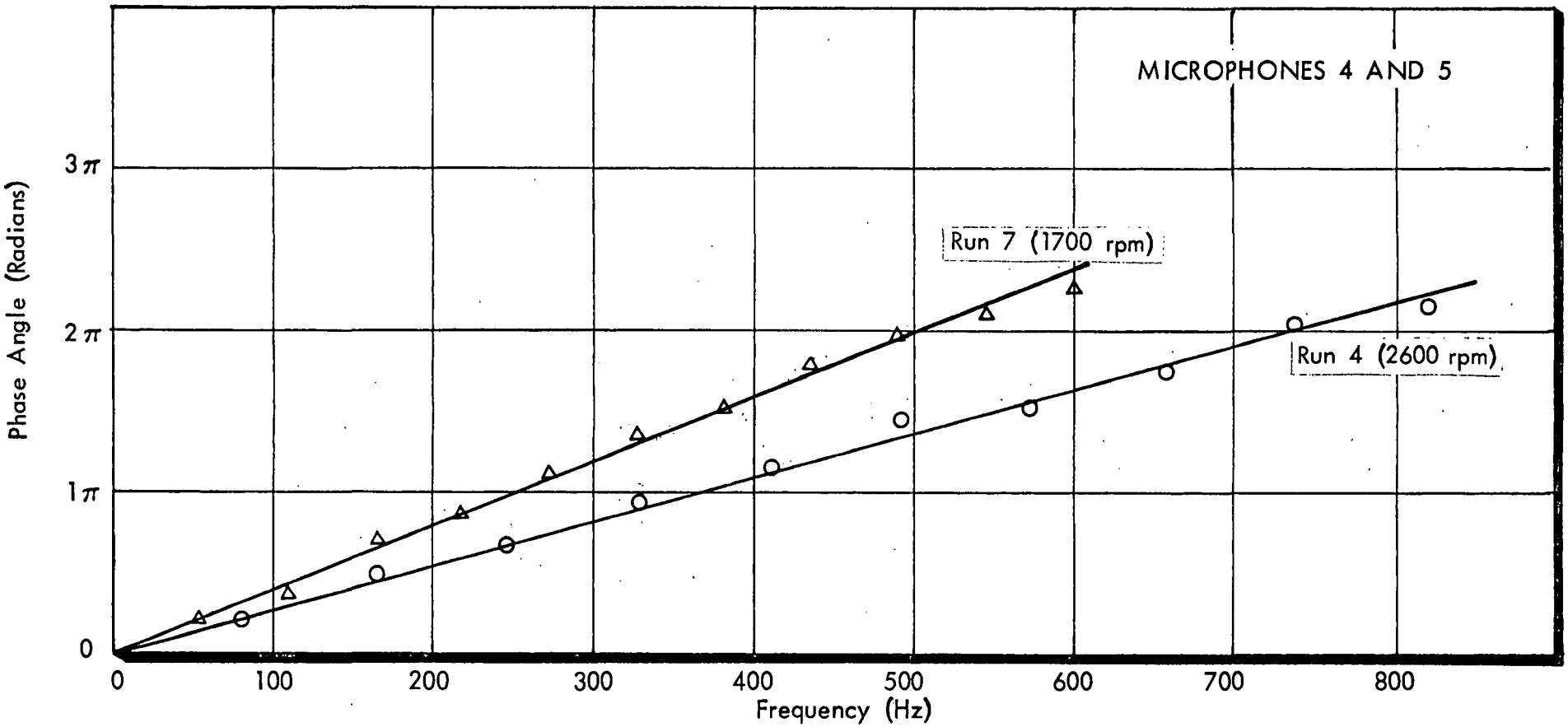

FIGURE 11. VARIATION OF CROSS-SPECTRUM PHASE ANGLE WITH FREQUENCY FOR PROPELLER NOISE COMPONENTS (Microphones 4 and 5)

Table 8

Estimated Trace Velocities

Test Run Engine RPM	4 2600	2 2400	5 2100	7 1700	Average
Microphone Pair	Trace Velocity* (m/s)				
Circumferential					
4 - 3	217	216	180	160	-
5 - 3	217	203	176	150	-
5 - 4	209	193	171	143	-
6 - 4	246	239	207	172	-
6 - 5	326	317	244	201	-
Longitudinal					
5 - 2	-97	-94	-79	-78	-
5 - 1	-153	-153	-132	-120	-
2 - 1	-	-	-	-	-608
5 - 7	98	95	80	60	-
5 - 8	129	131	118	109	-
5 - 9	-	-	-	-	334
5 - 10	-	-	-	-	369
7 - 8	-	-	-	-	445
7 - 9	-	-	-	-	413
7 - 10	-	-	-	-	394
8 - 9	-	-	-	-	417
8 - 10	-	-	-	-	391
9 - 10	-	-	-	-	353

*Positive sign indicates convection in rearward or upward directions.

is dominated by a potential pressure field which rotates with the propeller as a "rigid body." The trace velocities associated with such a model can be easily calculated by

$$U_c' = \frac{6\Omega d}{\alpha} \qquad (4)$$

where Ω is the propeller rpm and α is the angle subtended at the propeller center by the distance d between the pair of microphones. U_c' can then be compared with the measured values U_c in Table 8. The ratio U_c/U_c', of measured to calculated trace velocity, is given in Table 9, where the values of the ratio are seen to be close to unity. This result suggests that the hypothesis of the rotating aerodynamic pressure field is a possible physical explanation of the observed phenomenon.

TABLE 9

Ratio of Measured Circumferential Trace Velocity to Trace Velocity Based on Simple Pressure Field Model

Test Run	4	2	5	7	Average
Microphone Pair	Velocity Ratio* U_c/U_c'				
4-3	0.97	1.05	0.99	1.07	1.02
5-3	0.95	0.96	0.95	0.99	0.96
4-5	0.90	0.90	0.90	0.92	0.90
4-6	0.99	1.04	1.02	1.04	1.02
5-6	1.22	1.30	1.13	1.14	1.20

Velocity Ratio = (Measured Circumferential Trace Velocity from Table 7) ÷ Trace Velocity Calculated for "rigid body" Pressure Field) [See Equations (2) and (4)]

A similar analysis has been followed for the longitudinal direction, although the interpretation is somewhat different. The results show a more complicated pattern than do the circumferential data, as can be seen from a study of the example phase angle data in Figures 12-14. These figures again show the variation of pressure field phase angle with frequency for the propeller harmonics. Figure 12 contains data for Microphone pair 5-8, where one microphone, 5, is in the plane of rotation of the propeller; Figure 13 contains data for the Microphone pair 1-2 ahead of the plane of rotation; and Figure 14 presents results for Microphone pair 9-10 which is well aft of the plane of rotation.

These results show several different characteristics. The data in Figure 13 show a phase angle which is essentially independent of frequency at low frequencies; but above 200 Hz, ϕ decreases as frequency increases. The fitted regression line at high frequencies gives a highly supersonic trace velocity in the forward direction. The linear regression line fitted to data in Figure 14 gives a slightly supersonic velocity in the aft direction. There is, however, a certain amount of data scatter about the empirical curve; and this scatter is believed to be associated with acoustic reflections from the wing and ground. Finally, the data with Microphone 5 as reference (Figure 12) show a low frequency region where the phase angle is independent of frequency, followed by a region where the phase angle frequency relationship results in a subsonic trace velocity.

A summary of the estimated trace velocities in the longitudinal direction is given in Table 8, where it is seen that all pressure disturbances, either acoustic (supersonic trace velocity) or aerodynamic (subsonic velocity), propagate away from the plane of rotation of the propeller. The subsonic trace velocities occur

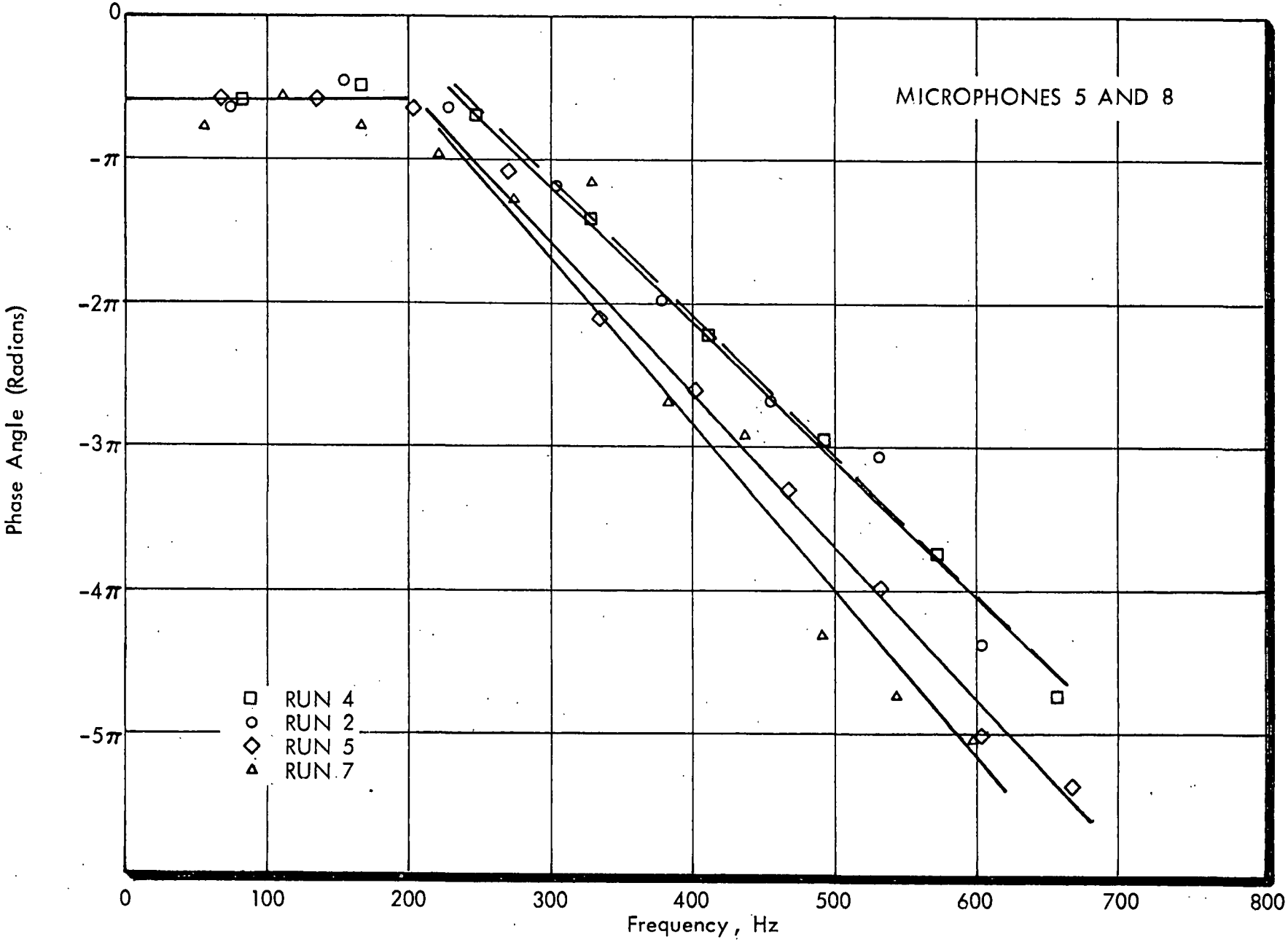

FIGURE 12. VARIATION OF CROSS-SPECTRUM PHASE ANGLE WITH FREQUENCY FOR PROPELLER NOISE COMPONENTS (Microphones 5 and 8)

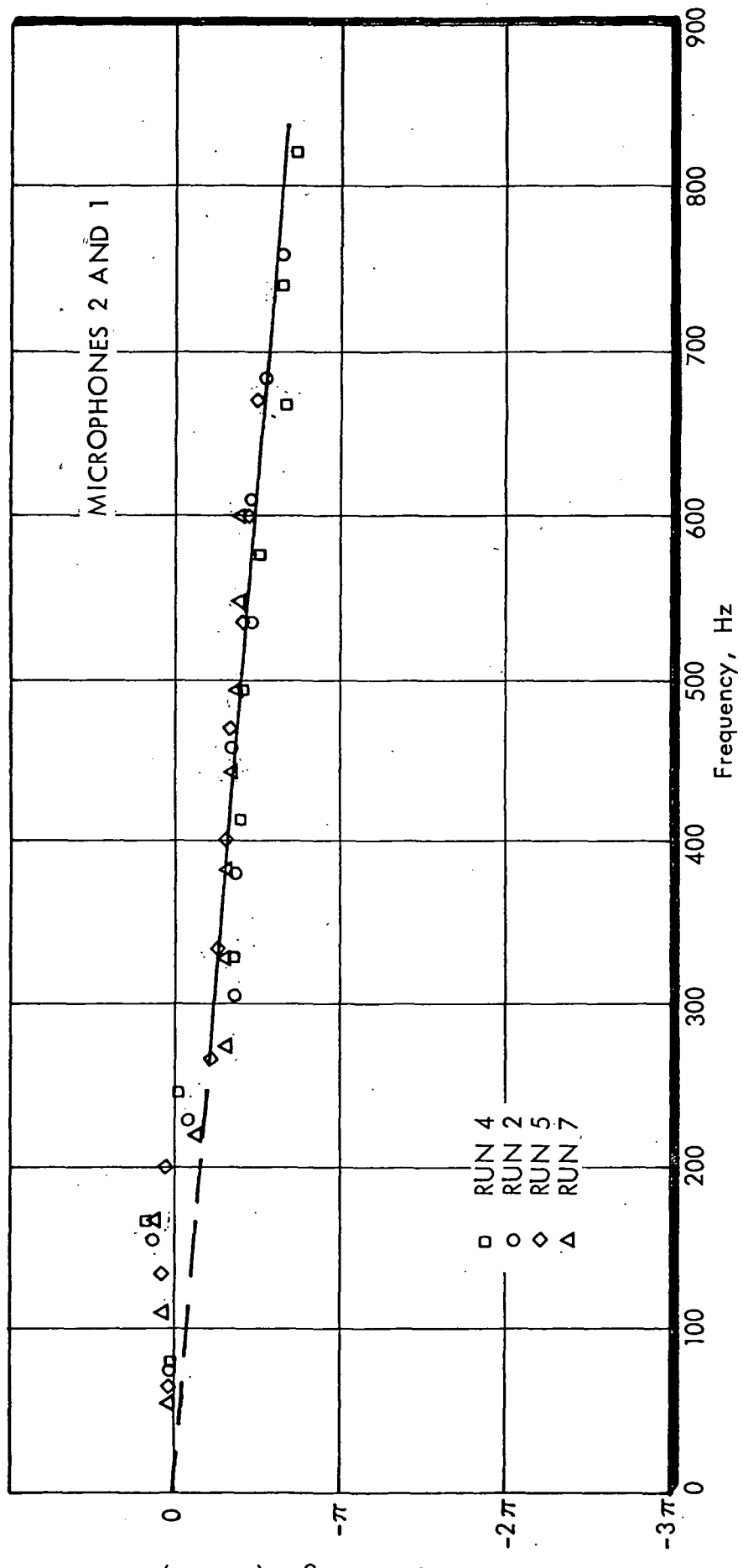

FIGURE 13. VARIATION OF CROSS-SPECTRUM PHASE ANGLE WITH FREQUENCY FOR PROPELLER NOISE COMPONENTS (Microphones 1 and 2)

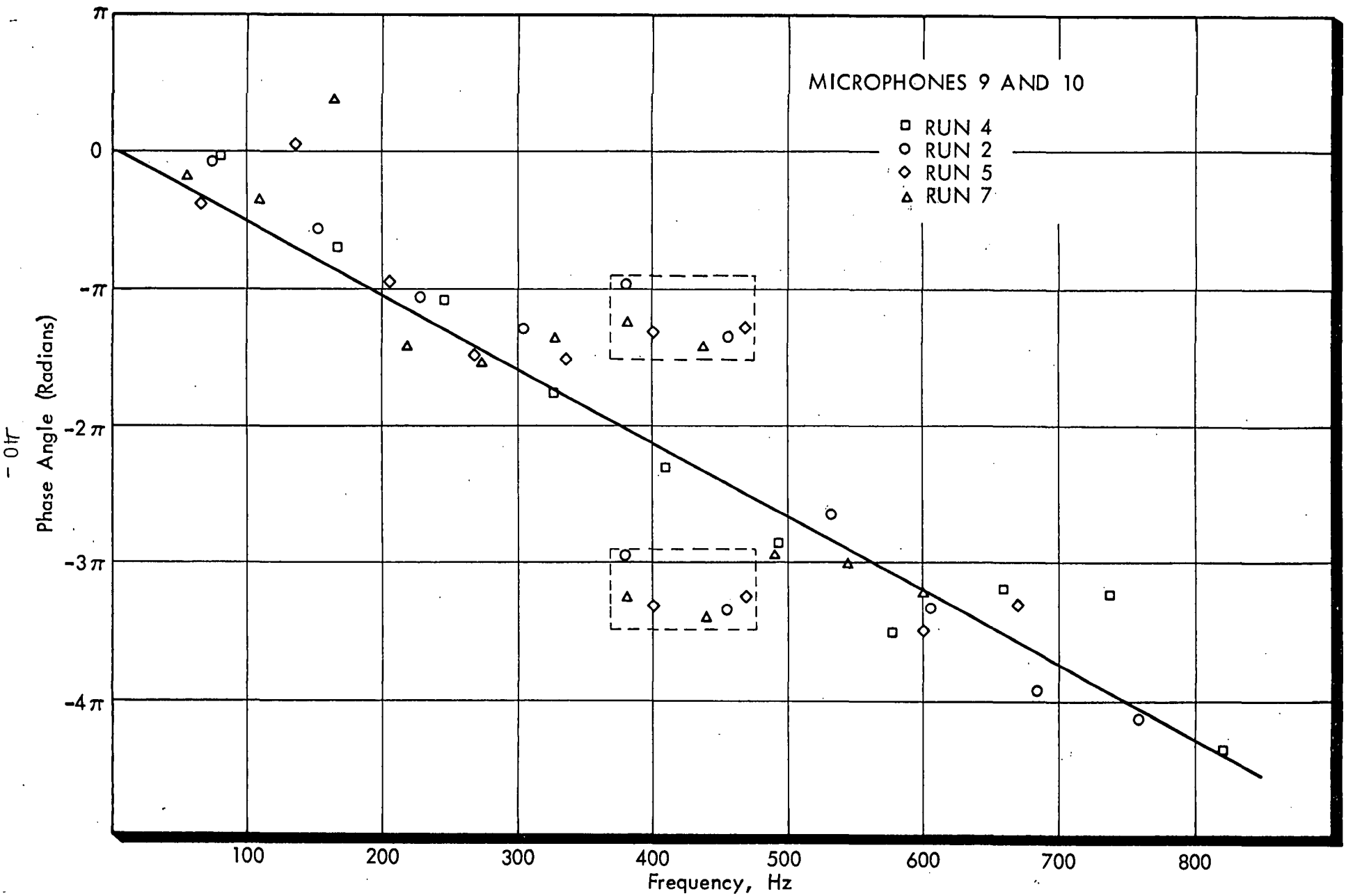

FIGURE 14. VARIATION OF CROSS-SPECTRUM PHASE ANGLE WITH FREQUENCY FOR PROPELLER NOISE COMPONENTS (MICROPHONES 9 AND 10)

when one of the microphones (specifically No. 5) lies in the plane of rotation of the propeller. It is possible that near-field components dominate these results. The frequency-independent phase angle at low frequencies may also be associated with near-field or aerodynamic factors, the pressure field rotating with the blades of the propeller. There is some indication in the data that the value of the subsonic trace velocity is dependent on propeller rotational speed, but the supersonic trace velocity is essentially independent of propeller rpm.

Whenever a supersonic trace velocity is measured, it is possible to use a simplified ray analysis to locate an effective source. To illustrate this method, it can be assumed that the trace velocity U_c is given by

$$U_c = c/\cos\ \theta \qquad (5)$$

where c is the speed of sound and θ is the angle of incidence of the sound wave on the structure. The effective source locations are then determined by geometric construction as indicated in Figure 15. In constructing Figure 15, the effect of local airflow velocities was neglected. Furthermore, the construction was made assuming a two-dimensional rather than a three-dimensional system. It is interesting to note, however, that the effective source locations lie between 30 percent and 75 percent of the propeller radius, on the fuselage side of the propeller center. Also, with some exceptions, the acoustic center moves towards the center of the propeller as the observation location moves away from the plane of rotation. Thus the results are physically reasonable within the constraints of the simplifying assumptions.

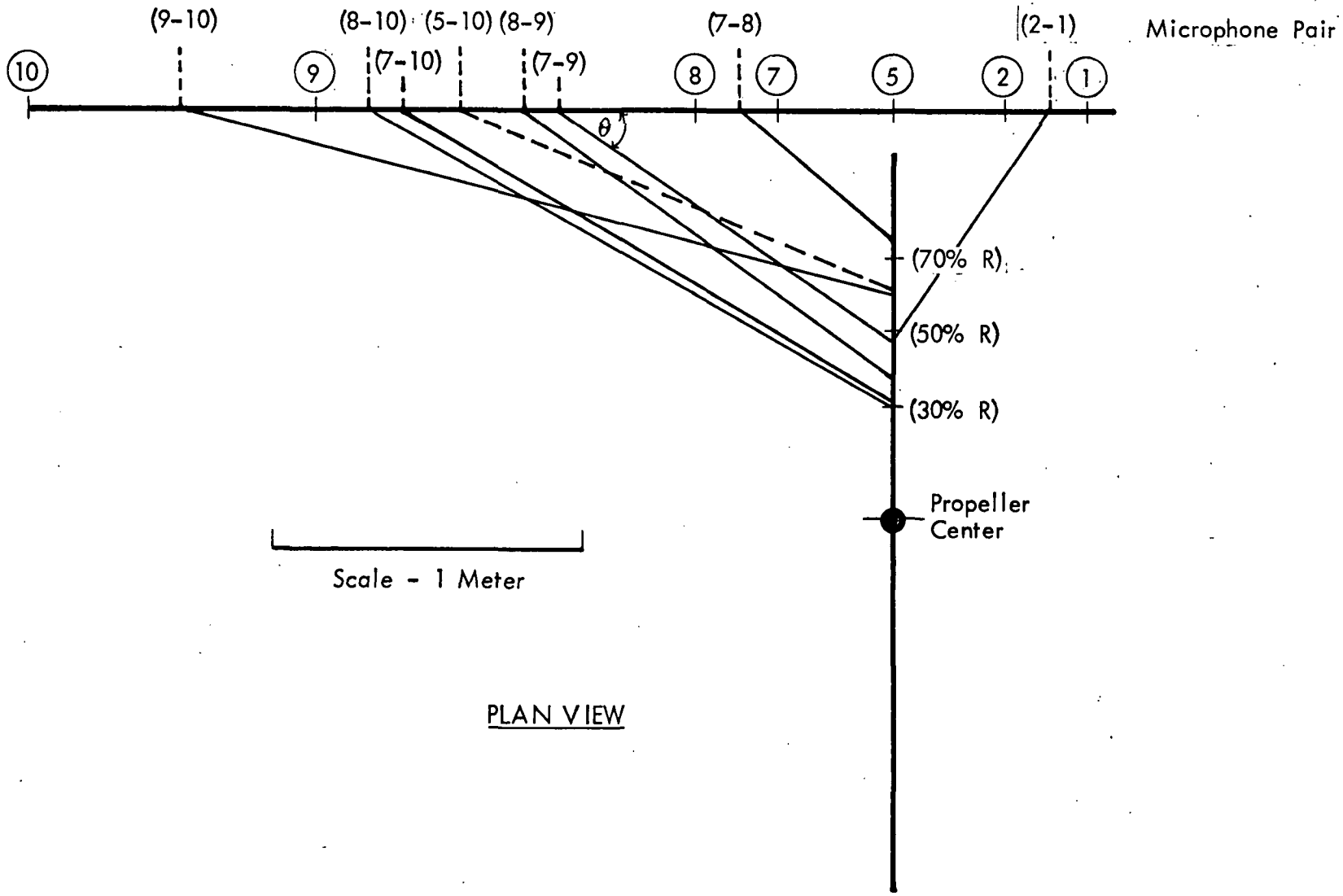

FIGURE 15. EFFECTIVE SOURCE LOCATION BASED ON TRACE VELOCITY ANALYSIS

4.4.2 Coherence

In many cases of aerodynamic or acoustic forcing fields on aerospace structures, it is possible to normalize the pressure coherence function in terms of the Strouhal number fd/U_c where d is a separation distance and U_c a trace velocity. For the present case, the pressure field is strongly inhomogeneous, and a data collapse using this Strouhal number may not be successful. The following discussion considers this topic.

Two sets of coherence data measured by microphones in the circumferential array are presented in Figures 16 and 17, with frequency non-dimensionalized with respect to d and U_c. For a given pair of microphones (fixed d) the data show a reasonable collapse; but this is not too significant as the variation in U_c is small for the test range of propeller rpm (see Table 8). If the data in Figures 16 and 17 are compared, it is immediately obvious that data associated with different values of d do not collapse onto a common spectrum shape.

An alternative non-dimensional system is shown in Figure 18 where the frequency is represented by the harmonic order. Although results are presented for only one propeller rpm, it is seen that the data collapse is much better than where the parameter fd/U_c is used. In this format, the coherence appears to fall off rapidly at about the 10th harmonic order

If one were to assume an exponential decay for the coherence in the form

$$\gamma^2 = e^{-n/a}$$

where n is the harmonic order and a is a decay factor, then the data in Figure 18 give a $\simeq$ 28.

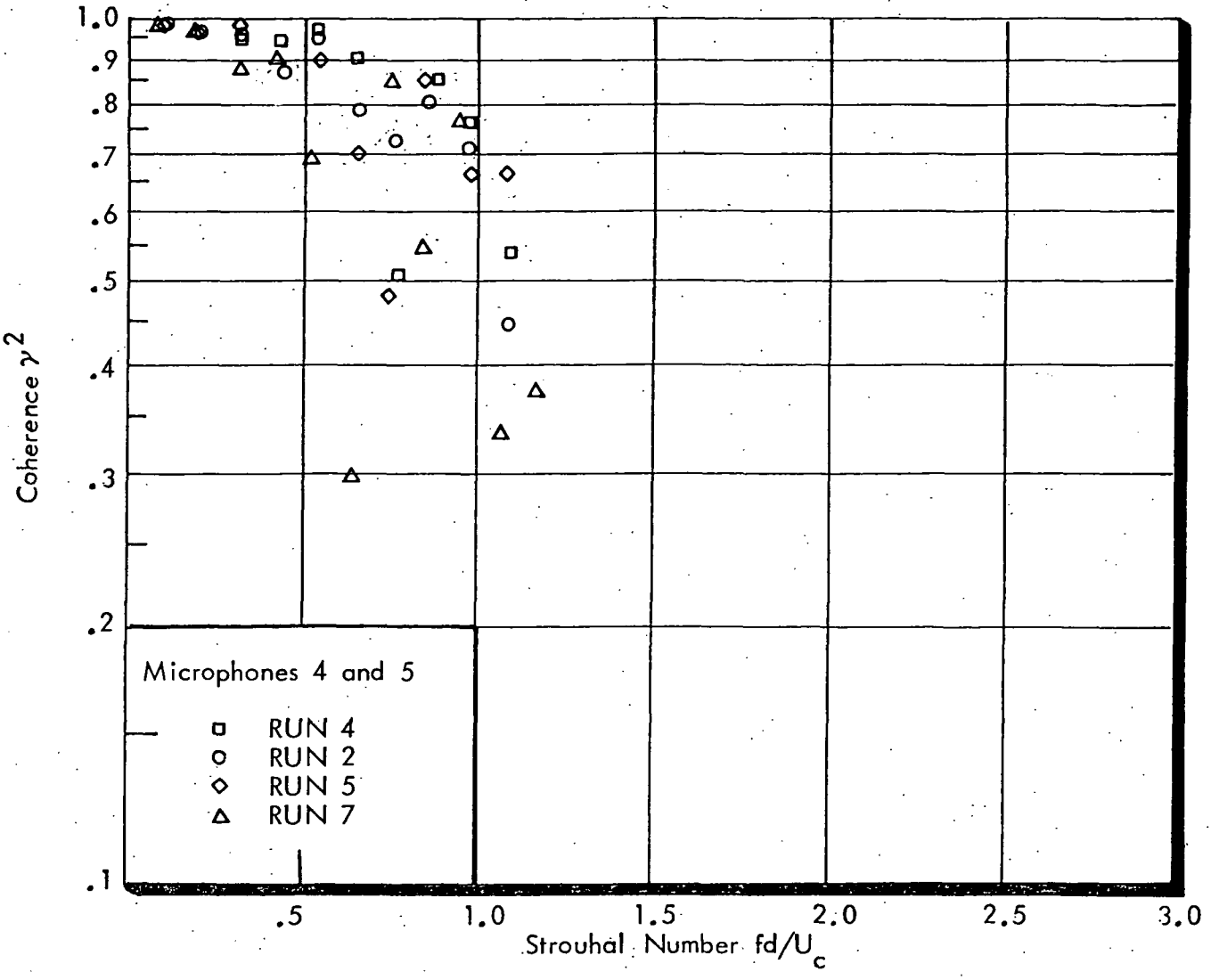

FIGURE 16. VARIATION OF COHERENCE WITH STROUHAL NUMBER FOR PROPELLER NOISE COMPONENTS (MICROPHONES 4 AND 5)

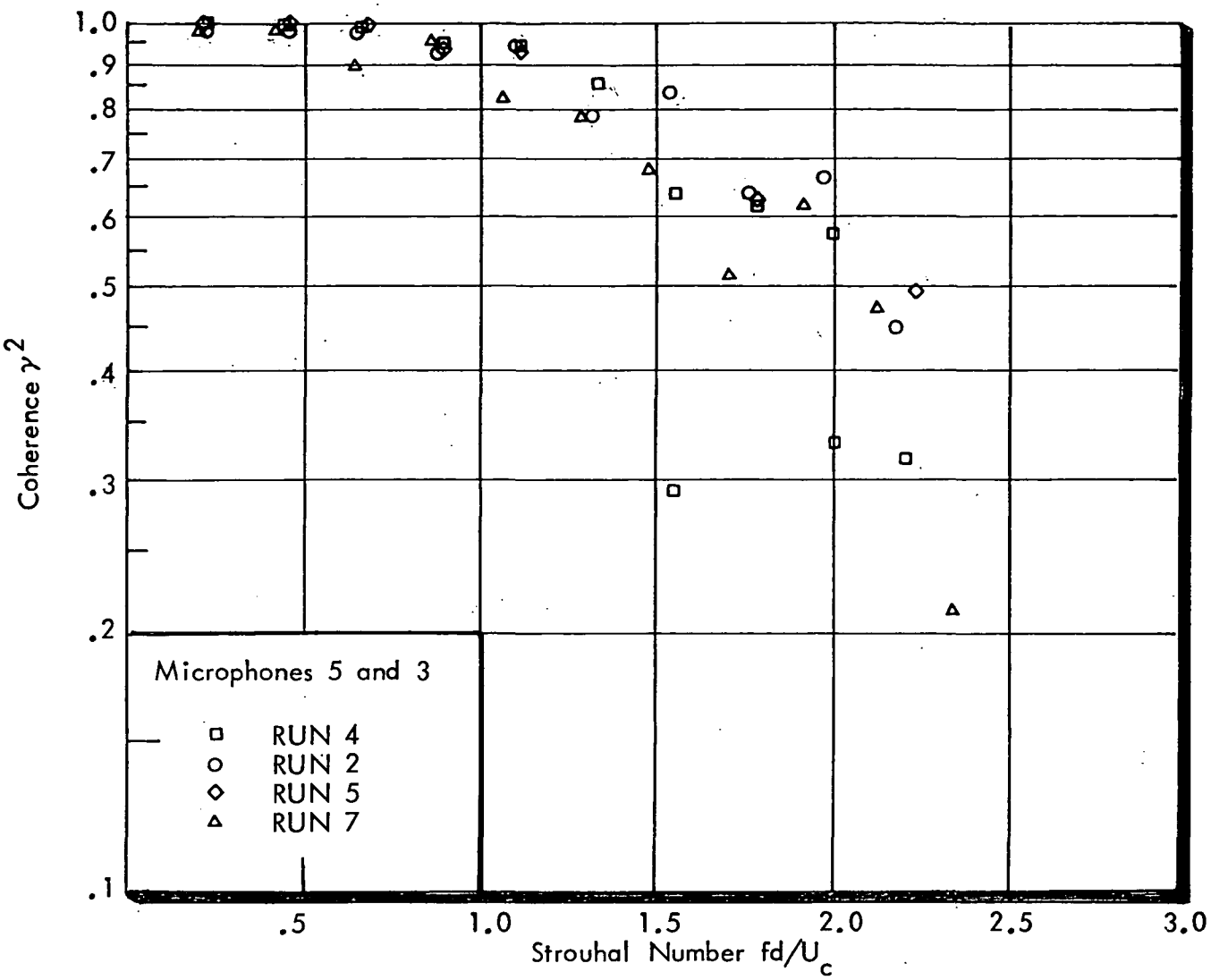

FIGURE 17. VARIATION OF COHERENCE WITH STROUHAL NUMBER FOR PROPELLER NOISE COMPONENTS (MICROPHONES 5 AND 3)

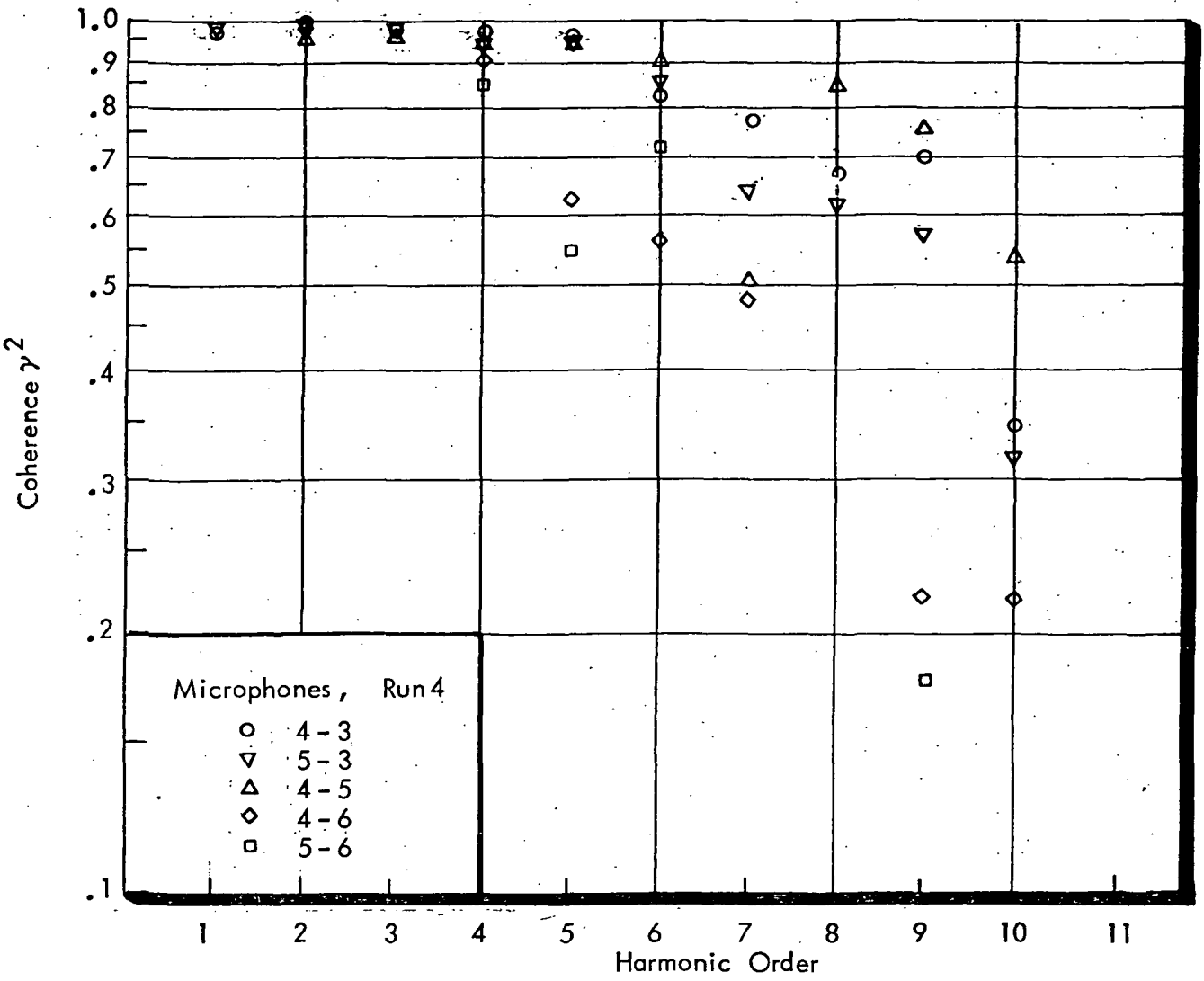

FIGURE 18. VARIATION OF COHERENCE WITH HARMONIC ORDER FOR PROPELLER NOISE COMPONENTS (MICROPHONES 3,4,5 AND 6)

When coherence spectra for the longitudinal direction are analyzed, it is again found that the Strouhal number fd/U_c provides a poor collapse of the data. The situation is, in any case, somewhat more complicated than in the circumferential direction, since the estimated trace velocities are not strictly applicable at low frequencies (as is discussed in Section 4.4.1).

Two example coherence spectra are shown in Figures 19 and 20, the data corresponding to the phase angle data presented in Figures 13 and 14, respectively. For the Microphone pair 2-1, the separation distance is small and the trace velocity high. Consequently, the range of fd/U_c is small, and the coherence remains high. In this region the pressure field is dominated by the propeller, as shown in Figure 5.

The coherence spectrum is quite different at the most rearward transducers, where there are also significant contributions from the engine exhaust (Figure 7). Figure 20 presents coherence data measured by the Microphone pair 9-10. In this case the range of values for fd/U_c is about seven times that in Figure 19. The coherence shows a wide range of values and the pattern is very irregular showing no particular relationship with Strouhal number. Even when plotted in terms of harmonic order, there is no well-defined relationship. In this structural region it is anticipated that reflections from the ground and structure will influence the data. Other factors include the effect of the aerodynamic wake from the propellers and the engine exhaust noise.

The third set of data considered is that associated with microphone pairs in the longitudinal array where one microphone lies in the plane of rotation of the propeller. For most of these cases, Table 8 shows that the mean trace velocity is subsonic, indicating

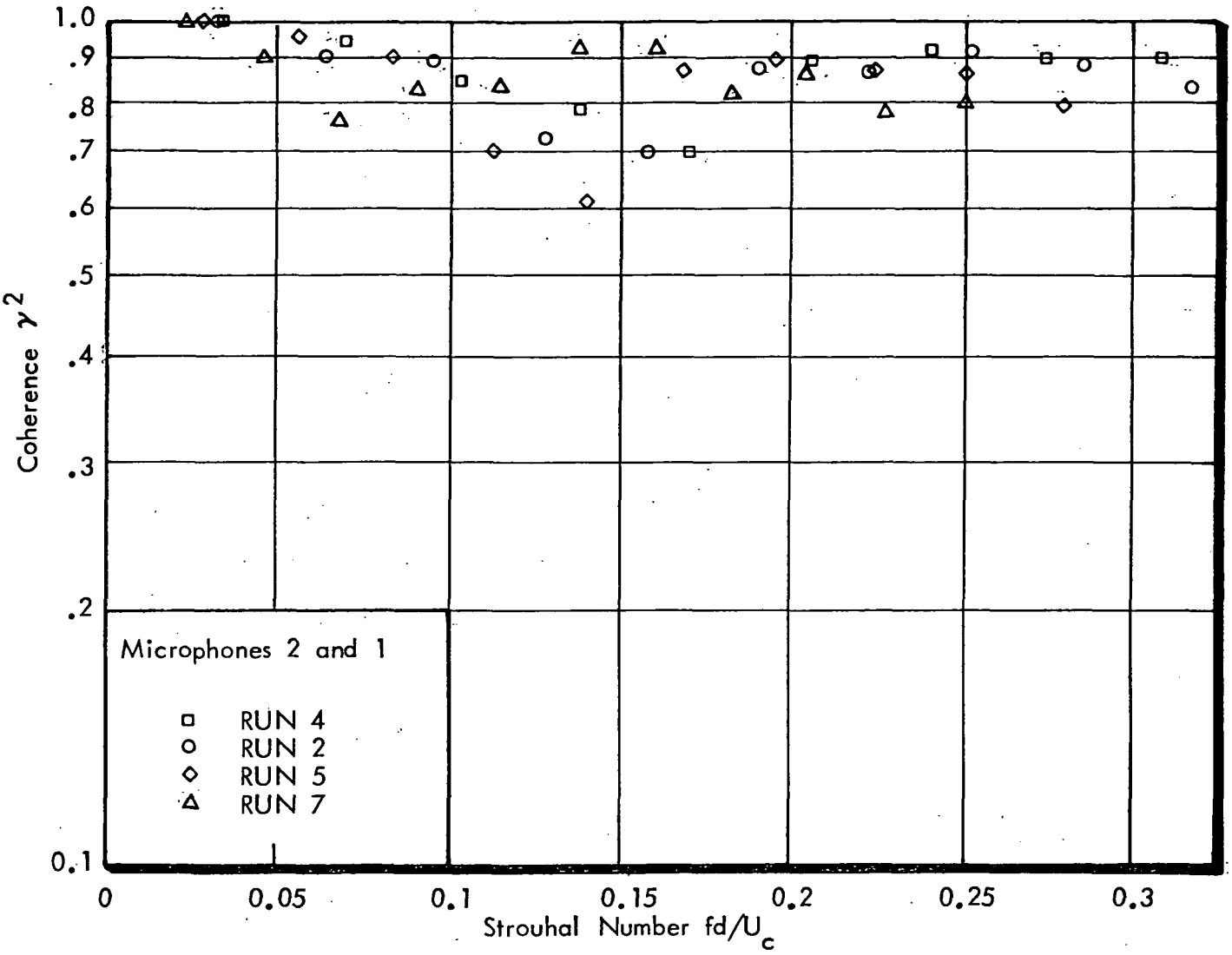

FIGURE 19. VARIATION OF COHERENCE WITH STROUHAL NUMBER FOR PROPELLER NOISE COMPONENTS (MICROPHONES 2 AND 1)

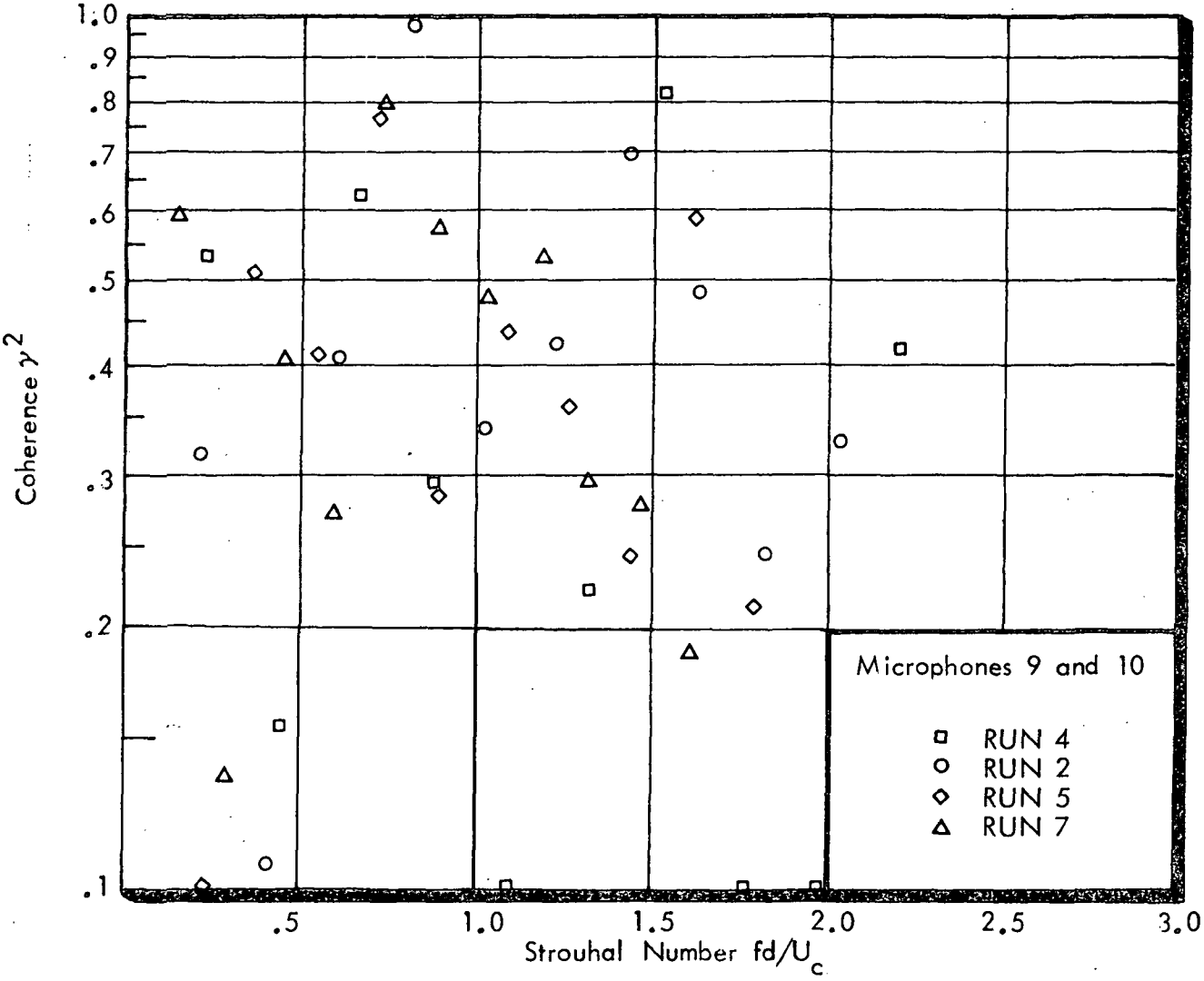

FIGURE 20. VARIATION OF COHERENCE WITH STROUHAL NUMBER FOR PROPELLER NOISE COMPONENTS (MICROPHONES 9 AND 10)

that the dominant pressure field is aerodynamic. Again the Strouhal frequency fd/V_c does not collapse the coherence spectra. Thus harmonic order was used as a non-dimensional frequency since it appeared to give an improved data collapse for the aerodynamic field propagating in the circumferential direction. Figure 21 contains coherence data for the Microphone pair 5-7, with harmonic order as the parameter on the abscissa. At low harmonic orders, where the phase angle is constant, the coherence remains high. Then the coherence decays rapidly with increasing harmonic order in the frequency range where the phase angle indicates subsonic trace velocities. Use of harmonic order gives reasonably good collapse of coherence data for the four lowest harmonic orders, but at higher orders there is very poor data collapse.

4.4.3 Summary of Correlation Analysis

A brief analysis of the coherence and phase angle data measured on the Aero Commander has shown that the pressure field has complicated characteristics. Consequently, it is not possible to fit simple analytical representations to the coherence and phase angle spectra.

Phase angle data show the existence of regions where the pressure field can be approximated as an incident acoustic field, other regions where the characterisitcs suggest the presence of a convected aerodynamic field, and other regions or frequency ranges where the pressure field appears to be a potential field rotating with the propeller. It is likely, however, that the situation would become more amenable to analysis if the twin-engined airplane had the plane of rotation of the propeller well forward of the cabin and the engine was a turboprop design.

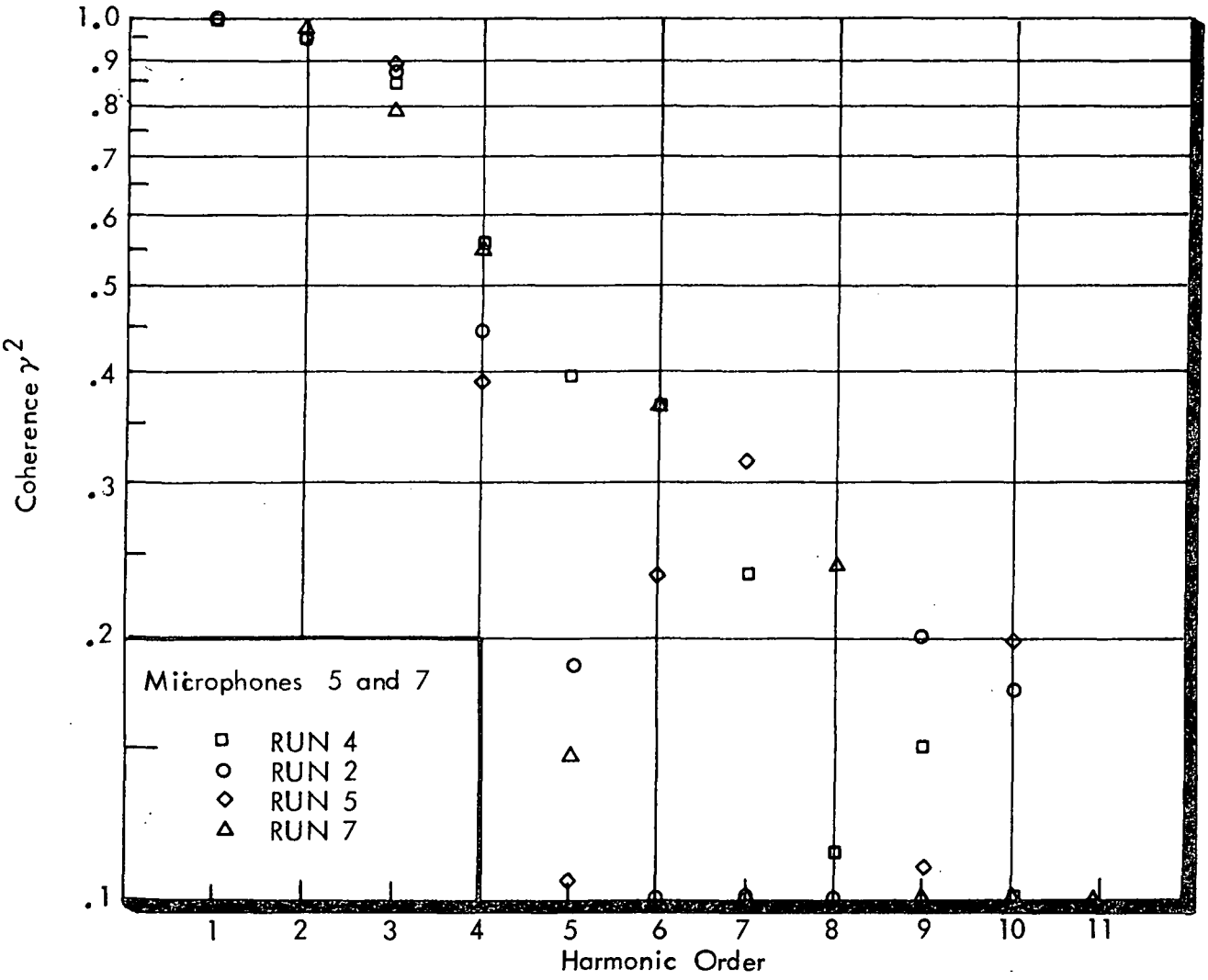

FIGURE 21. VARIATION OF COHERENCE WITH HARMONIC ORDER FOR PROPELLER NOISE COMPONENTS (MICROPHONES 5 AND 7)

A rather cursory analysis of the coherence spectra failed to identify any satisfactory non-dimensional frequency parameter which would allow good collapse of the data. Consequently, much more effort is required to search for a suitable description of the coherence for use in analytical models of structural response and interior noise.

REFERENCES

1. Mixson, J. S., C. K. Barton, and R. Vaicaitis, "Investigation of Interior Noise in a Twin-Engine Light Aircraft," *Journal of Aircraft,* Vol. 15, No. 4, pp 227-233, April 1978.

2. Bendat, J. S., *Principles and Applications of Random Noise Theory,* p. 380, John Wiley & Sons, New York, 1958.

3. Bliss, D. B., K. L. Claudiramani, and A. G. Piersol, "Data Analysis and Noise Prediction for the QF-1B Experimental Fan Stage," NASA CR 135066, Lewis Research Center, Ohio, August 1976.

4. "Prediction Procedure for Near-Field and Far-Field Propeller Noise," SAE Aerospace Information Report AIR 1407, May 1977.

5. Ungar, E. E., et al, "A Guide for Estimation of Aeroacoustic Loads on Flight Vehicle Surfaces," AFFDL-TR-76-91 Vol. I, February 1977.

APPENDIX A

Magnitude of Propeller Blade Passage Tones

TABLE A-1.

LOCATION 1 SPECTRAL VALUES - DB (4 Hz Resolution)

HARMONIC ORDER	RUN 1	RUN 2	RUN 3	RUN 4	RUN 5	RUN 6	RUN 7	RUN 8	RUN AV(7+8)	RUN AV(5+6)
1	128.1	131.1	131.8	132.0	128.7	127.8	123.6	123.3	123.5	128.3
2	115.4	117.4	120.5	122.1	117.0	113.2	109.0	108.3	108.7	115.1
3	115.4	115.5	116.2	118.0	113.3	112.0	104.8	107.3	106.1	112.7
4	112.4	115.4	119.3	119.4	109.5	110.8	103.0	105.2	104.1	110.2
5	109.0	111.7	113.0	115.6	108.0	107.8	102.2	104.5	103.4	107.9
6	110.2	110.3	113.2	114.8	107.9	108.6	102.8	103.6	103.2	108.3
7	108.3	109.2	114.0	114.7	107.1	107.5	101.1	101.1	101.1	107.3
8	105.9	108.9	109.4	110.5	105.0	104.9	98.9	100.5	99.7	105.0
9	105.4	106.9	111.8	112.1	104.3	105.6	100.2	100.9	100.6	105.0
10	103.6	107.3	108.3	109.6	102.9	104.7	97.3	98.2	97.8	103.8
11	103.3	104.9	107.8	106.4	101.8	104.0	97.8	97.8	97.8	102.9
12	102.2	105.1	107.2	107.8	101.7	102.9	95.1	96.7	95.9	102.3
13	98.8	103.4	104.5	104.9	99.8	101.6	94.3	95.6	95.0	100.7
14	100.4	101.4	104.7	103.9	99.5	101.0	94.7	94.4	94.5	100.3
15	96.9	100.9	102.4	101.4	97.6	99.1	93.7	93.2	93.5	98.3
16	95.9	100.0	100.9	100.4	97.3	98.6	92.0	91.9	92.0	97.9
17	96.1	99.0	101.5	100.0	97.0	97.8	92.1	90.9	91.5	97.4
18	94.4	99.4	99.0	98.2	95.9	97.7	90.5	90.9	90.7	96.8
19	94.5	97.4	100.1	98.7	95.6	96.7	90.4	89.8	90.1	96.2
20	94.4	97.2	97.3	96.9	94.6	96.2	88.4	88.8	88.6	95.4
21	92.3	96.5	0.0	0.0	93.2	94.8	89.0	88.4	88.7	94.0
22	91.5	0.0	0.0	0.0	92.5	93.6	87.9	0.0	0.0	93.1
23	91.3	0.0	0.0	0.0	92.9	92.9	86.5	0.0	0.0	92.9
24	90.5	0.0	0.0	0.0	92.3	92.5	87.1	0.0	0.0	92.4
25	0.0	0.0	0.0	0.0	0.0	0.0	86.4	0.0	0.0	0.0
26	0.0	0.0	0.0	0.0	0.0	0.0	85.4	0.0	0.0	0.0
27	0.0	0.0	0.0	0.0	0.0	0.0	84.9	0.0	0.0	0.0
28	0.0	0.0	0.0	0.0	0.0	0.0	84.9	0.0	0.0	0.0
OVERALL	128.9	131.7	132.7	133.1	129.3	128.4	124.0	123.8	123.9	128.8
RPM	2100.	2400.	2600.	2600.	2100.	2100.	1700.	1700.	1700.	2100.

TABLE A-2.

LOCATION 2 SPECTRAL VALUES - DB (4 Hz Resolution)

HARMONIC ORDER	RUN 1	RUN 2	RUN 3	RUN 4	RUN 5	RUN 6	RUN 7	RUN 8	RUN AV(7+8)	RUN AV(5+6)
1	132.3	135.0	135.9	136.1	132.4	131.8	127.5	127.2	127.4	132.1
2	123.1	126.1	128.0	129.4	123.9	121.8	118.0	116.9	117.5	122.9
3	118.2	121.1	122.9	123.1	118.8	116.4	112.4	111.5	112.0	117.6
4	115.0	118.5	120.1	120.4	113.2	112.2	108.1	107.5	107.8	112.7
5	109.0	111.9	111.9	114.3	107.3	108.6	104.9	104.7	104.8	108.0
6	108.4	110.8	112.3	114.4	107.6	108.7	103.7	104.6	104.2	108.2
7	106.7	109.4	115.6	115.9	106.9	106.9	101.9	102.6	102.3	106.9
8	104.6	107.9	110.2	109.9	104.5	104.4	100.8	100.8	100.8	104.5
9	102.8	106.4	110.8	111.1	103.8	104.2	99.9	100.3	100.1	104.0
10	102.2	106.7	106.6	108.7	102.3	104.3	98.0	98.9	98.5	103.3
11	101.9	104.1	106.7	106.5	101.3	103.7	97.6	98.0	97.8	102.5
12	100.8	103.8	105.4	105.9	101.1	102.1	94.2	95.4	94.8	101.6
13	97.8	101.2	103.3	103.1	99.4	101.0	94.1	94.7	94.4	100.2
14	98.3	100.3	103.2	103.3	98.6	100.6	94.1	94.0	94.1	99.6
15	95.2	100.0	101.2	101.4	97.2	98.8	92.7	93.6	93.1	98.0
16	95.0	99.4	100.0	99.4	96.8	97.6	91.0	91.7	91.4	97.2
17	94.6	98.4	99.8	99.5	96.3	96.8	90.4	91.0	90.7	96.5
18	93.7	97.7	98.6	98.4	95.8	96.1	90.1	90.2	90.2	95.9
19	92.7	98.0	97.8	98.1	95.1	95.6	90.2	89.4	89.8	95.3
20	91.9	95.9	97.4	98.0	94.5	94.9	89.0	88.9	89.0	94.7
21	91.0	96.3	0.0	0.0	92.7	93.3	88.4	88.1	88.2	93.0
22	0.0	0.0	0.0	0.0	92.7	93.1	88.1	0.0	0.0	92.9
23	0.0	0.0	0.0	0.0	92.7	92.8	87.6	0.0	0.0	92.7
24	0.0	0.0	0.0	0.0	0.0	0.0	87.0	0.0	0.0	0.0
25	0.0	0.0	0.0	0.0	0.0	0.0	86.3	0.0	0.0	0.0
26	0.0	0.0	0.0	0.0	0.0	0.0	85.6	0.0	0.0	0.0
27	0.0	0.0	0.0	0.0	0.0	0.0	84.5	0.0	0.0	0.0
28	0.0	0.0	0.0	0.0	0.0	0.0	84.9	0.0	0.0	0.0
OVERALL	133.1	135.8	136.9	137.3	133.2	132.5	128.2	127.8	128.0	132.8
RPM	2100.	2400.	2600.	2600.	2100.	2100.	1700.	1700.	1700.	2100.

TABLE A-3.

LOCATION 3 SPECTRAL VALUES - DB (4 Hz Resolution)

HARMONIC ORDER	RUN 1	RUN 2	RUN 3	RUN 4	RUN 5	RUN 6	RUN 7	RUN 8	RUN AV(7+8)	RUN AV(5+6)
1	130.0	132.1	133.2	133.5	129.6	129.2	124.3	124.3	124.3	129.4
2	127.4	129.9	131.6	131.7	126.3	125.6	121.2	120.5	120.9	126.0
3	123.9	127.0	128.1	128.4	123.1	122.7	118.1	117.6	117.9	122.9
4	119.7	122.9	126.1	125.7	119.2	119.2	114.9	114.8	114.9	119.2
5	116.7	120.9	123.7	123.2	115.6	115.7	111.5	111.1	111.3	115.7
6	114.8	117.9	121.0	120.3	113.2	113.8	109.1	109.5	109.3	113.5
7	111.9	114.4	118.2	118.1	110.4	111.2	106.0	105.7	105.9	110.8
8	108.9	112.2	116.4	115.1	106.4	108.0	103.1	103.1	103.1	107.2
9	107.1	110.7	117.0	116.9	105.1	107.4	101.1	101.1	101.1	106.3
10	105.8	111.9	115.1	115.8	102.5	105.1	97.5	98.6	98.1	103.8
11	106.9	110.1	113.6	114.5	103.3	104.1	96.0	97.3	96.7	103.7
12	107.6	108.3	114.0	114.7	104.3	105.1	93.8	94.9	94.3	104.7
13	105.9	108.4	114.3	115.2	101.7	103.9	92.5	92.9	92.7	102.8
14	103.8	108.4	112.6	113.5	101.0	101.7	91.8	91.6	91.7	101.4
15	103.6	107.2	112.0	112.7	99.6	100.9	92.3	92.8	92.5	100.3
16	103.2	104.8	112.6	112.7	98.4	101.1	89.9	90.9	90.4	99.8
17	101.6	105.4	111.1	112.0	97.4	100.2	87.8	88.8	88.3	98.8
18	99.0	104.7	110.2	110.2	95.0	97.8	86.4	87.2	86.8	96.4
19	99.3	103.0	110.4	110.3	93.8	97.5	87.1	86.9	87.0	95.6
20	98.8	102.4	108.6	108.6	93.1	97.3	86.3	87.6	86.9	95.2
21	96.4	102.7	0.0	0.0	92.8	96.1	85.2	86.5	85.9	94.4
22	95.6	99.7	0.0	0.0	91.1	95.1	83.2	85.0	84.1	93.1
23	95.8	0.0	0.0	0.0	91.1	94.7	82.3	83.3	82.8	92.9
24	95.0	0.0	0.0	0.0	89.9	94.1	83.1	83.5	83.3	92.0
25	0.0	0.0	0.0	0.0	0.0	0.0	82.8	83.6	83.2	0.0
26	0.0	0.0	0.0	0.0	0.0	0.0	81.6	0.0	0.0	0.0
27	0.0	0.0	0.0	0.0	0.0	0.0	80.8	0.0	0.0	0.0
28	0.0	0.0	0.0	0.0	0.0	0.0	81.4	0.0	0.0	0.0
OVERALL	133.1	135.6	137.3	137.4	132.3	132.0	127.2	127.0	127.1	132.1
RPM	2100.	2400.	2600.	2600.	2100.	2100.	1700.	1700.	1700.	2100.

TABLE A-4.

LOCATION 4 SPECTRAL VALUES - DB (4 Hz Resolution)

HARMONIC ORDER	RUN 1	RUN 2	RUN 3	RUN 4	RUN 5	RUN 6	RUN 7	RUN 8	RUN AV(7+8)	RUN AV(5+6)
1	131.3	133.9	135.4	135.3	130.7	130.3	125.6	126.0	125.8	130.5
2	127.9	130.1	132.1	131.9	126.4	125.8	122.2	121.8	122.0	126.1
3	122.4	126.0	128.1	127.7	121.7	121.1	116.8	117.5	117.2	121.4
4	120.0	123.9	126.5	126.0	119.0	119.0	114.3	113.8	114.1	119.0
5	117.4	121.5	124.3	123.7	116.1	116.2	112.3	111.9	112.1	116.2
6	114.9	118.6	122.8	121.9	113.8	114.7	110.6	110.6	110.6	114.3
7	113.5	116.5	119.0	118.3	112.5	112.4	107.6	106.1	106.9	112.5
8	109.8	112.4	116.8	116.6	109.4	108.7	104.9	103.5	104.2	109.1
9	107.6	111.6	115.6	114.6	107.3	106.6	103.2	101.8	102.5	107.0
10	106.4	108.1	112.7	112.4	105.7	105.1	100.3	98.3	99.3	105.4
11	103.4	107.2	112.0	110.9	102.4	101.9	97.7	96.1	96.9	102.2
12	102.1	104.8	109.1	108.2	101.5	101.7	95.8	94.8	95.3	101.6
13	98.9	102.7	108.8	107.5	97.9	99.5	93.7	92.8	93.2	98.7
14	98.4	101.2	106.3	105.1	97.0	97.7	91.3	90.9	91.1	97.4
15	94.4	99.0	104.4	103.6	94.7	96.3	89.0	89.0	89.0	95.5
16	93.9	97.9	102.0	101.5	93.9	95.5	87.8	87.8	87.8	94.7
17	91.9	96.1	101.0	101.2	92.7	93.7	85.3	87.0	86.2	93.2
18	91.4	95.5	99.2	99.5	90.6	93.5	84.3	85.8	85.0	92.0
19	90.3	93.7	97.9	98.7	89.7	93.3	84.0	85.3	84.6	91.5
20	89.9	94.8	94.4	95.5	89.1	93.0	82.2	0.0	0.0	91.1
21	0.0	92.9	0.0	0.0	89.2	92.2	83.2	0.0	0.0	90.7
22	0.0	0.0	0.0	0.0	89.7	91.8	0.0	0.0	0.0	90.7
23	0.0	0.0	0.0	0.0	91.5	92.2	0.0	0.0	0.0	91.8
24	0.0	0.0	0.0	0.0	88.4	89.4	0.0	0.0	0.0	88.9
25	0.0	0.0	0.0	0.0	0.0	87.6	0.0	0.0	0.0	0.0
26	0.0	0.0	0.0	0.0	0.0	0.0	0.0	0.0	0.0	0.0
27	0.0	0.0	0.0	0.0	0.0	0.0	0.0	0.0	0.0	0.0
28	0.0	0.0	0.0	0.0	0.0	0.0	0.0	0.0	0.0	0.0
OVERALL	133.8	136.5	138.4	138.1	132.9	132.5	128.1	128.2	128.2	132.7
RPM	2100.	2400.	2600.	2600.	2100.	2100.	1700.	1700.	1700.	2100.

TABLE A-5.

LOCATION 5 SPECTRAL VALUES - DB (4 Hz Resolution)

HARMONIC ORDER	RUN 1	RUN 2	RUN 3	RUN 4	RUN 5	RUN 6	RUN 7	RUN 8	RUN AV(7+8)	RUN AV(5+6)
1	128.2	131.1	132.6	132.5	127.8	127.8	122.0	121.9	122.0	127.8
2	121.0	123.7	125.2	125.4	120.3	120.2	116.0	115.9	116.0	120.3
3	117.4	121.0	122.3	122.2	117.7	117.0	112.2	111.1	111.7	117.4
4	116.0	119.8	120.4	119.8	113.8	113.8	108.5	108.4	108.5	113.8
5	111.4	114.2	117.5	117.0	110.8	109.6	105.6	104.2	104.9	110.2
6	107.9	111.2	115.5	114.7	107.7	106.9	104.3	103.9	104.1	107.3
7	106.8	109.8	113.1	112.6	106.0	105.7	98.1	97.7	97.9	105.9
8	102.6	105.2	109.3	109.6	102.2	101.5	99.8	97.7	98.7	101.9
9	99.5	103.9	106.9	106.6	100.7	99.8	94.8	94.8	94.8	100.3
10	98.0	101.5	102.5	102.4	98.3	97.2	91.7	90.2	91.0	97.8
11	96.7	97.3	102.1	102.5	97.2	96.7	86.8	89.6	88.2	96.9
12	93.4	97.5	99.3	100.8	95.5	95.0	87.9	88.5	88.2	95.3
13	92.5	97.1	98.8	99.4	93.5	93.4	86.2	86.1	86.2	93.5
14	91.3	94.0	95.1	96.7	92.8	94.1	84.9	88.1	86.5	93.4
15	91.3	93.5	96.0	96.6	92.9	93.4	82.5	86.1	84.3	93.1
16	88.0	93.4	95.7	96.2	93.0	92.6	82.4	83.2	82.8	92.8
17	88.7	92.0	95.2	96.2	90.7	92.2	83.7	83.3	83.5	91.5
18	89.0	92.3	95.0	96.5	91.5	91.1	84.0	83.2	83.6	91.3
19	89.9	91.8	95.2	95.3	89.7	89.5	82.3	83.7	83.0	89.6
20	92.2	92.8	94.7	96.5	90.4	89.8	81.5	0.0	0.0	90.1
21	87.8	93.5	0.0	0.0	90.8	89.9	81.2	0.0	0.0	90.4
22	0.0	0.0	0.0	0.0	91.4	91.2	80.3	0.0	0.0	91.3
23	0.0	0.0	0.0	0.0	89.9	90.2	0.0	0.0	0.0	90.0
24	0.0	0.0	0.0	0.0	90.6	0.0	0.0	0.0	0.0	0.0
25	0.0	0.0	0.0	0.0	0.0	0.0	0.0	0.0	0.0	0.0
26	0.0	0.0	0.0	0.0	0.0	0.0	0.0	0.0	0.0	0.0
27	0.0	0.0	0.0	0.0	0.0	0.0	0.0	0.0	0.0	0.0
28	0.0	0.0	0.0	0.0	0.0	0.0	0.0	0.0	0.0	0.0
OVERALL	129.6	132.6	134.1	134.0	129.1	129.1	123.6	123.4	123.5	129.1
RPM	2100.	2400.	2600.	2600.	2100.	2100.	1700.	1700.	1700.	2100.

TABLE A-6.

LOCATION 6 SPECTRAL VALUES - DB (4 Hz Resolution)

HARMONIC ORDER	RUN 1	RUN 2	RUN 3	RUN 4	RUN 5	RUN 6	RUN 7	RUN 8	RUN AV(7+8)	RUN AV(5+6)
1	124.9	127.9	129.3	129.1	124.5	124.5	128.9	128.5	128.7	124.5
2	114.1	117.7	121.3	121.4	114.2	113.5	119.1	118.5	118.8	113.9
3	111.1	111.4	115.5	115.8	110.5	110.0	114.5	114.2	114.4	110.3
4	113.5	118.9	118.9	119.5	108.5	109.1	114.6	111.6	113.1	108.8
5	101.6	104.2	108.4	107.8	101.8	102.2	110.7	106.6	108.7	102.0
6	105.4	103.9	104.9	105.2	103.4	102.9	102.8	107.4	105.1	103.2
7	94.4	105.0	107.8	104.2	98.0	97.2	106.9	104.4	105.7	97.6
8	98.9	97.1	105.9	105.6	97.7	96.8	101.0	104.6	102.8	97.2
9	92.1	99.1	97.5	98.1	95.3	95.1	97.9	98.6	98.2	95.2
10	98.7	96.1	101.6	102.3	99.4	97.3	103.9	100.1	102.0	98.3
11	95.5	97.2	97.8	100.6	92.8	94.4	94.5	98.5	96.5	93.6
12	93.9	94.3	96.9	98.8	94.4	94.9	97.5	99.9	98.7	94.7
13	89.7	94.5	96.2	94.8	92.9	94.2	95.2	99.1	97.2	93.6
14	89.4	93.0	95.6	96.7	93.2	94.0	96.1	95.9	96.0	93.6
15	88.9	92.3	93.5	95.4	91.4	92.6	95.8	94.9	95.3	92.0
16	88.9	92.7	95.3	96.0	90.2	92.0	92.4	93.1	92.7	91.1
17	87.4	93.0	97.8	101.3	90.0	91.3	91.6	92.7	92.2	90.6
18	88.3	0.0	95.2	0.0	89.7	89.8	93.9	93.1	93.5	89.8
19	90.7	0.0	97.9	0.0	91.1	90.9	91.0	0.0	0.0	91.0
20	92.3	0.0	0.0	0.0	0.0	0.0	91.9	0.0	0.0	0.0
21	0.0	0.0	0.0	0.0	0.0	0.0	89.8	0.0	0.0	0.0
22	0.0	0.0	0.0	0.0	0.0	0.0	0.0	0.0	0.0	0.0
23	0.0	0.0	0.0	0.0	0.0	0.0	0.0	0.0	0.0	0.0
24	0.0	0.0	0.0	0.0	0.0	0.0	0.0	0.0	0.0	0.0
25	0.0	0.0	0.0	0.0	0.0	0.0	0.0	0.0	0.0	0.0
26	0.0	0.0	0.0	0.0	0.0	0.0	0.0	0.0	0.0	0.0
27	0.0	0.0	0.0	0.0	0.0	0.0	0.0	0.0	0.0	0.0
28	0.0	0.0	0.0	0.0	0.0	0.0	0.0	0.0	0.0	0.0
OVERALL	125.8	128.9	130.5	130.4	125.2	125.2	129.7	129.2	129.5	125.2
RPM	2100.	2400.	2600.	2600.	2100.	2100.	1700.	1700.	1700.	2100.

TABLE A-7.

LOCATION 7 SPECTRAL VALUES - DB (4 Hz Resolution)

HARMONIC ORDER	RUN 1	RUN 2	RUN 3	RUN 4	RUN 5	RUN 6	RUN 7	RUN 8	RUN AV(7+8)	RUN AV(5+6)
1	128.9	131.8	132.8	133.0	129.7	128.6	124.0	124.1	124.1	129.2
2	122.2	124.3	125.1	125.0	122.5	120.2	116.2	115.2	115.7	121.4
3	115.8	118.4	121.2	120.9	115.9	112.9	108.9	107.7	108.3	114.4
4	116.9	119.2	119.1	120.5	111.5	112.8	105.4	106.8	106.1	112.2
5	106.2	110.5	112.1	113.0	104.5	106.1	101.4	104.5	103.0	105.3
6	110.3	110.4	109.9	112.3	107.6	108.4	101.9	105.5	103.7	108.0
7	107.1	108.5	111.1	109.7	108.5	108.0	99.4	102.6	101.0	108.3
8	103.2	107.8	111.8	112.3	104.4	104.8	103.0	104.8	103.9	104.6
9	102.2	109.0	111.6	112.3	104.6	105.2	95.9	98.9	97.4	104.9
10	104.6	107.1	104.5	108.0	102.2	104.9	94.4	98.6	96.5	103.6
11	104.0	104.3	107.7	106.5	103.6	104.9	94.2	96.9	95.6	104.3
12	99.7	105.4	105.8	106.0	103.5	102.5	93.9	97.2	95.6	103.0
13	98.2	102.8	105.2	105.2	100.7	101.9	92.7	96.4	94.5	101.3
14	98.1	102.9	102.9	102.0	100.9	101.7	93.0	94.9	94.0	101.3
15	96.1	100.3	104.2	101.8	100.4	100.4	91.9	93.0	92.5	100.4
16	96.4	100.7	101.9	101.4	99.8	99.6	90.2	90.9	90.6	99.7
17	93.6	100.7	103.3	101.9	98.1	98.5	89.5	91.3	90.4	98.3
18	94.7	99.5	100.3	99.5	98.4	98.9	89.4	90.3	89.8	98.7
19	95.5	98.2	100.7	99.6	98.6	97.6	89.5	90.3	89.9	98.1
20	93.6	97.9	99.0	99.4	97.9	97.7	87.5	90.0	88.8	97.8
21	92.9	97.5	0.0	0.0	96.9	97.6	86.3	0.0	0.0	97.2
22	91.8	96.5	0.0	0.0	95.0	95.4	88.1	0.0	0.0	95.2
23	92.7	0.0	0.0	0.0	95.1	95.3	87.7	0.0	0.0	95.2
24	0.0	0.0	0.0	0.0	93.8	94.4	86.7	0.0	0.0	94.1
25	0.0	0.0	0.0	0.0	92.7	0.0	86.4	0.0	0.0	0.0
26	0.0	0.0	0.0	0.0	0.0	0.0	85.8	0.0	0.0	0.0
27	0.0	0.0	0.0	0.0	0.0	0.0	84.3	0.0	0.0	0.0
28	0.0	0.0	0.0	0.0	0.0	0.0	84.8	0.0	0.0	0.0
OVERALL	130.3	133.0	134.0	134.2	130.8	129.6	124.9	125.0	125.0	130.2
RPM	2100.	2400.	2600.	2600.	2100.	2100.	1700.	1700.	1700.	2100.

TABLE A-8.

LOCATION 8 SPECTRAL VALUES - DB (4 Hz Resolution)

HARMONIC ORDER	RUN 1	RUN 2	RUN 3	RUN 4	RUN 5	RUN 6	RUN 7	RUN 8	RUN AV(7+8)	RUN AV(5+6)
1	123.8	127.5	128.7	128.9	125.2	123.9	119.9	120.6	120.3	124.6
2	115.5	116.7	119.0	119.8	114.8	112.4	107.3	108.3	107.8	113.6
3	109.8	112.4	124.3	123.7	108.7	108.1	110.7	109.2	110.0	108.4
4	121.6	122.9	124.2	124.8	117.3	116.9	102.7	104.1	103.4	117.1
5	108.4	112.8	113.6	115.0	108.8	109.8	102.3	103.2	102.8	109.3
6	110.9	111.2	112.3	113.6	107.7	109.4	104.1	107.4	105.8	108.6
7	108.0	111.7	113.8	115.9	107.7	107.6	101.7	102.4	102.1	107.7
8	107.1	108.1	106.7	108.4	106.9	106.3	100.6	103.8	102.2	106.6
9	104.8	104.4	106.9	106.6	104.9	105.8	97.2	100.3	98.7	105.4
10	99.8	106.2	111.5	111.0	104.9	106.5	97.8	99.8	98.8	105.7
11	100.2	109.4	110.3	110.3	101.4	103.8	95.7	98.4	97.1	102.6
12	102.4	107.5	105.8	106.3	101.2	104.1	94.6	96.9	95.7	102.7
13	102.2	102.9	105.5	104.9	102.6	104.3	92.5	94.4	93.5	103.5
14	98.3	103.0	103.3	103.0	101.3	101.4	92.7	93.9	93.3	101.4
15	96.9	102.0	102.4	101.3	101.8	101.5	94.7	93.9	94.3	101.7
16	97.1	101.3	102.0	101.5	100.1	101.6	93.8	95.0	94.4	100.9
17	95.6	99.8	102.2	102.6	99.1	99.3	91.9	92.9	92.4	99.2
18	95.5	100.4	100.6	102.0	98.2	98.5	90.8	90.9	90.8	98.4
19	95.7	99.7	99.7	100.2	98.0	99.3	90.8	90.9	90.8	98.7
20	95.1	99.0	100.1	100.7	98.6	99.2	88.9	90.1	89.5	98.9
21	93.6	0.0	0.0	0.0	95.4	97.2	88.4	0.0	0.0	96.3
22	0.0	0.0	0.0	0.0	95.2	96.8	88.8	0.0	0.0	96.0
23	0.0	0.0	0.0	0.0	96.1	95.8	88.2	0.0	0.0	95.9
24	0.0	0.0	0.0	0.0	95.3	95.1	88.2	0.0	0.0	95.2
25	0.0	0.0	0.0	0.0	0.0	0.0	87.2	0.0	0.0	0.0
26	0.0	0.0	0.0	0.0	0.0	0.0	86.1	0.0	0.0	0.0
27	0.0	0.0	0.0	0.0	0.0	0.0	86.5	0.0	0.0	0.0
28	0.0	0.0	0.0	0.0	0.0	0.0	86.8	0.0	0.0	0.0
OVERALL	126.7	129.6	131.7	131.9	126.7	125.7	121.0	121.7	121.4	126.2
RPM	2100.	2400.	2600.	2600.	2100.	2100.	1700.	1700.	1700.	2100.

TABLE A-9.

LOCATION 9 SPECTRAL VALUES - DB (4 Hz Resolution)

HARMONIC ORDER	RUN 1	RUN 2	RUN 3	RUN 4	RUN 5	RUN 6	RUN 7	RUN 8	RUN AV(7+8)	RUN AV(5+6)
1	111.1	114.7	119.0	119.6	113.6	112.0	111.2	111.8	111.5	112.8
2	114.0	112.4	112.4	114.5	116.3	116.1	106.2	105.2	105.7	116.2
3*	113.4	126.1	130.0	130.1	114.4	111.1	112.8	116.1	114.5	112.8
4*	125.7	125.6	123.2	124.3	123.0	122.6	109.9	107.1	108.5	122.8
5	109.2	106.4	111.5	110.4	107.7	108.2	106.0	103.6	104.8	108.0
6	107.5	114.0	115.8	117.6	106.3	105.2	104.4	105.3	104.9	105.8
7*	114.0	116.0	116.6	117.7	113.9	112.7	98.7	100.8	99.8	113.3
8	109.3	106.8	114.2	114.9	104.8	105.7	104.9	102.0	103.5	105.3
9	103.1	108.2	109.1	108.9	104.7	104.8	101.5	102.1	101.8	104.8
10	106.8	106.0	112.1	113.1	104.6	105.0	102.0	101.1	101.6	104.8
11	103.1	108.0	108.8	110.0	101.4	102.4	95.3	96.7	96.0	101.9
12	104.1	104.7	110.7	111.2	102.3	102.1	96.2	94.0	95.1	102.2
13	102.0	106.2	108.1	109.2	102.7	103.4	93.6	96.7	95.1	103.1
14	102.2	103.2	102.1	104.1	98.5	99.9	93.0	94.5	93.8	99.2
15	102.0	98.3	99.1	99.0	100.8	102.3	94.6	93.3	93.9	101.6
16	99.0	99.4	102.7	102.2	98.2	98.7	94.2	92.5	93.4	98.5
17	94.4	99.1	0.0	101.2	96.2	95.7	90.6	90.9	90.7	96.0
18	95.2	98.6	0.0	99.3	97.3	96.7	92.4	91.7	92.0	97.0
19	97.5	0.0	0.0	0.0	96.5	96.9	90.8	92.4	91.6	96.7
20	95.0	0.0	0.0	0.0	94.6	95.1	89.4	89.3	89.3	94.9
21	93.7	0.0	0.0	0.0	96.0	96.4	86.8	89.6	88.2	96.2
22	0.0	0.0	0.0	0.0	93.9	93.7	87.0	0.0	0.0	93.8
23	0.0	0.0	0.0	0.0	93.7	94.1	86.5	0.0	0.0	93.9
24	0.0	0.0	0.0	0.0	0.0	96.5	88.6	0.0	0.0	0.0
25	0.0	0.0	0.0	0.0	0.0	0.0	0.0	0.0	0.0	0.0
26	0.0	0.0	0.0	0.0	0.0	0.0	0.0	0.0	0.0	0.0
27	0.0	0.0	0.0	0.0	0.0	0.0	0.0	0.0	0.0	0.0
28	0.0	0.0	0.0	0.0	0.0	0.0	0.0	0.0	0.0	0.0
OVERALL*	127.0	129.6	131.7	132.1	125.4	124.8	117.9	118.9	118.3	125.1
RPM	2100.	2400.	2600.	2600.	2100.	2100.	1700.	1700.	1700.	2100.

*Data at most propeller blade passage harmonics may be influenced by engine exhaust tones at similar frequencies; propeller harmonics 3, 4, and 7 in particular appear to be heavily contaminated.

TABLE A-10.

LOCATION 10 | SPECTRAL VALUES - DB (4 Hz Resolution)

HARMONIC ORDER	RUN 1	RUN 2 **	RUN 3	RUN 4	RUN 5	RUN 6	RUN 7	RUN 8	RUN AV(7+8)	RUN AV(5+6)
1	110.0	84.0	114.5	113.0	109.8	108.7	106.1	106.0	106.1	109.3
2	111.4	84.1	115.1	116.1	114.4	113.8	103.5	103.8	103.7	114.1
3 *	117.1	84.3	126.7	126.7	116.0	116.4	115.1	117.8	116.5	116.2
4 *	124.3	82.3	124.7	125.5	122.2	121.7	110.7	109.7	110.2	122.0
5	107.1	78.7	115.0	115.0	104.3	103.5	103.2	103.4	103.3	103.9
6	110.7	72.7	112.6	113.8	109.2	108.5	104.2	105.0	104.6	108.9
7 *	106.9	78.7	123.3	123.3	110.7	109.2	103.1	101.9	102.5	110.0
8	102.0	77.1	109.3	111.0	103.3	108.4	105.8	104.4	105.1	105.9
9	105.0	68.8	106.9	109.1	110.4	109.5	101.1	97.7	99.4	110.0
10	105.0	69.0	108.8	110.3	106.1	105.2	101.5	97.5	99.5	105.7
11	98.8	69.2	99.5	100.4	96.6	99.5	99.2	98.3	98.7	98.1
12	95.2	73.8	107.2	107.3	96.0	96.4	92.5	96.5	94.5	96.2
13	98.8	78.3	105.9	105.5	99.5	99.9	90.4	92.7	91.6	99.7
14	98.2	74.4	103.3	104.4	94.4	97.1	89.2	90.5	89.9	95.7
15	100.5	0.0	107.5	105.6	98.5	99.1	87.3	89.1	88.2	98.8
16	95.5	0.0	103.2	102.8	94.5	97.5	89.1	89.7	89.4	96.0
17	95.5	0.0	0.0	0.0	94.3	97.0	86.8	88.1	87.5	95.6
18	96.2	0.0	0.0	0.0	93.7	96.1	89.2	88.3	88.7	94.9
19	98.9	0.0	0.0	0.0	95.4	97.9	89.7	0.0	0.0	96.7
20	99.4	0.0	0.0	0.0	0.0	0.0	87.2	0.0	0.0	0.0
21	99.0	0.0	0.0	0.0	0.0	0.0	88.0	0.0	0.0	0.0
22	0.0	0.0	0.0	0.0	0.0	0.0	0.0	0.0	0.0	0.0
23	0.0	0.0	0.0	0.0	0.0	0.0	0.0	0.0	0.0	0.0
24	0.0	0.0	0.0	0.0	0.0	0.0	0.0	0.0	0.0	0.0
25	0.0	0.0	0.0	0.0	0.0	0.0	0.0	0.0	0.0	0.0
26	0.0	0.0	0.0	0.0	0.0	0.0	0.0	0.0	0.0	0.0
27	0.0	0.0	0.0	0.0	0.0	0.0	0.0	0.0	0.0	0.0
28	0.0	0.0	0.0	0.0	0.0	0.0	0.0	0.0	0.0	0.0
OVERALL *	125.8	91.2	130.5	130.8	124.6	124.2	118.2	119.5	118.7	124.4
RPM	2100.	2400.	2600.	2600.	2100.	2100.	1700.	1700.	1700.	2100.

*Data at most propeller blade passage harmonics may be influenced by engine exhaust tones at similar frequencies; propeller harmonics 3, 4, and 7 in particular appear to be heavily contaminated.

**Data suspect due to auto-ranging of data acquisition equipment

TABLE A-11.

LOCATION 11 SPECTRAL VALUES - DB (4 Hz Resolution)

HARMONIC ORDER	RUN 1	RUN 2	RUN 3	RUN 4	RUN 5	RUN 6	RUN 7	RUN 8	RUN AV(7+8)	RUN AV(5+6)
1	102.4	105.8	106.6	106.6	95.0	95.4	92.3	92.1	92.2	95.2
2	99.6	99.9	102.0	101.7	98.9	97.6	86.7	88.3	87.5	98.2
3	90.6	94.5	94.6	97.0	89.6	91.0	92.3	94.8	93.6	90.3
4	91.4	99.9	103.4	103.4	88.7	87.7	81.7	83.7	82.7	88.2
5	90.9	83.0	95.5	96.3	87.0	87.0	77.3	74.7	76.0	87.0
6	90.2	89.3	90.9	91.1	86.0	85.9	85.5	84.3	84.9	86.0
7	86.5	82.5	90.2	90.9	84.4	84.3	75.7	77.5	76.6	84.3
8	81.2	85.0	82.7	84.4	75.7	77.6	78.5	80.1	79.3	76.7
9	81.9	76.4	79.5	79.8	77.3	78.5	73.4	74.3	73.9	77.9
10	74.2	76.6	79.2	77.9	70.1	73.6	71.1	70.4	70.8	71.9
11	74.4	74.5	77.5	78.2	72.6	73.9	69.2	73.4	71.3	73.3
12	72.9	74.1	73.3	75.3	66.4	70.4	66.4	70.3	68.4	68.4
13	71.7	71.1	71.1	73.0	69.3	72.1	61.6	61.6	61.6	70.7
14	68.2	68.6	70.1	71.5	66.8	69.4	62.1	61.9	62.0	68.1
15	0.0	67.3	73.7	71.5	60.2	62.5	58.7	63.4	61.1	61.4
16	0.0	65.8	74.3	73.4	60.8	63.0	62.8	59.5	61.2	61.9
17	0.0	67.8	0.0	69.0	58.5	62.6	59.8	60.0	59.9	60.6
18	0.0	64.9	0.0	67.4	58.9	59.6	54.7	0.0	0.0	59.3
19	0.0	64.6	0.0	68.2	59.6	60.8	53.9	0.0	0.0	60.2
20	0.0	0.0	0.0	0.0	61.4	63.9	51.2	0.0	0.0	62.7
21	0.0	0.0	0.0	0.0	56.7	59.9	50.2	0.0	0.0	58.3
22	0.0	0.0	0.0	0.0	0.0	58.3	50.5	0.0	0.0	0.0
23	0.0	0.0	0.0	0.0	0.0	59.0	50.5	0.0	0.0	0.0
24	0.0	0.0	0.0	0.0	0.0	58.2	53.1	0.0	0.0	0.0
25	0.0	0.0	0.0	0.0	0.0	0.0	0.0	0.0	0.0	0.0
26	0.0	0.0	0.0	0.0	0.0	0.0	0.0	0.0	0.0	0.0
27	0.0	0.0	0.0	0.0	0.0	0.0	0.0	0.0	0.0	0.0
28	0.0	0.0	0.0	0.0	0.0	0.0	0.0	0.0	0.0	0.0
OVERALL	105.1	107.9	109.7	109.8	101.4	101.0	96.6	97.8	97.2	101.2
RPM	2100.	2400.	2600.	2600.	2100.	2100.	1700.	1700.	1700.	2100.

TABLE A-12. PORT ENGINE OPERATION, SPECTRAL VALUES - DB (4 Hz RESOLUTION)

HARMONIC ORDER	LOCATION NUMBER (SEE FIGURE 1)										
	1	2	3	4	5	6	7	8	9	10	11
1	94.2	97.2	106.8	103.6	100.5	99.5	102.3	103.0	102.4	99.6	102.1
2	96.9	96.5	101.2	102.0	98.3	96.6	101.6	101.7	101.0	98.0	88.7
3	89.8	91.0	88.1	86.8	89.8	96.1	92.6	95.8	91.0	88.3	84.7
4	102.7	102.4	97.9	96.4	105.2	106.6	106.2	105.9	91.2	97.9	85.2
5	80.9	81.1	79.1	80.8	81.2	80.9	80.4	81.8	82.1	81.7	76.6
6	85.6	85.8	84.1	85.8	84.7	92.4	86.5	87.3	79.9	87.4	73.4
7	81.5	82.3	85.5	78.3	83.2	84.7	85.2	86.8	92.6	88.2	74.3
8	77.9	76.7	74.1	77.7	74.6	82.4	74.0	77.5	81.3	85.6	64.2
9	83.7	84.9	75.4	74.5	83.8	84.1	85.5	85.9	87.8	89.6	66.6
10	74.7	73.3	74.3	70.3	75.4	73.2	75.4	77.5	81.6	75.1	62.9
11	70.0	73.1	74.3	75.5	70.5	73.6	75.7	77.0	79.0	80.9	67.9
12	71.3	77.2	72.1	78.4	75.0	77.6	71.7	74.0	76.8	77.2	67.1
13	72.8	71.1	77.6	73.6	77.3	81.0	78.6	79.2	76.3	87.7	64.1
14	76.8	75.5	75.1	75.0	71.6	73.5	78.0	77.6	77.2	78.4	66.8
15	71.7	72.0	72.6	72.4	74.4	76.7	73.9	75.5	83.1	77.3	60.0
16	70.4	70.7	73.5	71.4	72.3	72.8	74.5	75.3	76.0	79.7	58.5
17	69.6	70.0	72.2	73.8	74.1	74.5	75.8	76.5	77.6	74.7	61.2
18	69.7	70.7	71.2	72.6	73.1	70.8	75.5	78.5	76.8	77.3	59.4
19	70.1	69.3	70.3	70.8	70.0	-	75.5	75.5	74.1	71.5	-
20	68.9	72.3	-	70.8	70.8	-	72.7	76.6	79.0	-	-

TABLE A-13. 1700 RPM OPERATION, SPECTRAL VALUES - DB (2 Hz RESOLUTION)

HARMONIC ORDER	RUN NO. 7, LOCATION NUMBER (SEE FIGURE 1)									
	1	2	3	4	5	6	7	8	9	10
1	123.0	127.1	123.5	124.8	121.8	128.0	123.4	119.2	109.4	104.3
2	108.2	116.9	119.9	120.7	115.2	117.3	114.9	105.9	101.1	97.4
3	103.2	111.4	117.3	115.6	111.7	112.9	107.7	100.4	107.5	107.4
4	99.6	106.3	114.3	113.3	107.6	105.8	100.2	95.9	98.4	96.3
5	99.4	102.3	110.5	110.9	104.5	106.1	100.1	98.6	100.0	99.0
6	100.6	102.1	108.2	109.2	103.4	100.7	100.1	102.2	102.9	102.3
7	98.6	99.3	104.9	106.2	97.2	104.9	97.6	100.0	96.8	100.3
8	96.3	97.6	102.4	103.5	98.1	98.5	101.3	98.3	103.3	104.7
9	96.4	97.2	100.1	101.2	90.9	90.6	93.6	95.3	94.9	91.0
10	94.6	95.1	96.3	98.2	90.1	94.8	91.6	95.9	94.9	89.7
11	93.6	95.0	94.8	96.3	84.9	91.3	91.3	93.3	92.8	92.6
12	91.3	91.7	92.6	94.0	85.5	94.4	90.9	92.0	93.4	88.8
13	91.0	91.4	91.2	91.5	83.9	90.9	90.4	90.2	90.9	87.2
14	91.2	90.6	91.0	89.7	82.6	93.3	90.2	89.7	90.2	94.7
15	90.5	89.4	91.1	86.4	80.2	92.0	89.0	92.1	91.5	84.1
16	88.2	87.8	88.3	85.0	79.7	88.8	87.4	91.0	91.0	84.6
17	88.5	87.1	86.5	82.5	81.1	87.5	86.1	88.9	87.3	83.9
18	86.5	86.9	85.0	81.1	80.9	90.3	86.6	87.6	89.2	85.8
19	87.1	87.0	85.2	80.9	79.3	87.5	86.2	87.7	87.5	86.7
20	84.4	85.0	83.7	78.5	78.9	88.1	84.2	85.5	86.1	83.1
Overall	123.3	127.0	126.3	127.1	123.2	128.6	124.2	119.8	113.7	112.2

TABLE A-14. 2100 RPM OPERATION, SPECTRAL VALUES - DB (2 Hz RESOLUTION)

HARMONIC ORDER	RUN NO. 5, LOCATION NUMBER (SEE FIGURE 1)									
	1	2	3	4	5	6	7	8	9	10
1	127.8	131.3	128.2	129.4	127.1	123.1	128.4	123.9	111.5	107.6
2	116.7	123.5	125.8	125.8	120.3	113.5	122.1	114.2	108.0	103.9
3	112.1	117.5	121.9	120.4	116.8	108.7	114.8	107.3	106.3	105.4
4	107.2	111.6	117.2	117.0	112.5	105.5	108.3	104.3	103.6	101.2
5	106.1	105.6	114.3	115.1	109.7	98.9	103.1	107.3	104.9	99.2
6	105.6	105.6	111.0	111.6	105.9	100.4	105.8	105.5	102.5	106.4
7	104.3	104.7	108.0	110.2	103.8	94.9	106.1	105.0	110.0	108.2
8	102.7	102.3	104.7	106.8	100.1	94.4	101.4	104.4	100.0	99.9
9	101.4	101.0	101.2	104.5	98.3	91.7	101.9	101.9	101.1	107.0
10	99.9	99.2	101.6	102.3	94.9	91.0	99.2	102.8	99.6	94.9
11	98.9	97.9	102.9	99.4	94.4	86.8	100.7	99.3	93.6	90.9
12	98.8	97.8	103.6	98.6	93.4	90.0	100.7	98.3	98.1	93.5
13	96.8	96.1	101.9	94.9	90.8	90.1	97.8	99.9	98.7	93.3
14	96.7	95.3	100.3	94.0	90.3	90.3	98.5	98.6	94.4	90.6
15	94.4	94.0	98.7	91.7	89.8	87.6	97.7	98.6	97.3	95.1
16	94.2	93.5	98.2	91.0	90.5	86.7	96.7	96.9	94.7	90.0
17	93.9	93.1	96.5	89.1	87.5	86.3	95.0	95.9	91.5	89.0
18	92.5	92.4	93.7	87.4	89.3	86.4	95.1	94.8	93.5	89.7
19	92.4	91.7	92.6	86.9	86.7	87.8	95.1	94.5	92.0	--
20	91.3	91.1	91.3	85.6	87.1	--	94.5	95.2	89.7	--
Overall	128.4	132.2	131.2	131.7	128.5	123.9	129.6	124.8	116.8	115.1

TABLE A-15. 2400 RPM OPERATION, SPECTRAL VALUES - DB (2 Hz RESOLUTION)

HARMONIC ORDER	RUN NO. 2, LOCATION NUMBER (SEE FIGURE 1)								
	1	2	3	4	5	6	7	8	9
1	130.5	134.1	130.9	132.9	130.6	126.7	130.6	126.7	112.7
2	116.3	124.9	128.3	128.8	122.8	116.2	122.6	115.1	105.5
3	113.8	119.3	125.0	124.1	119.7	109.3	116.4	110.6	109.6
4	108.2	114.7	120.5	121.6	115.7	104.9	111.1	108.5	103.7
5	109.4	109.5	118.8	119.3	112.4	102.2	108.4	110.9	102.4
6	108.3	108.4	115.8	116.4	109.4	101.1	107.5	108.5	111.7
7	106.4	106.7	112.1	114.2	107.6	102.4	105.4	109.2	113.4
8	106.3	105.0	109.3	110.1	102.1	94.0	104.6	105.1	103.7
9	104.4	103.7	108.0	108.9	101.0	94.4	105.8	100.8	105.4
10	104.6	103.4	109.4	105.3	98.5	91.9	103.5	102.9	103.1
11	101.6	101.1	107.3	104.3	94.3	94.2	100.5	106.0	105.3
12	101.5	100.7	105.5	101.8	94.5	91.0	101.6	104.1	101.8
13	100.4	98.0	105.4	99.4	94.2	90.8	99.0	98.8	103.4
14	98.5	97.3	105.4	97.8	90.9	87.6	99.1	99.8	100.1
15	97.5	96.8	104.3	95.7	90.5	88.1	96.5	98.2	94.7
16	97.1	95.0	101.9	95.1	90.8	88.8	96.8	97.7	95.7
17	96.2	95.1	102.5	92.9	88.6	87.9	96.6	96.2	95.4
18	94.3	93.9	101.6	92.2	89.1	90.4	95.4	96.6	92.7
19	94-4	93.7	99.9	90.4	88.5	--	94.4	95.8	91.8
20	92.9	92.2	99.7	90.8	89.1	--	93.9	95.2	--
Overall	130.9	134.8	134.0	135.2	131.8	127.2	131.5	127.5	119.5

TABLE A-16. 2600 RPM OPERATION, SPECTRAL VALUES - DB (2 Hz RESOLUTION)

HARMONIC ORDER	RUN NO. 4 LOCATION NUMBER (SEE FIGURE 1)									
	1	2	3	4	5	6	7	8	9	10
1	132.2	136.2	133.1	134.9	132.8	129.1	132.4	128.9	118.7	112.5
2	121.0	128.3	130.2	130.5	124.6	120.2	123.3	118.2	112.9	109.2
3	116.6	122.3	126.8	126.3	121.6	115.0	119.4	114.0	109.4	109.6
4	111.9	118.5	124.0	124.0	118.5	109.6	112.0	112.5	109.1	105.5
5	113.3	111.6	121.3	121.5	115.7	103.9	110.7	112.0	107.2	99.8
6	113.1	111.9	118.5	119.3	113.0	102.9	109.3	111.5	112.3	107.2
7	112.6	113.8	115.8	115.9	110.9	101.9	106 4	114.1	116.0	122.0
8	108.3	107.5	113.1	114.1	107.4	98.9	109.1	105.5	111.5	108.6
9	109.9	108.4	114.4	112.0	104.7	94.7	109.3	103.6	106.3	102.8
10	107.2	106.2	113.7	109.9	100.4	99.5	104.1	108.6	110.3	97.6
11	103.7	103.5	111.8	108.1	100.1	97.3	102.5	107.5	107.2	92.3
12	105.4	103.3	112.4	105.7	98.1	95.1	102.5	103.3	108.3	103.0
13	101.9	100.1	112.4	104.5	96.5	91.3	101.3	101.5	106.2	102.9
14	101.2	99.6	111.2	102.4	93.2	92.6	98.2	99.7	100.9	100.8
15	98.0	98.0	109.7	100.5	93.3	91.4	98.7	98.2	95.2	102.4
16	97.1	96.9	110.0	98.4	93.3	91.7	97.1	97.7	98.8	99.2
17	96.5	96.1	109.8	97.7	92.3	94.3	97.9	97.5	96.2	99.6
18	95.0	95.2	107.3	95.8	93.3	94.0	95.5	98.1	95.9	--
19	95.5	94.9	107.0	95.0	92.2	94.5	96.1	96.7	--	--
20	93.4	94.4	105.5	92.1	93.5	92.8	94.8	97.3	--	--
Overall	132.9	137.1	136.3	137.2	133.9	129.9	133.2	129.9	123.4	123.5

APPENDIX B

Typical Probability Density Plots for Propeller Blade Passage Tone Stability Studies - Test Run 4, Location No. 6

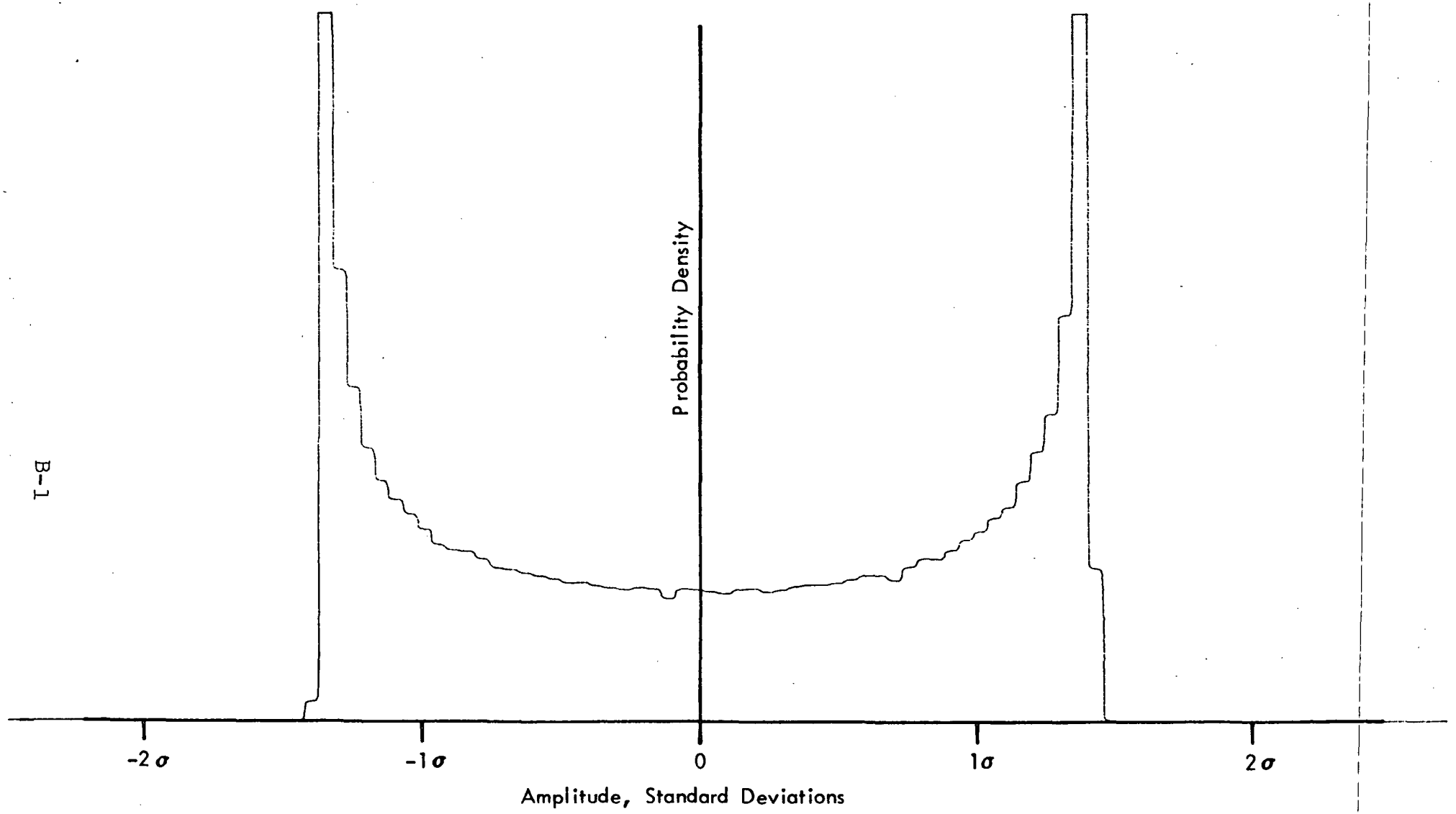

FIGURE B-1. PROBABILITY DENSITY FUNCTION OF CALIBRATION SINE WAVE

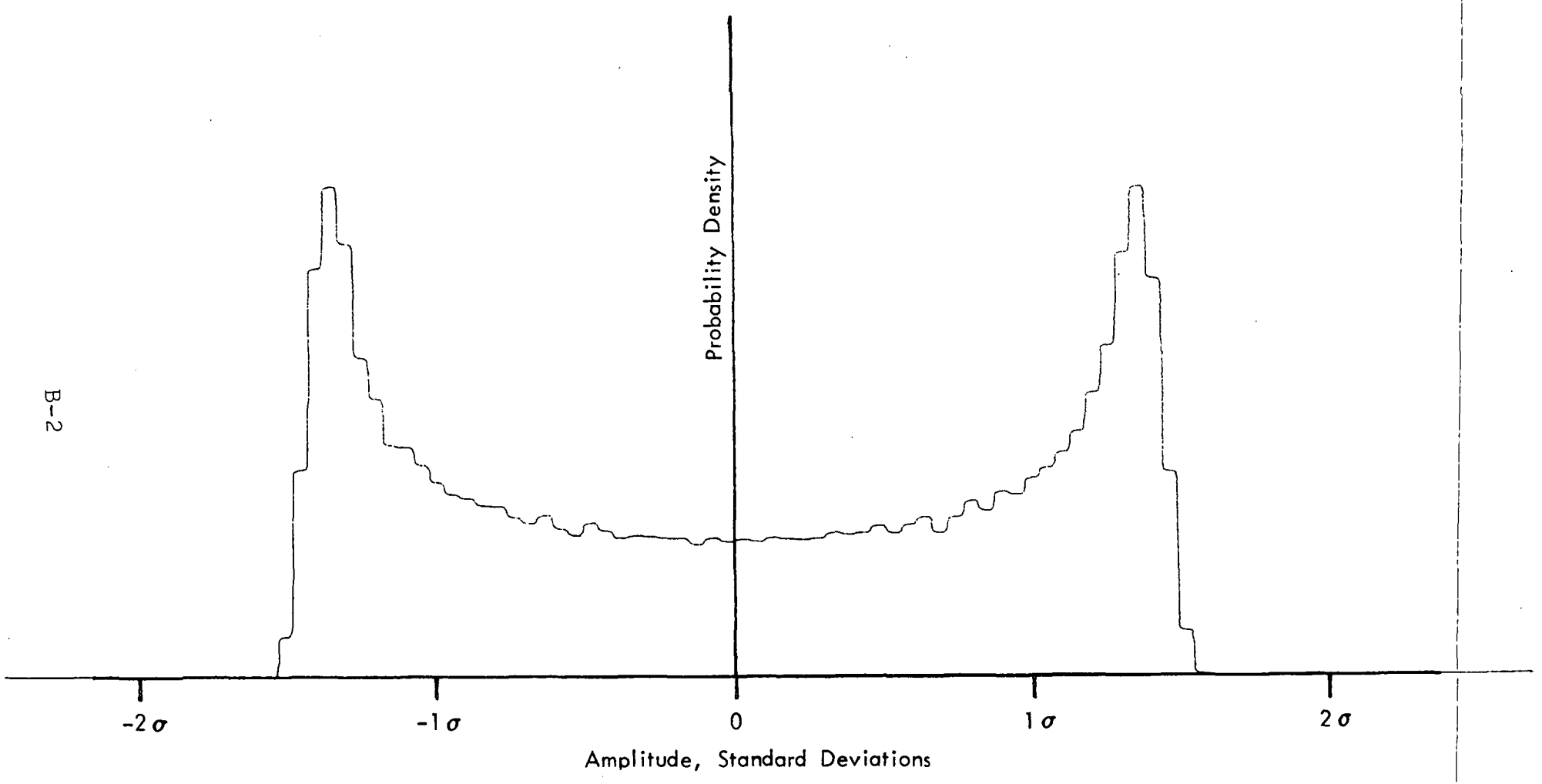

FIGURE B-2. PROBABILITY DENSITY FUNCTION OF FIRST HARMONIC, TEST RUN 4, LOCATION NO.6

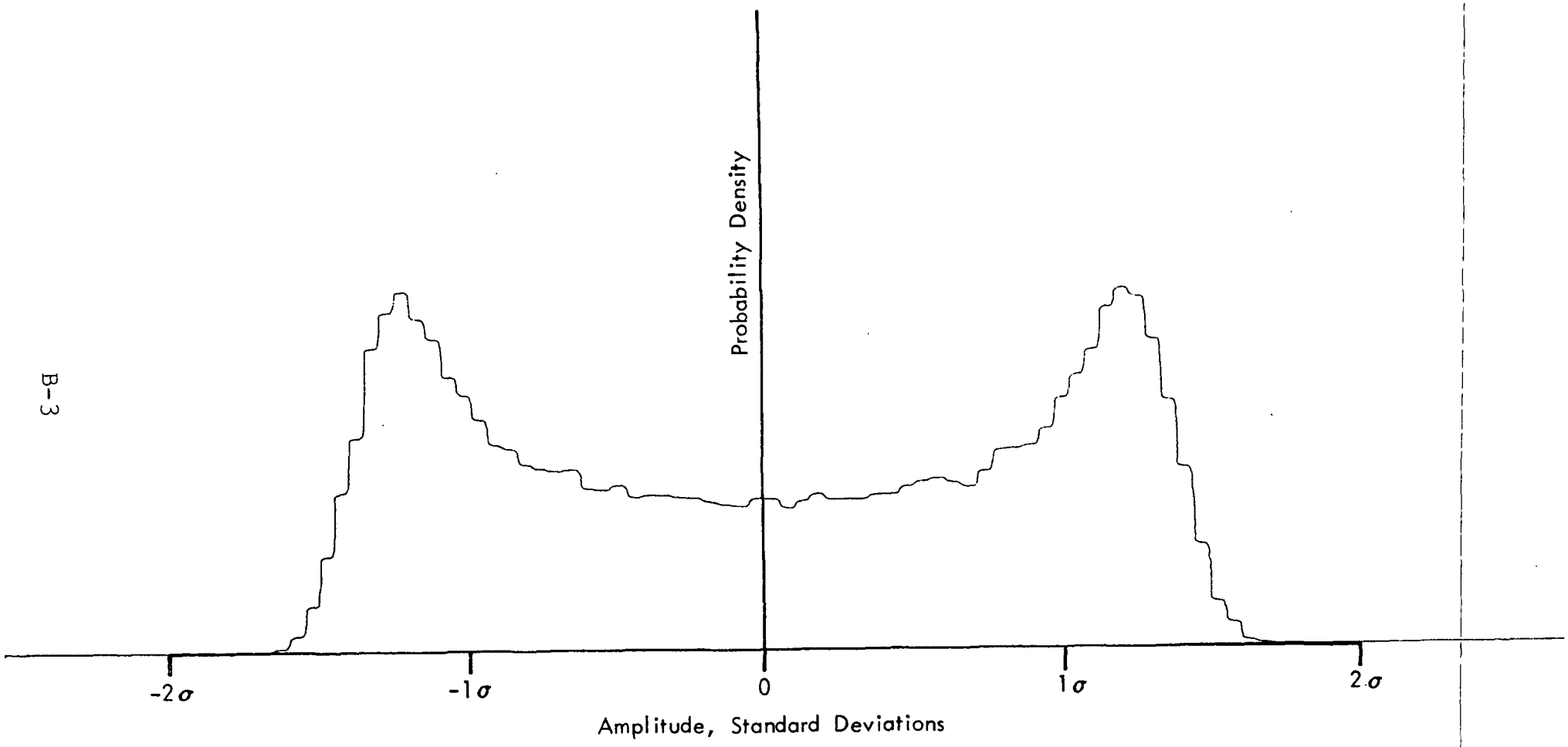

FIGURE B-3. PROBABILITY DENSITY FUNCTION OF SECOND HARMONIC, TEST RUN 4, LOCATION NO.6

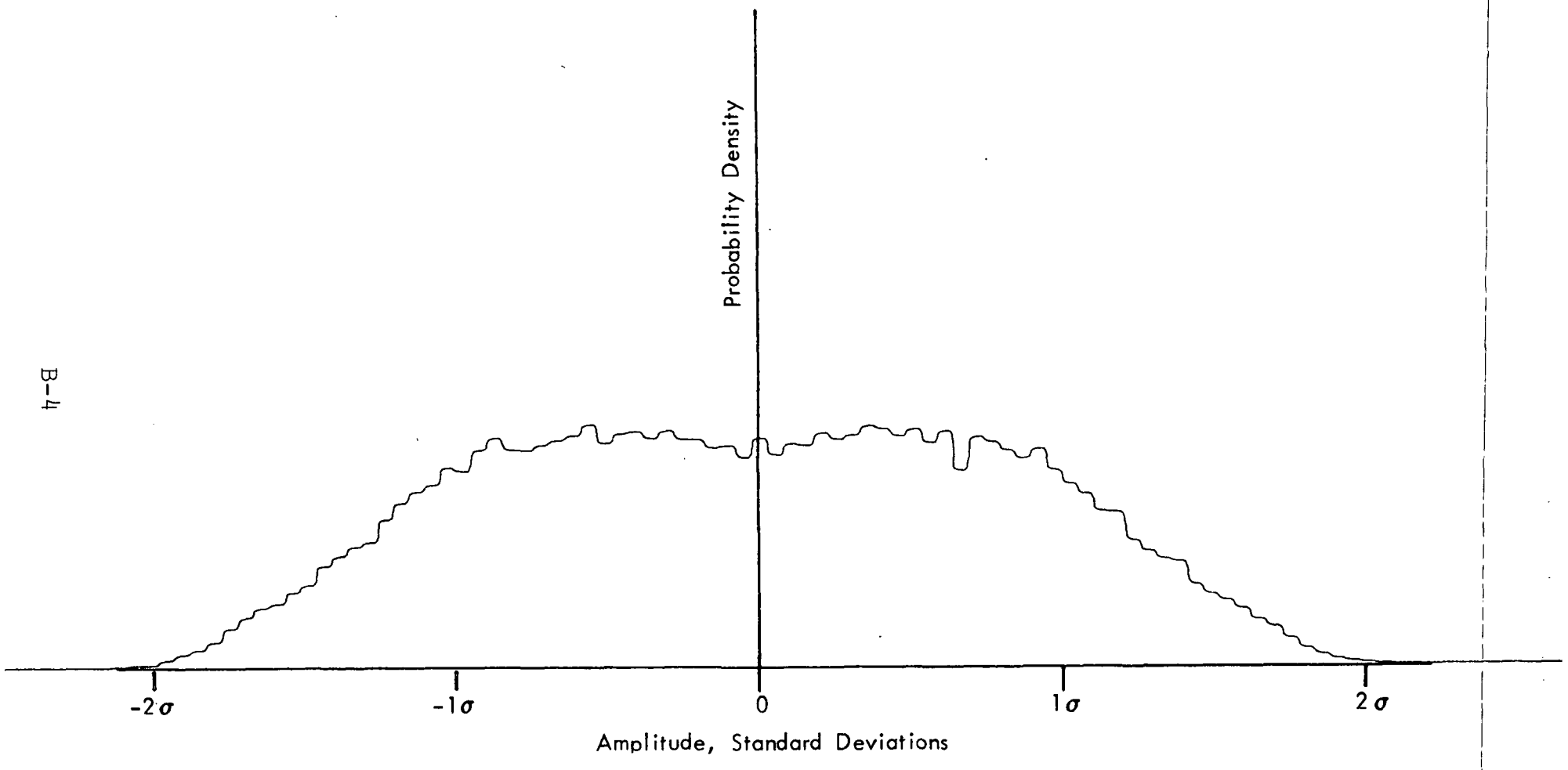

FIGURE B-4. PROBABILITY DENSITY FUNCTION OF THIRD HARMONIC, TEST RUN 4, LOCATION NO.6

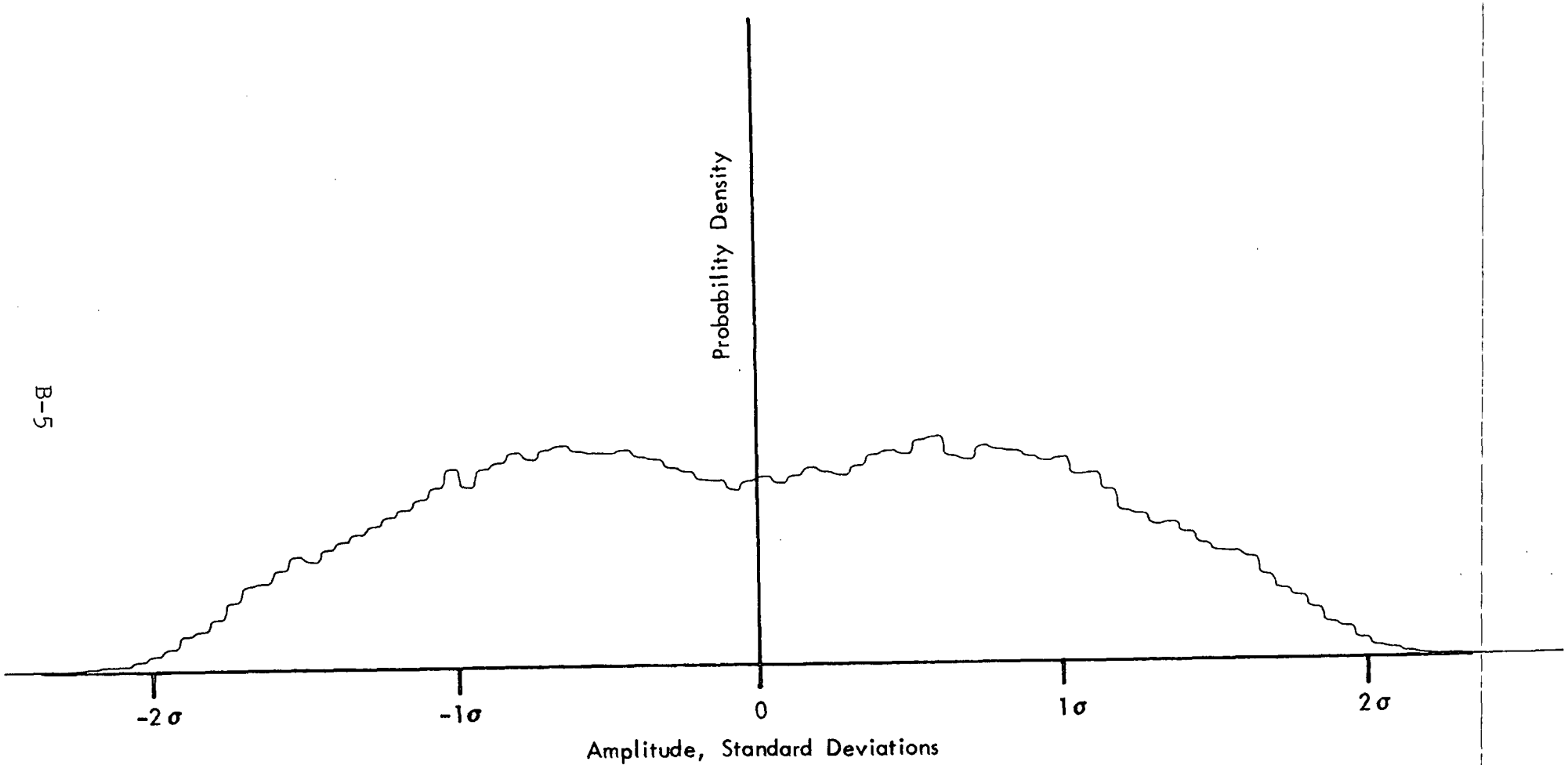

FIGURE B-5. PROBABILITY DENSITY FUNCTION OF FOURTH HARMONIC, TEST RUN 4, LOCATION NO.6

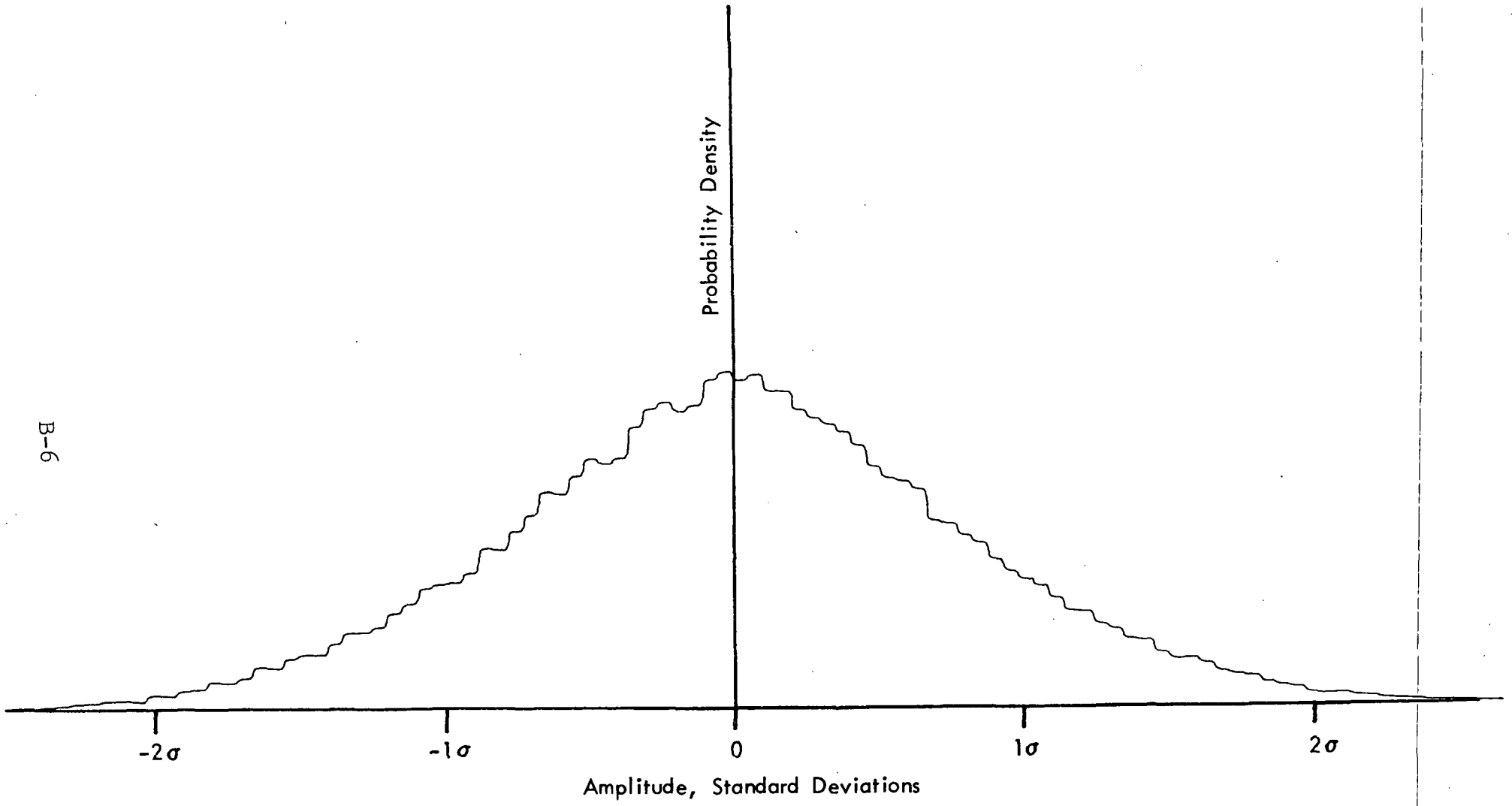

FIGURE B-6. PROBABILITY DENSITY FUNCTION OF FIFTH HARMONIC, TEST RUN 4, LOCATION NO.6

APPENDIX C

Pressure Coherence and Phase Angle Data

APPENDIX C

Pressure Coherence and Phase Angle Data

This appendix presents measured values of coherence and phase angle for several pairs of microphones and several test conditions.

Sample spectral plots are given for four microphone pairs, all the spectra being associated with Test Run 4. Figures C1-C4 contain coherence spectra for Microphone pairs 4-5, 2-1, 5-8, and 9-10, respectively, the coherence by definition having a value in the range $0 \leq \gamma^2 \leq 1$. Figures C5-C8 present phase angle spectra for the same microphone pairs. The phase angle ϕ is presented such that $-\pi \leq \phi \leq \pi$. Consequently, when ϕ reaches $\pm\pi$ the plot switches over to $\mp\pi$, respectively, showing a full-scale sweep on the figure, as can be clearly seen in Figure C6.

For present purposes, interest is concentrated on the contributions from the propeller pressure field. Consequently, values for coherence and phase angle at the propeller harmonic frequencies were read directly from the digital meter on the SD360 analyzer, and the resulting values are listed in a series of tables presented in this appendix.

COHERENCE AND PHASE ANGLE

Harmonic Order	Run 4 - 2600 rpm		Run 2 - 2400 rpm		Run 5 - 2100 rpm		Run 7-1700 rpm	
	Coherence	Phase (deg)	Coherence	Phase (deg)	Coherence	Phase (deg)	Coherence	Phase (deg)
Microphones 5 and 2								
1	.99	47	.99	49	.99	53	.99	48
2	.96	53	.95	56	.96	59	.94	56
3	.90	46	.91	40	.94	44	.82	28
4	.77	- 2	.75	- 1	.61	25	.70	23
5	.18	-112	.23	- 64	.17	- 76	.33	- 34
6	.27	94	.12	154	.29	135	.50	-122
7	.07	64	.05	55	.05	25	.16	147
8	.02	-100	.00	- 14	.25	- 81	.21	-180
9	.09	149	.13	-160	.14	141	.07	-157
10	.01	- 30	.07	89	.11	103	.11	170
11							.25	117
Microphones 5 and 1								
1	.99	47	.99	51	.99	57	.99	52
2	.84	85	.79	80	.90	77	.90	69
3	.70	42	.69	34	.76	51	.53	50
4	.42	- 76	.35	- 74	.11	- 18	.51	- 21
5	.53	146	.28	-174	.34	167	.34	-113
6	.45	33	.24	85	.43	86	.49	171
7	.10	- 19	.11	- 23	.06	- 52	.18	93
8	.07	118	.00	-106	.13	-156	.09	94
9	.12	46	.17	105	.10	77	.11	109
10	.00	138	.11	- 32	.23	14	.08	76
11							.07	18

COHERENCE AND PHASE ANGLE

Harmonic Order	Run 4 - 2600 rpm		Run 2 - 2400 rpm		Run 5 - 2100 rpm		Run 7 - 1700 rpm	
	Coherence	Phase (deg)	Coherence	Phase (deg)	Coherence	Phase (deg)	Coherence	Phase (deg)
Microphones 2 and 1								
1	1.00	0	1.00	2	1.00	4	.99	1
2	.94	30	.91	22	.96	17	.91	15
3	.85	- 4	.90	-12	.91	4	.77	21
4	.79	-63	.73	-66	.70	-40	.83	-27
5	.70	-73	.69	-63	.61	-48	.84	-55
6	.90	-73	.88	-61	.88	-57	.93	-55
7	.93	-91	.88	-82	.89	-61	.92	-56
8	.90	-116	.93	-84	.88	-75	.82	-68
9	.89	-118	.89	-100	.87	-81	.86	-67
10	.85	-130	.84	-116	.79	-90	.78	-73
11							.80	-72
Microphones 5 and 7								
1	1.00	-90	1.00	-94	1.00	-93	.99	-111
2	.95	-93	.95	-92	.97	-93	.98	-89
3	.85	-91	.88	-88	.89	-97	.79	-115
4	.56	-164	.44	-158	.40	-123	.55	-109
5	.40	44	.19	81	.11	33	.15	118
6	.37	-88	.03	123	.24	-35	.37	86
7	.24	-69	.00	-130	.32	131	.05	-96
8	.11	149	.02	-84	.05	134	.24	110
9	.15	-8	.20	72	.11	-138	.07	30
10	.02	-161	.18	-100	.20	-16	.03	-152
11							.03	4

COHERENCE AND PHASE ANGLE

Harmonic Order	Run 4 - 2600 rpm		Run 2 - 2400 rpm		Run 5 - 2100 rpm		Run 7 - 1700 rpm	
	Coherence	Phase (deg)	Coherence	Phase (deg)	Coherence	Phase (deg)	Coherence	Phase (deg)
Microphones 5 and 8								
1	.97	-105	.98	-111	.98	-108	.97	-137
2	.88	-86	.84	-83	.90	-100	.86	-97
3	.71	-125	.68	-111	.69	-112	.43	-134
4	.35	104	.34	147	.06	173	.16	-174
5	.51	-37	.33	3	.18	-20	.09	134
6	.40	-168	.30	-122	.45	-106	.16	151
7	.31	48	.07	170	.11	127	.31	-124
8	.11	-126	.05	-70	.10	8	.16	-163
9	.06	-68	.01	-153	.28	177	.03	-49
10	.02	-142	.08	-140	.14	118	.12	-128
11							.05	176
Microphones 5 and 9								
1	.66	-93	.54	-67	.07	-72	.47	137
2	.21	148	.02	-120	.18	143	.02	174
3	.25	-33	.51	-45	.44	5	.04	7
4	.26	95	.53	122	.01	-37	.81	-47
5	.45	-49	.29	-60	.08	-14	.26	76
6	.14	71	.34	134	.09	-109	.28	-165
7	.22	152	.06	175	.27	87	.05	-104
8	.16	53	.19	94	.19	119	.38	60
9	.23	178	.39	-88	.23	12	.14	-180
10	.03	13	.16	94	.34	-154	.07	89
11							.01	-15

COHERENCE AND PHASE ANGLE

Harmonic Order	Run 4 - 2600 rpm		Run 2 - 2400 rpm		Run 5 - 2100 rpm		Run 7 - 1700 rpm	
	Coherence	Phase (deg)	Coherence	Phase (deg)	Coherence	Phase (deg)	Coherence	Phase (deg)
Microphones 5 and 10								
1	.72	-92	.54	-46	.16	11	.56	106
2	.27	18	.01	-57	.16	-33	.05	109
3	.55	98	.18	124	.43	-162	.05	-41
4	.35	98	.15	-128	.01	-63	.33	20
5	.09	-112	.07	115	.24	32	.32	170
6	.27	12	.16	-149	.12	137	.57	-47
7	.20	-145	.03	25	.45	-127	.14	105
8	.16	17	.05	-130	.23	14	.47	169
9	.27	137	.21	-44	.26	148	.24	23
10	.00	-4	.15	128	.27	-116	.13	-110
11							.17	79
Microphones 7 and 8								
1	.99	-15	.98	-16	.99	-13	.98	-25
2	.94	6	.92	7	.96	-8	.92	-9
3	.89	-30	.91	-28	.90	-18	.67	-12
4	.71	-73	.71	-49	.38	-37	.65	4
5	.86	-86	.84	-77	.77	-74	.08	-46
6	.77	-97	.41	-91	.28	-68	.26	13
7	.21	155	.11	-149	.24	-58	.31	-36
8	.30	168	.26	178	.59	-90	.12	-37
9	.25	-129	.49	-162	.19	-124	.79	-92
10	.17	-88	.46	-127	.36	-167	.28	-113
11							.25	-120

COHERENCE AND PHASE ANGLE

Harmonic Order	Run 4 - 2600 rpm		Run 2 - 2400 rpm		Rpm 5 - 2100 rpm		Run 7 - 1700 rpm	
	Coherence	Phase (deg)	Coherence	Phase (deg)	Coherence	Phase (deg)	Coherence	Phase (deg)
Microphones 7 and 9								
1	.66	-3	.53	27	.08	12	.46	-109
2	.37	-128	.01	-67	.14	-133	.05	-103
3	.50	-13	.69	51	.64	99	.16	-157
4	.46	-85	.27	-40	.18	-19	.54	-41
5	.56	-100	.42	-131	.44	-73	.33	-26
6	.36	114	.15	-20	.23	-166	.29	70
7	.09	-134	.38	-30	.14	-3	.16	130
8	.45	-108	.23	-76	.02	97	.47	-86
9	.70	166	.64	-151	.03	90	.11	70
10	.51	131	.31	161	.24	-121	.18	-55
11							.12	148
Microphones 7 and 10								
1	.72	-3	.46	48	.12	99	.55	-145
2	.33	104	.05	72	.17	90	.09	176
3	.67	169	.55	-148	.60	-68	.03	-37
4	.44	-86	.74	134	.24	59	.50	-6
5	.12	-154	.14	-93	.05	21	.56	70
6	.18	112	.42	86	.22	-97	.61	-150
7	.15	-95	.23	-124	.57	109	.51	-116
8	.21	-82	.17	12	.25	-84	.47	54
9	.09	-89	.29	-161	.28	-3	.07	106
10	.36	61	.07	176	.09	-120	.04	-145
11							.09	-34

COHERENCE AND PHASE ANGLE

Harmonic Order	Run 4 - 2600 rpm		Run 2 - 2400 rpm		Run 5 - 2100 rpm		Run 7 - 1700 rpm	
	Coherence	Phase (deg)	Coherence	Phase (deg)	Coherence	Phase (deg)	Coherence	Phase (deg)
Microphones 8 and 9								
1	.67	12	.53	41	.06	16	.43	-82
2	.39	-134	.08	-91	.37	-123	.08	-86
3	.43	36	.60	81	.69	121	.48	173
4	.74	-3	.86	-56	.82	-146	.46	-75
5	.52	-16	.55	-45	.70	4	.34	-116
6	.42	-152	.63	-86	.06	32	.81	24
7	.68	110	.30	-136	.26	-107	.18	11
8	.32	115	.36	146	.06	166	.43	-103
9	.22	-110	.10	59	.29	-149	.13	-171
10	.66	-166	.37	-119	.35	86	.14	-174
11							.35	174
Microphones 8 and 10								
1	.70	11	.41	68	.12	121	.52	-120
2	.37	101	.11	110	.21	103	.13	-167
3	.75	-156	.63	-118	.65	-50	.22	-142
4	.26	11	.61	73	.06	-82	.73	-30
5	.27	-68	.14	-103	.11	101	.26	-9
6	.08	174	.10	30	.41	-113	.50	144
7	.35	-168	.41	74	.09	81	.25	-144
8	.10	179	.15	-100	.58	21	.23	-40
9	.14	-36	.06	-6	.20	-95	.10	136
10	.26	144	.10	-148	.08	130	.28	3
11							.12	-93

COHERENCE AND PHASE ANGLE

Harmonic Order	Run 4 - 2600 rpm		Run 2 - 2400 rpm		Run 5 - 2100 rpm		Run 7 - 1700 rpm	
	Coherence	Phase (deg)	Coherence	Phase (deg)	Coherence	Phase (deg)	Coherence	Phase (deg)
Microphones 9 and 10								
1	.53	-3	.31	-14	.02	-70	.59	-35
2	.16	-128	.11	-105	.51	9	.14	-61
3	.62	166	.41	168	.42	-172	.40	67
4	.29	37	.98	128	.77	92	.27	104
5	.01	-57	.34	-176	.28	89	.80	87
6	.22	-157	.43	116	.44	125	.58	114
7	.82	88	.70	-119	.36	131	.48	134
8	.02	148	.48	121	.24	-114	.53	107
9	.03	140	.24	12	.59	94	.29	-168
10	.42	-68	.33	-21	.21	125	.27	-180
11							.19	140
Microphones 5 and 11								
1	.41	-49						
2	.56	-15						
3	.79	-65						
4	.05	66						
5	.81	177						
6	.40	31						
7	.26	-135						
8	.53	30						
9	.30	-60						
10	.10	-120						
11								

COHERENCE AND PHASE ANGLE

Harmonic Order	Run 4 - 2600 rpm		Run 2 - 2400 rpm		Run 5 - 2100 rpm		Run 7 - 1700 rpm	
	Coherence	Phase (deg)	Coherence	Phase (deg)	Coherence	Phase (deg)	Coherence	Phase (deg)
Microphones 4 and 3								
1	.98	-46	.97	-45	1.00	-40	.98	-41
2	1.00	-69	.99	-65	1.00	-63	.99	-62
3	.98	-118	.99	-110	1.00	-107	.96	-92
4	.97	-152	.94	-148	.93	-156	.97	-143
5	.98	168	.98	176	.96	173	.91	172
6	.83	121	.91	135	.86	133	.57	139
7	.77	80	.70	93	.77	77	.82	101
8	.67	34	.69	50	.70	34	.90	58
9	.71	-10	.70	6	.32	-36	.85	19
10	.35	-95	.43	-31	.59	-53	.64	-17
11							.39	-61
Microphones 5 and 3								
1	.99	-83	.98	-79	1.00	-78	1.00	-77
2	1.00	-154	.99	-142	.99	-141	.99	-128
3	.98	126	.98	133	.99	130	.89	138
4	.94	46	.93	53	.96	44	.96	60
5	.95	-40	.95	-21	.93	-31	.82	-12
6	.86	-128	.79	-106	.78	-107	.77	-81
7	.65	174	.84	172	.30	160	.68	-162
8	.62	80	.65	95	.62	58	.52	99
9	.57	-4	.67	11	.33	-9	.62	29
10	.32	-77	.45	-87	.49	-67	.47	-48
11							.21	-131

COHERENCE AND PHASE ANGLE

Harmonic Order	Run 4 - 2600 rpm		Run 2 - 2400 rpm		Run 5 - 2100 rpm		Run 7 - 1700 rpm	
	Coherence	Phase (deg)	Coherence	Phase (deg)	Coherence	Phase (deg)	Coherence	Phase (deg)
Microphones 4 and 5								
1	.98	36	.98	33	.99	38	.98	37
2	.97	84	.97	77	.98	77	.97	67
3	.96	117	.97	117	.98	123	.88	127
4	.94	163	.87	159	.89	160	.90	153
5	.97	-152	.95	-163	.91	-157	.69	-163
6	.91	-104	.79	-116	.71	-116	.30	-117
7	.51	-92	.73	-84	.48	-55	.85	-89
8	.86	-48	.81	-45	.86	-37	.55	-39
9	.76	1	.71	-12	.67	-29	.77	-8
10	.54	23	.45	40	.54	16	.34	14
11							.38	43
Microphones 4 and 6								
1	.97	66	.97	66	.99	72	.97	78
2	.99	166	.98	158	.96	158	.96	142
3	.98	-145	.94	-155	.97	-149	.92	-140
4	.91	-80	.71	-99	.91	-86	.76	-83
5	.63	-27	.70	-29	.74	-17	.64	-48
6	.57	57	.43	60	.03	-3	.36	36
7	.49	119	.29	125	.27	93	.00	176
8	.13	-122	.34	161	.22	-166	.12	-131
9	.22	-92	.04	178	.01	47	.04	-67
10	.22	4	.15	-73	.75	20	.02	-99
11							.02	6

COHERENCE AND PHASE ANGLE

Harmonic Order	Run 4 - 2600 rpm		Run 2 - 2400 rpm		Run 5 - 2100 rpm		Run 7 - 1700 rpm	
	Coherence	Phase (deg)	Coherence	Phase (deg)	Coherence	Phase (deg)	Coherence	Phase (deg)
Microphones 5 and 6								
1	.99	28	.99	32	.99	34	.99	41
2	.96	79	.97	80	.97	77	.96	74
3	.97	98	.93	87	.96	90	.79	90
4	.85	117	.47	99	.82	115	.54	123
5	.55	126	.73	131	.61	141	.21	137
6	.72	158	.34	155	.09	-141	.15	-163
7	.01	171	.01	48	.08	43	.14	-88
8	.10	-75	.24	-156	.17	-114	.16	-28
9	.18	-71	.11	151	.10	170	.12	-61
10	.04	49	.01	73	.13	28	.12	-8
11							.03	-30

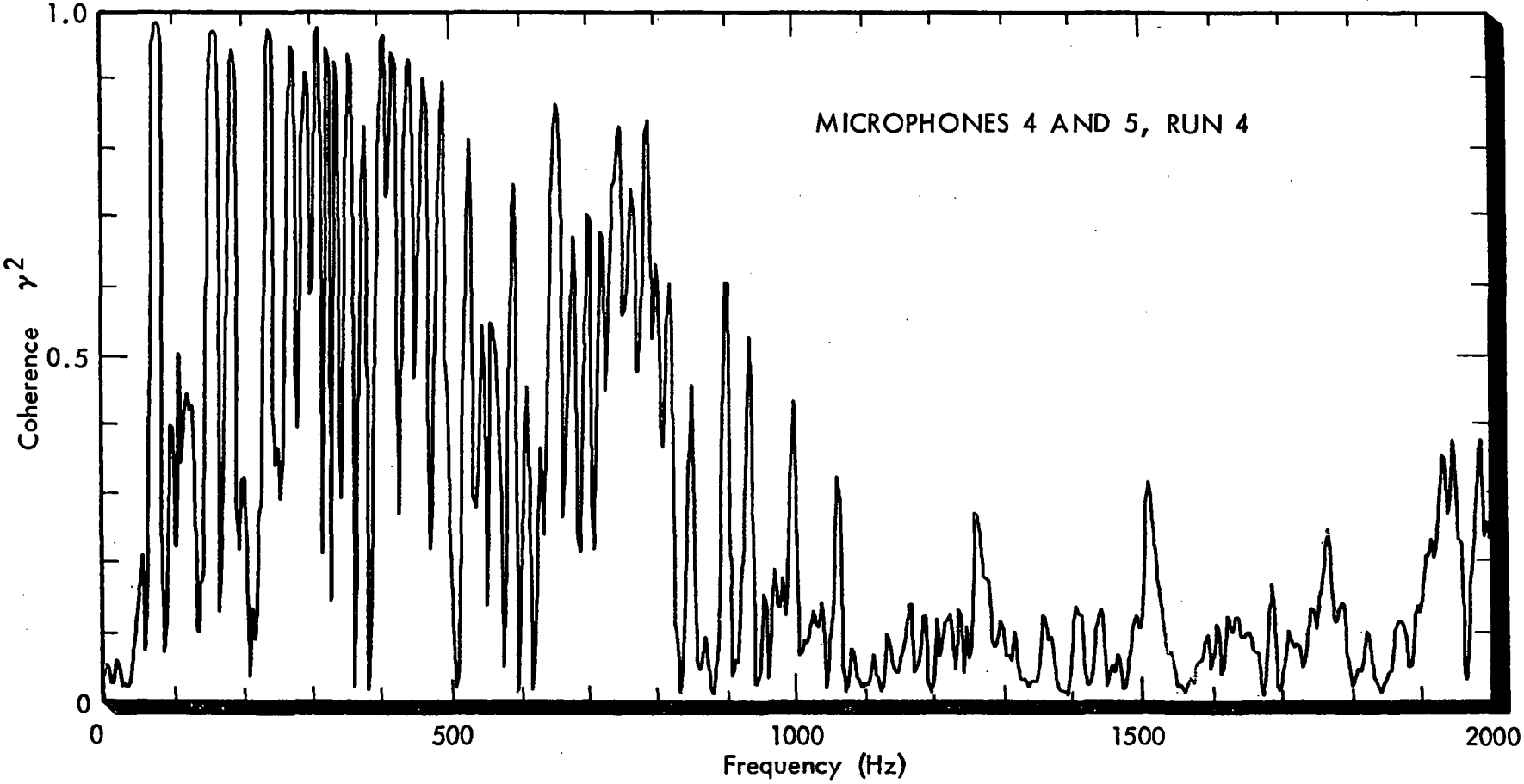

FIGURE C1. COHERENCE SPECTRUM FOR MICROPHONES 4 AND 5, TEST RUN 4

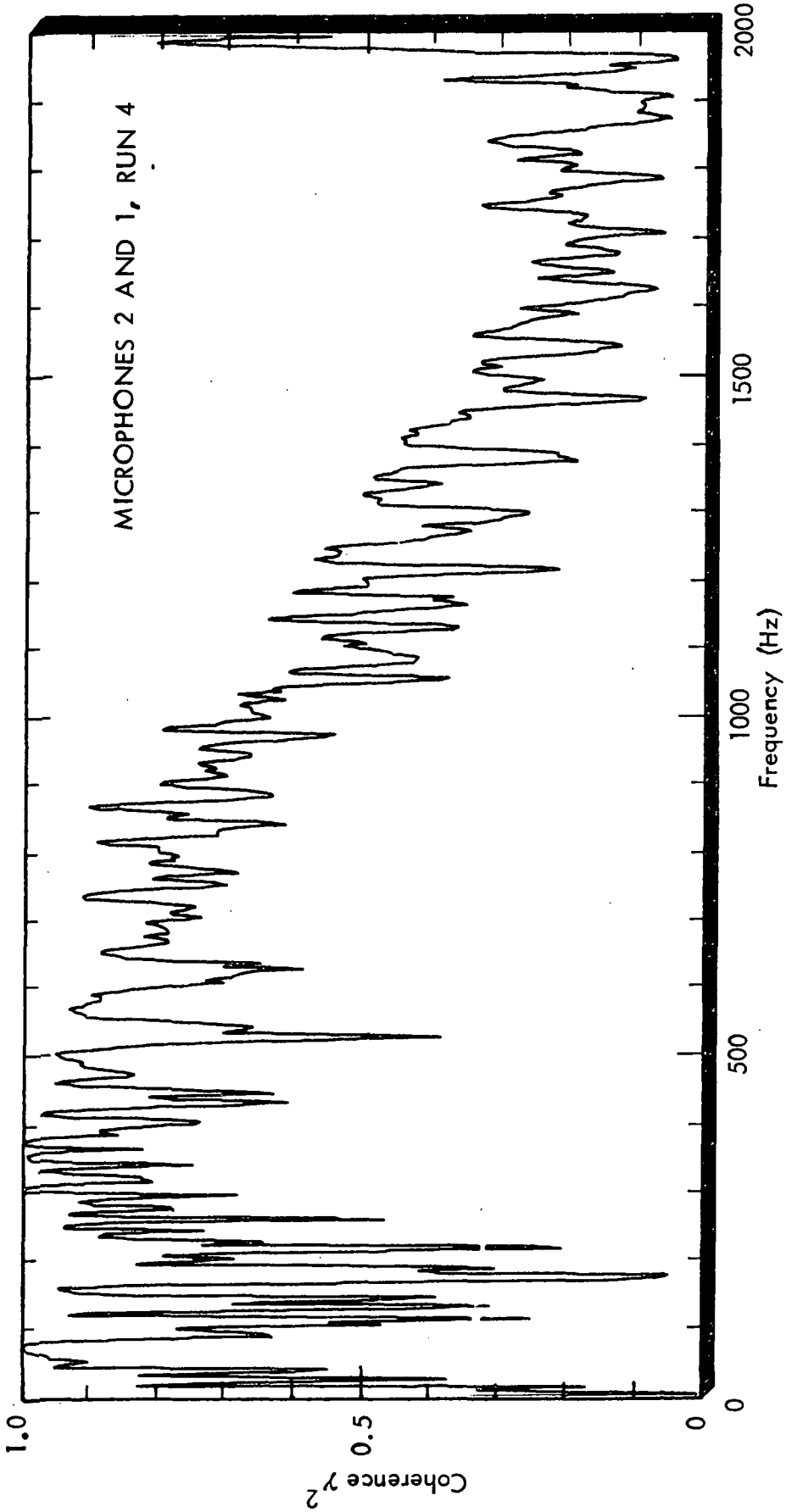

FIGURE C-2. COHERENCE SPECTRUM FOR MICROPHONES 2 AND 1, TEST RUN 4

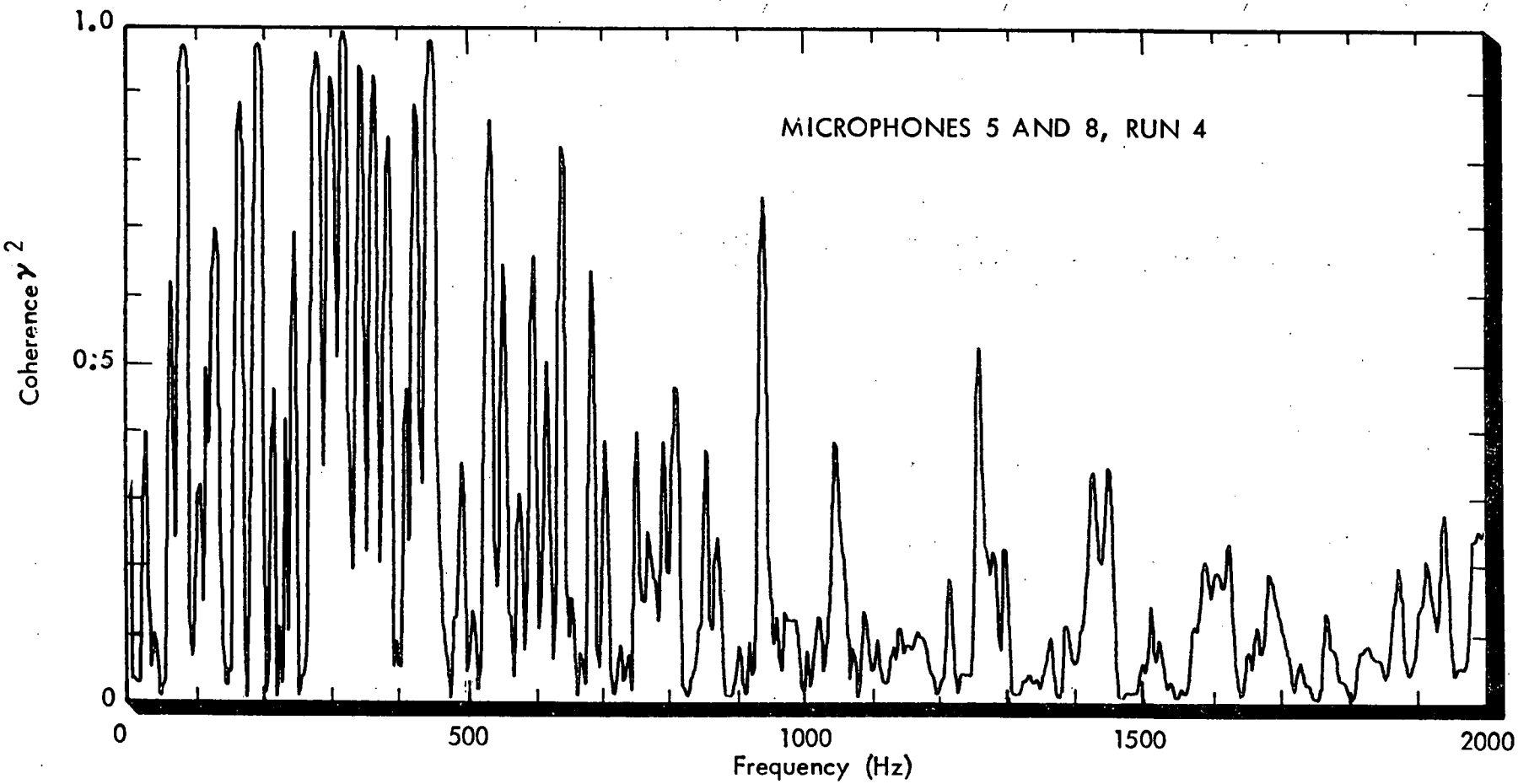

FIGURE C-3. COHERENCE SPECTRUM FOR MICROPHONES 5 AND 8, TEST RUN 4

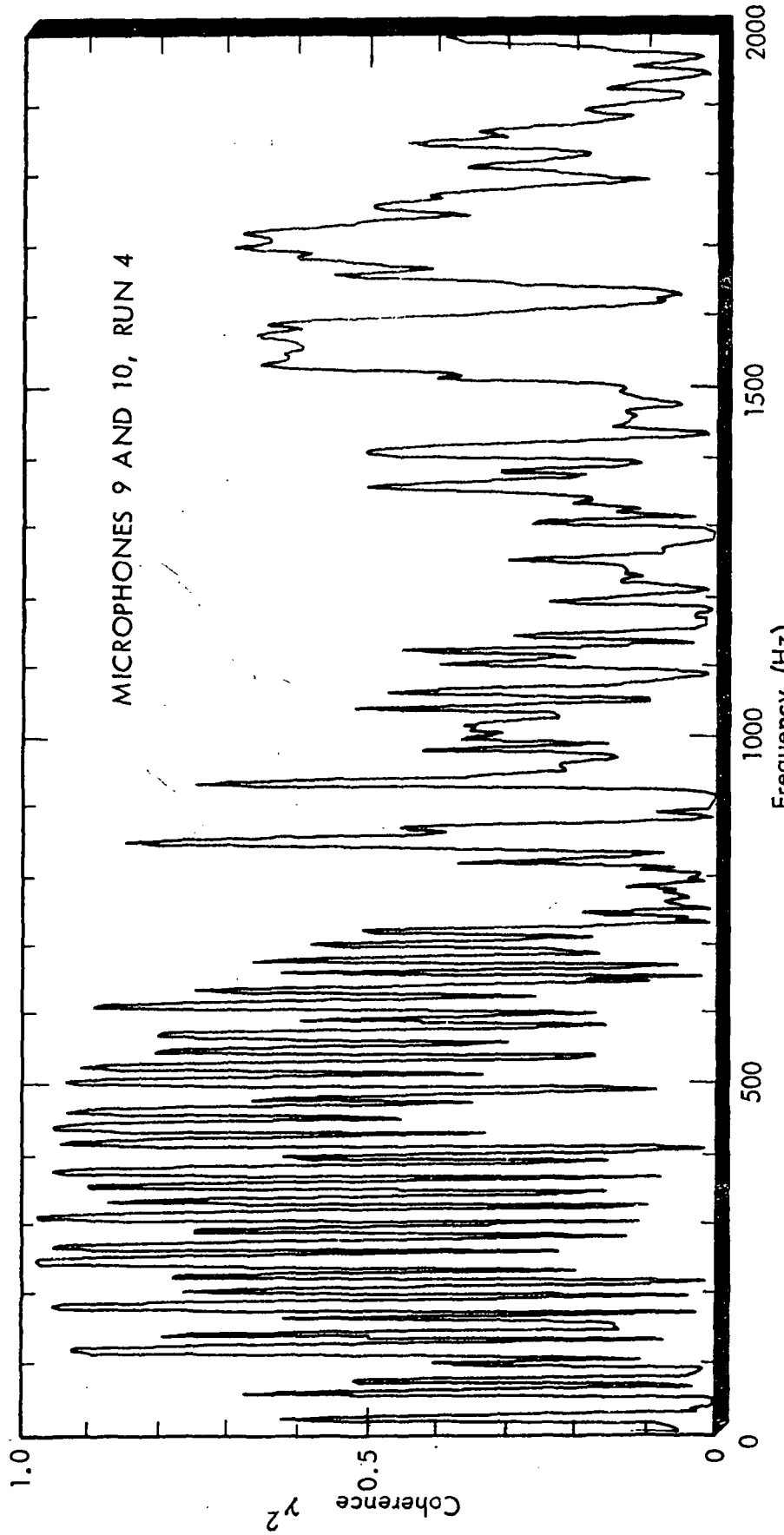

FIGURE C4. COHERENCE SPECTRUM FOR MICROPHONES 9 AND 10, TEST RUN 4

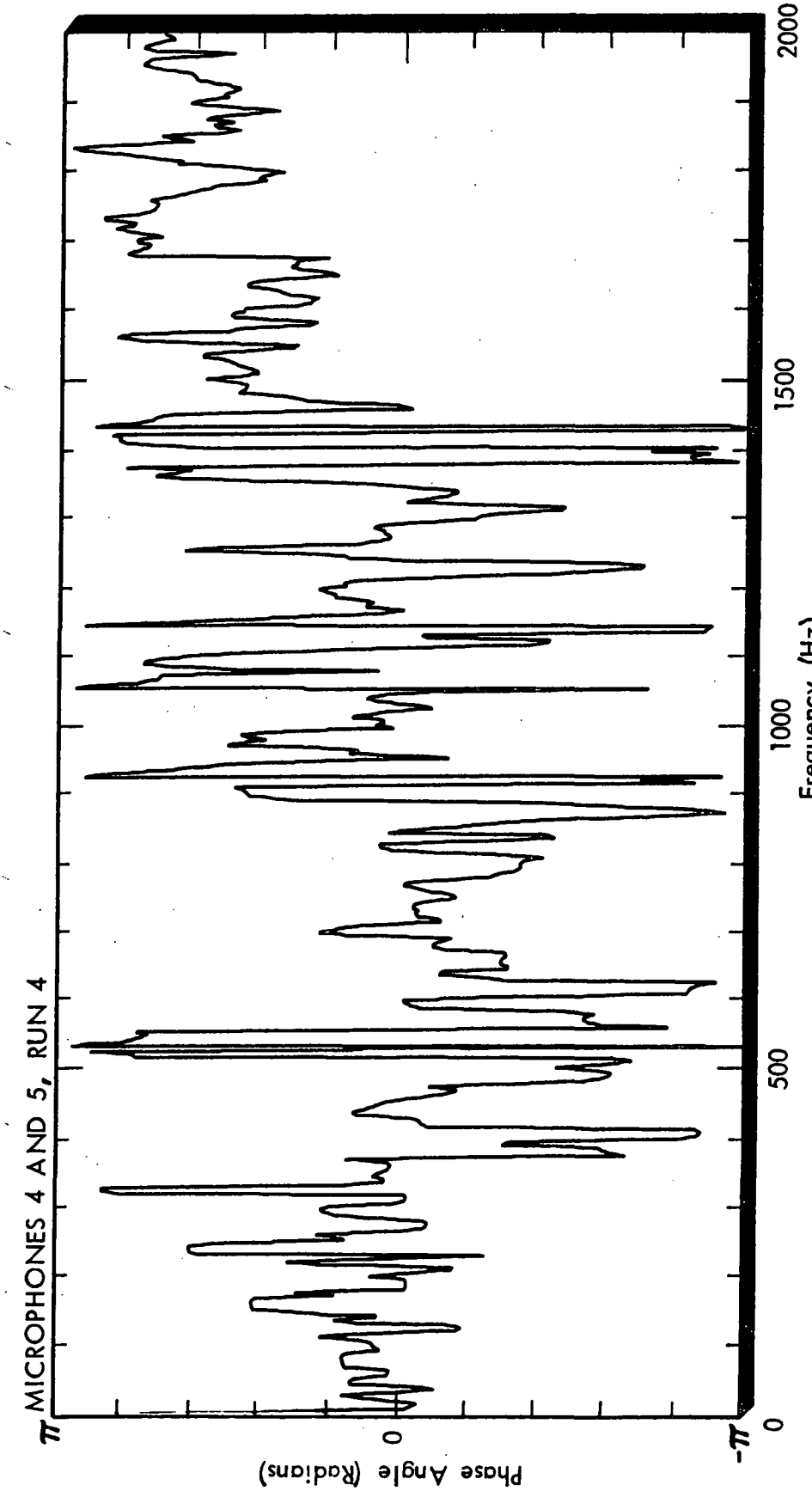

FIGURE C5. PHASE SPECTRUM FOR MICROPHONES 4 AND 5, TEST RUN 4

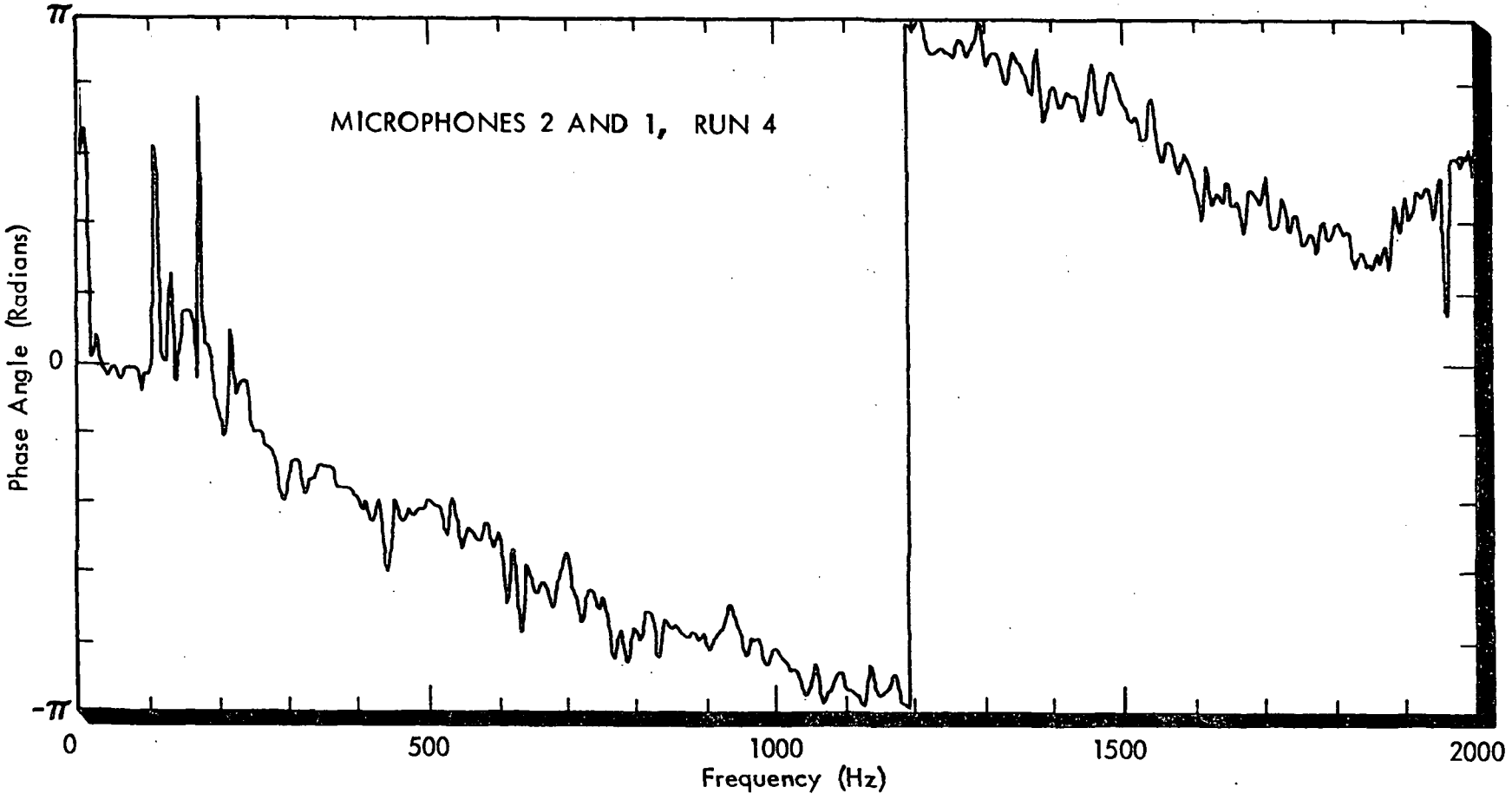

FIGURE C-6. PHASE SPECTRUM FOR MICROPHONES 2 AND 1, TEST RUN 4

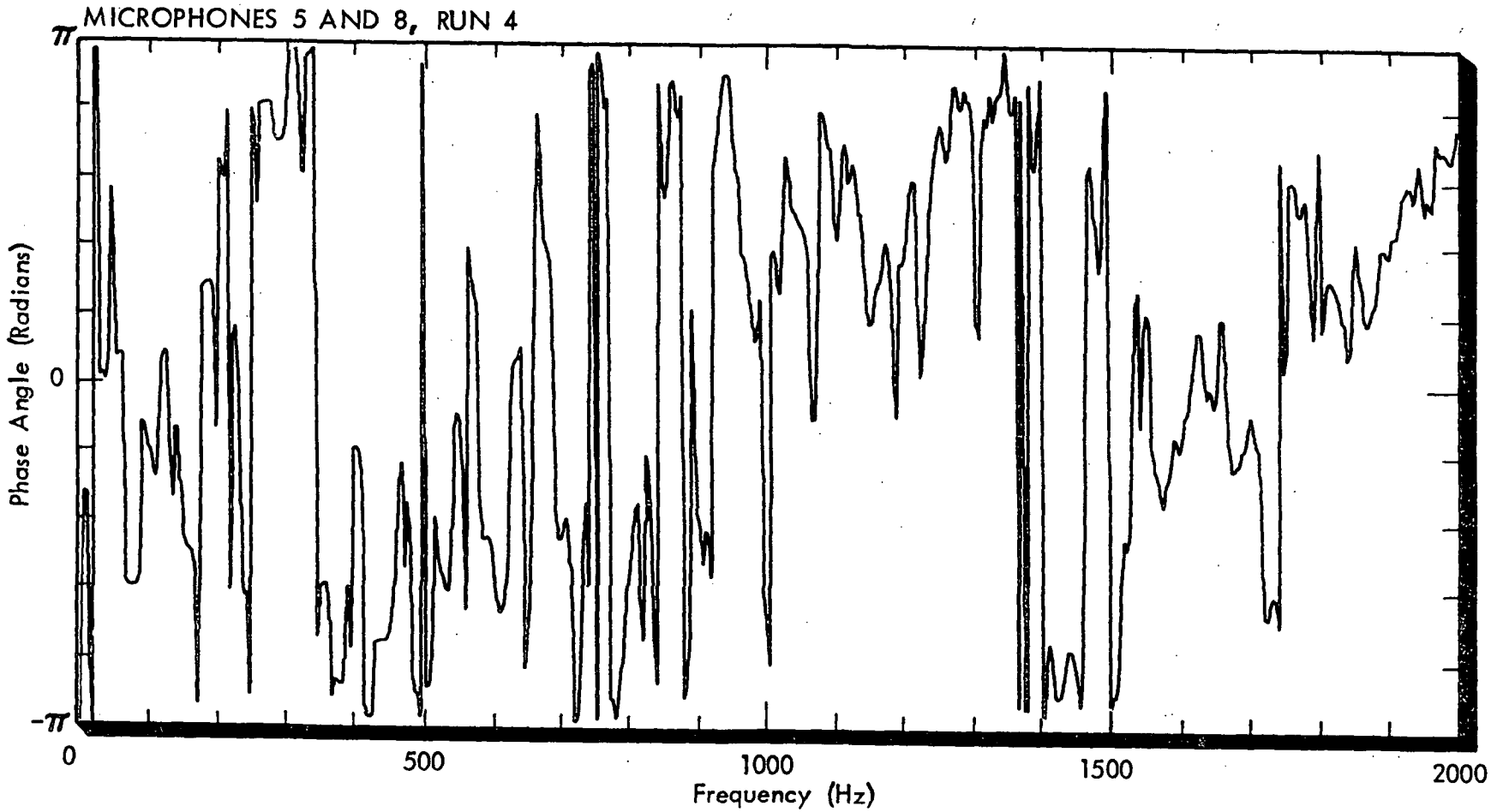

FIGURE C7. PHASE SPECTRUM FOR MICROPHONES 5 AND 8, TEST RUN 4

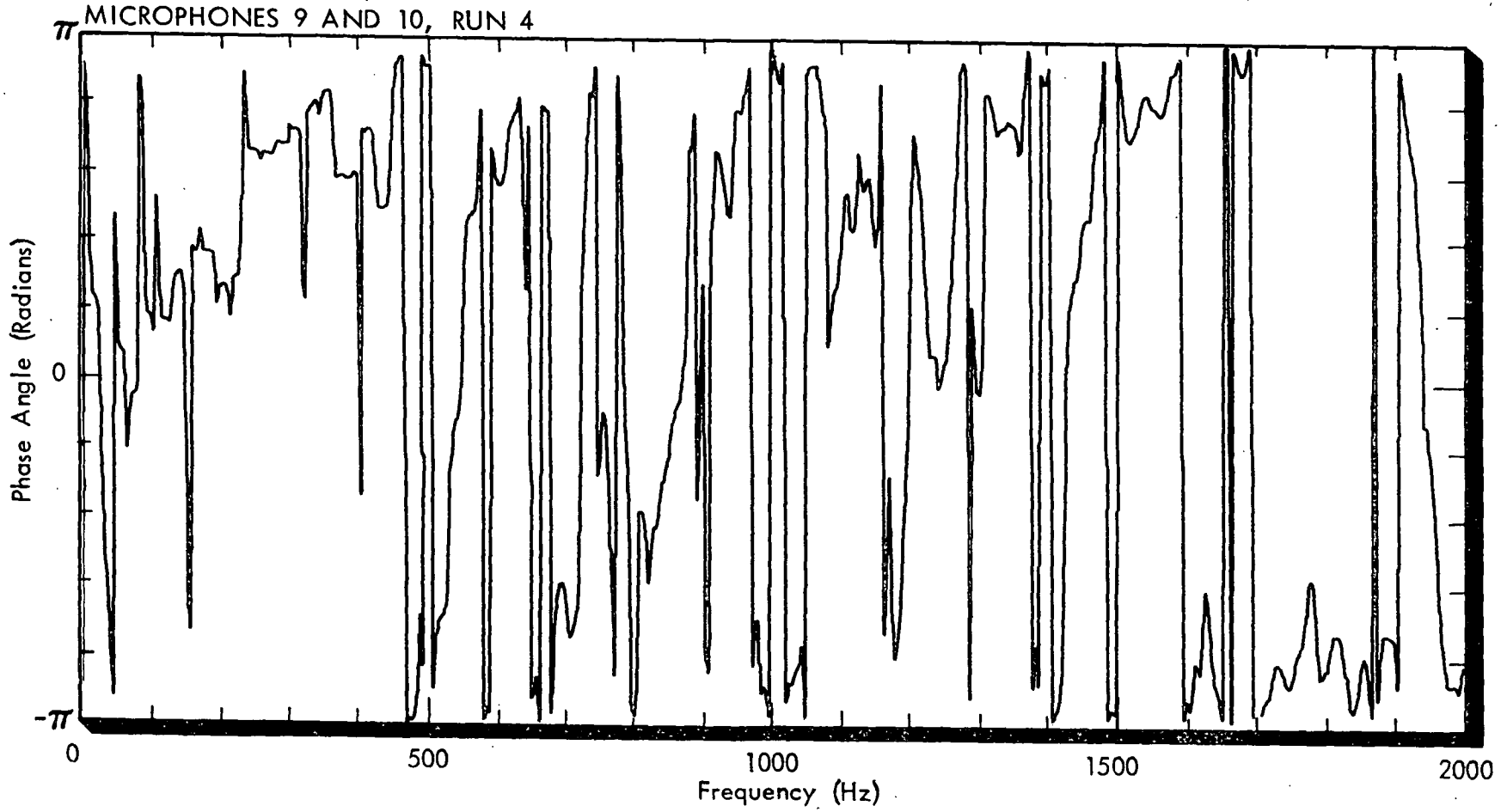

FIGURE C8. PHASE SPECTRUM FOR MICROPHONES 9 AND 10, TEST RUN 4